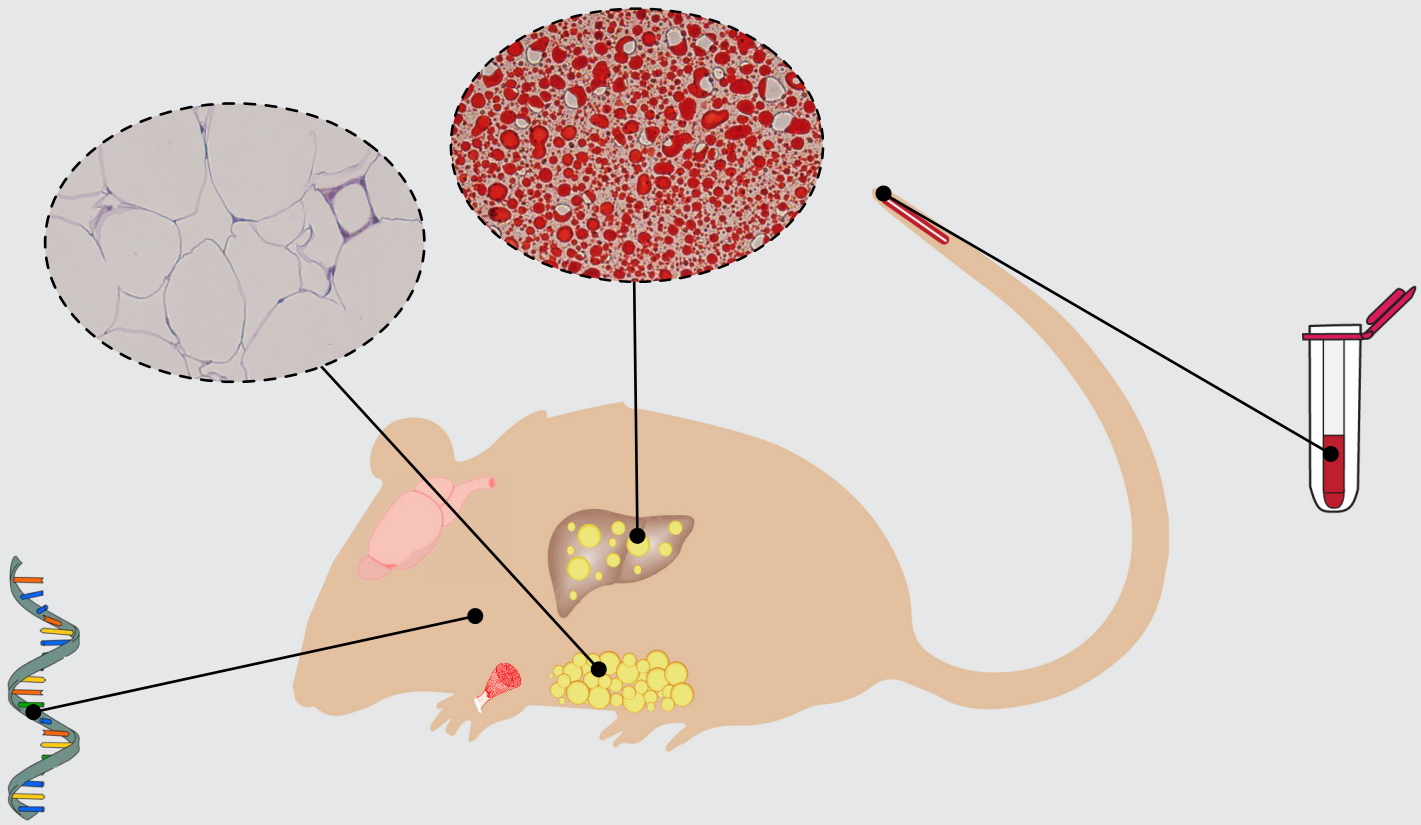

Patrícia Marques Diogo Valério

INSIGHTS INTO THE ROLE OF SIRTUIN 2 IN OBESITY AND INSULIN RESISTANCE

Dissertação de Mestrado em Biologia Celular e Molecular

Agosto 2017

· U C ·

UNIVERSIDADE DE COIMBRA

Patrícia Marques Diogo Valério

Insights into the role of sirtuin 2 in obesity and insulin resistance

Dissertação de Mestrado em Biologia Celular e Molecular, orientada pelo Doutor Pedro Gomes (Centro de Neurociências e Biologia Celular, Universidade de Coimbra) e pela Professora Doutora Emília Duarte (Departamento de Ciência da Vida, Universidade de Coimbra) e apresentada ao Departamento de Ciências da Vida da Universidade de Coimbra.

Agosto de 2017

UNIVERSIDADE DE COIMBRA

O trabalho aqui apresentado foi realizado no grupo de Neuroendocrinologia e Envelhecimento do Centro de Neurociências e Biologia Celular (Universidade de Coimbra, Portugal), liderado pela Professora Doutora Cláudia Cavadas, e orientado pelo Doutor Pedro Gomes.

O trabalho foi financiado pelo FEDER (QREN) através do Programa Mais Centro, no âmbito dos projetos CENTRO-07-ST24-FEDER-002006; pelo Programa Operacional Fatores de Competitividade - COMPETE 2020; e por Fundos Nacionais pela FCT - Fundação para a Ciência e Tecnologia através do Projeto Estratégico (UID/NEU/04539/2013) e HEALTHYAGING 2020 (CENTRO-01-0145-FEDER-000012).

The present work was performed in the Neuroendocrinology and Aging group of the Center for Neuroscience and Cell Biology (University of Coimbra, Portugal), headed by Professor Doctor Cláudia Cavadas, and under scientific guidance of Doctor Pedro Gomes.

This work was funded by FEDER (QREN) through Programa Mais Centro, under projects CENTRO-07-ST24-FEDER-002006; the Operational Programme Factors Competitiveness - COMPETE 2020; and National Funds through FCT - Foundation for Science and Technology under the Strategic Project (UID/NEU/04539/2013) and HEALTHYAGING 2020 (CENTRO-01-0145-FEDER-000012).

Agradecimentos

À Professora Doutora Cláudia Cavadas por me ter aceite e dado a oportunidade de desenvolver este projeto de mestrado no seu grupo de investigação. Muito obrigada pela confiança depositada no meu trabalho, pelos conselhos, compreensão e ajuda disponibilizada que me orientaram e encaminharam até ao fim deste ano.

Ao meu orientador, Doutor Pedro Gomes, por toda a orientação científica, compreensão e ajuda durante todo este ano de muita aprendizagem. Muito obrigada por todo o apoio nestes primeiros passos como cientista. Tenho a certeza que tudo o que aprendi este ano será uma mais valia no futuro.

A todos os elementos do grupo, desde os mais 'graúdos' aos mais 'verdinhos'. Trabalhar no laboratório de 'Neuroendocrinologia e Envelhecimento' foi a minha primeira grande aventura no caminho de me tornar uma boa investigadora. Aprendi muito, mas mesmo muito com vocês, e sei que irei levar toda essa aprendizagem comigo para onde quer que vá. Um especial obrigada à Célia, à Marisa, e à Mariana, que de uma maneira mais predominante me ajudaram a 'ganhar mão' em várias práticas laboratoriais essenciais ao meu trabalho. Um enorme obrigada também à Helena pela ajuda indispensável, à Magda por toda a orientação, e ao João pelo sua disponibilidade e boa disposição, nesta fase final da minha tese. Mais uma vez, obrigada a todos vocês.

A todos os meus colegas de mestrado, presentes e não presentes durante este ano, pois fizeram deste mestrado uma experiência, não para repetir, mas inesquecível. Levo comigo todos os momentos de convívio vividos e as conversas divertidas nas pausas de trabalho. Fizeram-me ver que todos 'sobrevivemos' a estes dois anos tão intensos. Um grande obrigada.

À Marta, que mesmo longe, se disponibilizou a ajudar-me em tudo o que precisei para continuar a desenvolver o seu trabalho. Obrigada por tudo.

À Nês, minha amiga de longa data e que muito bem me conhece, que para além de em anos passados, também esteve sempre disponível para me ouvir, apoiar e aconselhar durante este ano. Foi um período de grandes emoções, tanto espetaculares como frustrantes, e estiveste sempre por perto. Vimo-nos uma a outra a completar várias etapas da vida, esta é mais uma, uma de muitas outras que sei que virão. Um enorme obrigada.

Ao Tozé, que tornou estes últimos dois anos muito mais incríveis do que deveriam ter sido. Para além de ter tido de trabalhar para completar este mestrado, também tive de trabalhar para te conquistar. Obrigada por me teres deixado entrar na tua vida, por me deixares ser tua companheira nas mais diversas aventuras. Foi, está a ser, e sei que continuará a ser, um privilégio ser tua namorada. Obrigada por todos os abraços fortes e revitalizadores, por todas as parvoíces e

brincadeiras, por todos os sorrisos de orelha a orelha, que tanto me enchem a alma e me fazem ser mais forte para conquistar seja o que for. Obrigada por me mostrares, que a dois, tudo vale a pena. Obrigada por seres quem és, é enorme o orgulho que tenho de ti. Um gigantesco obrigada.

Aos pais do Tozé, por todo o apoio e preocupação que tiveram comigo durante este ano, e desde que entrei no vosso seio familiar. Quero que saibam que as idas à vossa terra, tão pacata e cheia de natureza, muito me ajudaram, e têm vindo a ajudar a crescer e a recarregar energias para enfrentar qualquer adversidade que apareça. Acima de tudo, as vossas palavras ajudaram-me a ter mais força para fazer sempre o meu melhor e completar este ano de trabalho. Muito obrigada por tudo.

Aos meus avós, por todo o vosso 'amor de avós ' e imenso apoio para conseguir alcançar as minhas ambições e ter sucesso na vida. Obrigada avó Palmira e avô Quim, que mesmo ausentes para acompanhar esta etapa, em muito me deram força e alento para completar esta ano árduo. Obrigada avó Alice, por estares sempre presente para acompanhar os teus netos em tudo, e os apoiares da melhor maneira que te é possível. Obrigada por todo o mimo que me deram e dão desde pequena, sou uma pessoa bem mais rica graças a isso, indispensável no completar deste mestrado. Muito obrigada por tudo.

Porque os últimos são sempre os mais importantes, aos meus pais, que são a quem mais tenho de agradecer por mais esta conquista. Obrigada pai e mãe, por tudo o que me proporcionaram desde que era um pequeno rebento até agora, já uma mulher adulta. Nunca deixaram que me faltasse seja o que fosse, e podem ter a certeza que em muito compensou o vosso esforço, pois agora aqui estou eu a completar mais uma fase importante da minha vida. Para além disso, tenho de agradecer mais ainda por todo o amor e carinho, conselhos e apoio que me deram, durante este ano, e em todos os outros anteriores, que tanto me ajudaram a ser mais forte e mais assertiva nas minhas escolhas e mais empenhada e dedicada em qualquer coisa que faço. Em já muito me acompanharam, e irão continuar a acompanhar, os valores e ensinamentos que me transmitiram. Um enorme obrigada a vocês os dois.

"Science, my lad, is made up of mistakes, but they are mistakes which it is useful to make, because they lead little by little to the truth"

Jules Verne

Table of Contents

Table of Figures

List of Tables

Abbreviations

ACAD	Acyl-CoA dehydrogenases
ACC	Acetyl-CoA carbolxylase
AceCS2	Acetyl-CoA-synthetase 2
ACLY	ATP-citrate lyase
ADP	Adenosine diphosphate
AgRP	Agouti-related protein
APC/C	Anaphase promoting complex
ARC	Arcuate nucleus
ATGL	Adipose triglyceride lipase
ATP	Adenosine triphosphate
BAT	Brown adipose tissue
BBB	Blood-brain-barrier
BCA	Bicinchoninic acid
BMR	Basal metabolic rate
CART	Cocaine- and amphetamine-regulated transcript
CD	Chow diet
ChREBP	Carbohydrate-responsive element-binding protein
CNC	Center for Neuroscience and Cell Biology
CNS	Central nervous system
CPT-1	Carnitine palmitoyltranferase 1
CR	Caloric restriction
CSP1	Carbamoyl phosphate synthetase 1
DAG	Diacylglycerol
DMH	Dorsomedial hypothalamic nuclei

DOC	Deoxycholate
DTT	Dithiothreitol
ECF	Enhanced chemifluorescence substrate
EE	Energy expenditure
EGTA	Egtazic acid
eWAT	Epididymal white adipose tissue
FA	Fatty acids
FAO	Fatty acid oxidation
FasN	Fatty acid synthase
FBP	Fructose-1,6-bisphosphate
FI	Food intake
FOXO1	Forkhead box protein 1
GCK	Glucokinase
GDH	Glutamate dehydrogenase
GKRP	Glucokinase regulatory protein
GLUT	Glucose transporters
GIT	Gastro-intestinal tract
GP	Glycogen phosphorylase
GS	Glycogen synthase
GSK3 β	Glycogen synthase kinase 3 beta
G6P	Glucose-6-phosphate
H	Histone
H&E	Hematoxylin & Eosin
HD	Huntington disease
HFD	High-fat diet

HGP	Hepatic glucose production
HSL	Hormone-sensitive lipase
HTT	Huntingtin
IL-6	Interleukin-6
IKK-β	IκB kinase-β
ipGTT	intraperitoneal glucose tolerance test
ipITT	intraperitoneal insulin tolerance test
IRS	Insulin receptor substrate proteins
IR	Insulin receptor
ISO	Isoproterenol
JNK	C-Jun amino-terminal kinase
LCAD	Long chain acyl-CoA dehydrogenase
LCFA	Long chain fatty acid
LD	Lipid droplet
LHA	Lateral hypothalamic area
LPL	Lipoprotein lipase
KO	Knockout
MAG	Monoacylglycerol
MAPK	Mitogen-activated protein kinase
MCAD	Medium chain acyl-CoA dehydrogenase
MCH	Melanin concentrating hormone
MCR	Melanocortin receptors
ME	Median eminence
mRNA	Messenger RNA
NA	Noradrenaline
NAD	Nicotinamide adenine dinucleotide

NAFLD	Non-alcoholic liver disease
NASH	Non-alcoholic steatohepatitis
NAM	Nicotinamide
NF-κB	Nuclear factor kappa B
NPY	Neuropeptide Y
NTS	Nucleus tractus solitarius
OD	Optical density
ORO	Oil Red O
PBMC	Peripheral blood mononuclear cells
PCR	Polymerase chain reaction
PD	Parkinson disease
PEPCK1	Phosphoenolpyruvate carboxykinase
PFK	Phosphofructokinase
PGC-1 α	PPAR-γ coactivator- 1 alpha
PI3K	phosphatidylinositol-4,5-bisphosphate 3-kinase
PKA	cAMP dependent protein kinase
PKB/C	Protein kinase B/C
PMSF	Phenylmethylsulfonylfluoride
POA	Preoptic area
POMC	Pro-opiomelanocortin
PPAR	Peroxisome proliferator-activated receptor
PTM	Post-translational modification
PVH	Paraventricular nucleus
rDNA	Ribosomal deoxyribonucleic acid
RIPA	Radioimmunoprecipitation assay
RNA	Ribonucleic acid

RT	Real time
SAR	Structure-activity relationships
SCD	Stearoyl-CoA desaturase
SDS	Sodium dodecyl sulphate
SDS–PAGE	Sulphate-polyacrylamide gel electrophoresis
SEM	Standard error of the mean
Ser	Serine
SFA	Saturated fatty acid
SIRT	Sirtuin
Sir2	Silent information regulator 2
SirReals	Sirtuin rearranging ligands
SNS	Sympathetic nervous system
SREBP	Sterol regulatory element-binding protein
TCA	Citric acid cycle
TG	Triglycerides
TLR4	Toll-like receptor 4
TNF-α	Tumor necrosis factor alpha
Tyr	Tyrosine
UCP1	Uncoupling protein 1
VLDL	Very low-density lipoproteins
VMH	Ventromedial nucleus
α-MSH	Alpha-melanocyte-stimulating hormone

Abstract

Metabolic disorders, such as obesity and type 2 diabetes, are associated with abnormal and excessive fat accumulation, increased body weight gain, hyperglycemia, hyperinsulinemia, glucose intolerance and insulin resistance. The prevalence of these diseases is growing at an alarming rate, which requires the development of novel therapeutic approaches to prevent or counteract their progression. The sirtuin family (SIRT1-7) of NAD^+-dependent protein deacetylases have gained increased recognition as crucial regulators of several cellular processes, such as stress response, aging, and also metabolic regulation. SIRT2, one of the least understood sirtuin isoforms, has been studied, mostly in *in vitro* models, as a key player in various metabolic processes, such as adipogenesis, fatty acid oxidation and insulin sensitivity. However, the role of SIRT2 in the development of obesity and related abnormalities has not been explored in an *in vivo* mouse model. Therefore, our group performed a thorough metabolic characterization of SIRT2-knockout (SIRT2-KO) mice fed a regular chow diet (CD) or a high-fat diet (HFD) for 4 weeks. Despite apparently normal under CD feeding, SIRT2-KO mice showed increased body weight gain, enlarged epididymal white adipose tissue (eWAT) mass, hypertriglyceridemia, hyperglycemia and insulin resistance when fed a HFD. Taking into account these results, the present study aimed to explore, at the histological and molecular level, the underlying mechanisms that could explain the exacerbated metabolic dysfunction in SIRT2-KO mice fed a HFD. Despite being insulin resistant, SIRT2-KO mice exhibited normal insulin signaling pathway activation when fed a HFD. Moreover, these animals revealed adipocyte hypertrophy in eWAT and exacerbated lipid accumulation in the liver. This hepatic overload was consistent with upregulated gene expression of lipogenic enzymes. Our findings reveal that SIRT2 plays a crucial role in the liver and adipose tissue, although further studies are required to fully address SIRT2 metabolic actions. In conclusion, this study provides critical insights into the role of SIRT2 in the pathogenesis of metabolic disorders and suggests that SIRT2 stimulation may be a therapeutic strategy to counteract obesity and associated metabolic complications.

Keywords: Sirtuin 2, high-fat diet, metabolic dysfunction, insulin resistance

Resumo

As doenças metabólicas, como a obesidade e diabetes tipo 2, estão associadas a uma acumulação excessiva e anormal de gordura, maior ganho de peso corporal, hiperglicemia, hiperinsulinemia, intolerância à glucose, e resistência à insulina. A prevalência destas doenças está a aumentar de forma exponencial, o que requer o desenvolvimento de novas abordagens terapêuticas para prevenir ou combater a sua progressão. A família das sirtuínas (SIRT1-7), proteínas com atividade deacetilase dependente de NAD^+, ganhou reconhecimento como reguladora crucial de vários processos celulares, como a resposta ao stresse, envelhecimento, e também regulação metabólica. A SIRT2, uma das isoformas menos estudadas, tem sido investigada, maioritariamente em modelos *in vitro*, como uma proteína-chave em vários processos metabólicos, como a adipogénese, oxidação de ácidos gordos e sensibilidade à insulina. No entanto, o papel da SIRT2 no desenvolvimento da obesidade e complicações associadas à mesma não foi explorado num modelo animal *in vivo.* Deste modo, o nosso grupo realizou uma caracterização metabólica detalhada de murganhos knockout para SIRT2 (SIRT2-KO), alimentados durante 4 semanas com uma dieta normal, ou com uma dieta rica em gordura. Apesar de aparentemente incólumes com a dieta normal, os murganhos SIRT2-KO apresentaram aumento de ganho de peso corporal e do tecido adiposo epididimal, hipertrigliceridemia, hiperglicemia e resistência à insulina quando alimentados com uma dieta rica em gordura. Tendo em conta estes resultados, o presente estudo teve como objetivo explorar, a nível histológico e molecular, os mecanismos subjacentes à disfunção metabólica exacerbada nos murganhos SIRT2-KO. Apesar de serem resistentes à insulina, os murganhos SIRT2-KO apresentaram uma ativação normal da via de sinalização da insulina quando alimentados com uma dieta rica em gordura. Estes animais apresentaram ainda uma hipertrofia dos adipócitos no tecido adiposo epididimal e acumulação exacerbada de lípidos no fígado. Esta sobrecarga hepática de lípidos foi consistente com o aumento da expressão génica de enzimas da lipogénese. Os nossos resultados sugerem que a SIRT2 desempenha um papel crucial no fígado e no tecido adiposo, embora sejam necessários mais estudos para uma compreensão mais detalhada das suas ações metabólicas. Em conclusão, este estudo

contribuiu com conhecimentos cruciais acerca do papel da SIRT2 na patogénese de doenças metabólicas, e sugere que a ativação da SIRT2 pode ser uma estratégia terapêutica para combater a obesidade e suas complicações metabólicas.

Palavras-chave: Sirtuína 2, dieta rica em gordura, disfunção metabólica, resistência à insulina

Chapter I. Introduction

1.1. Metabolic disorders

An unhealthy lifestyle with overnutrition and sedentarism is becoming highly prevalent in many regions of the world. Nutritional needs are met with diets containing high-energy dense foods, that are rich in sugars and fat, and poor in fiber, vitamins and other micronutrients. Concomitantly, physical activity is also low or inexistent [1]. This can lead to an unbalance of the body energetic state and dysregulation of metabolic homeostasis, promoting the development of metabolic disorders, such as obesity and type 2 diabetes [2]. The prevalence of these pathologies is growing at an alarming rate, being difficult to implement effective health treatments. There is, therefore, an urgent need to develop novel therapeutic approaches to prevent or counteract the development of these metabolic disorders [3,4].

1.1.1. Obesity

Obesity has recently been recognized as a chronic disease [5]. This disorder is characterized by an abnormal and excessive fat accumulation, increased body weight and a body-mass index of 30 kg/m^2 or greater [1,6]. This disorder is also defined by adipocyte hypertrophy and enlargement of the visceral white adipose tissue (WAT) mass, strongly associated with human dietary patterns [7]. Besides the alteration of body weight and body composition, the storage and secretion of several molecules by the adipose tissue is also affected. This tissue releases substantial amounts of fatty acids (FA) [8], hormones [9], proinflammatory cytokines [10,11] and other factors, collectively designated as adipokines [9]. Adipose tissue dysregulation promotes the development of obesity-related metabolic diseases. Thus, obesity is considered a major risk factor for the development of insulin resistance and type 2 diabetes [2,12], hypertension and dyslipidemia [13,14], liver pathologies [15], cardiovascular diseases [2,14,16]and cancer [17,18].

Obesity represents a heavy clinical and economic burden both in developed and developing countries [1,3,19]. At the beginning of the 21st century, the approximate number of obese adult population was 937 million, and by 2030 it is estimated to rise to 1.35 billion [3]. Therefore, it is critical to develop safer and more effective health strategies for prevention and treatment of obesity [20].

1.1.2. Type 2 diabetes

Type 2 diabetes is the most prevalent form of *diabetes mellitus*, and is characterized by persistent hyperglycemia, that is, increased levels of blood glucose [21,22]. This chronic disease has been associated to a dysfunction of insulin secretion by pancreatic β-cells in response to glucose [23–25] and resistance to the actions of insulin [8,26,27].

This metabolic disorder has an epidemic profile estimated to rise from 171 million people affected in the beginning of the century to about 400 million affected by 2030 [28,29]. Current treatments for type 2 diabetes are diverse [30,31]. Some of them, such as metformin [32] and thiazolidinediones [33], have several side effects, which increases the necessity to improve existing treatments and develop more effective therapeutic approaches [34]. Prevention of body weight gain and tight glycemic control can reduce the development of diabetes-associated morbidities [35,36]. The overwhelming burden of this disease on health systems can also be decreased, promoting an improvement of population healthspan [2,37].

1.2. Metabolic homeostasis

1.2.1. Energy metabolism

Energy homeostasis is achieved when there is a match between energy consumption and energy expenditure. This balance of food intake and energy expenditure is crucial for survival and is dependent on multiple and complex mechanisms that regulate and maintain body weight. Energy intake relies on feeding behavior, and energy expenditure on physical activity, basal metabolism and adaptive thermogenesis [38]. When energy intake exceeds energy expenditure, there is a positive energy balance, which in a chronic manner, promotes obesity and obesity-related disorders. In contrary, negative energy balance occurs when energy expenditure exceeds energy intake, which in long term promotes weight disorders, such as anorexia [39]. The central nervous system (CNS) is essential for energy balance regulation and maintenance. CNS receives and integrates whole-body hormonal and nutritional signals in several brain structures, promoting adaptive body weight changes [40] (Figure 1).

Food intake

Food intake (FI) is regulated by a multi-structured small area in the brain, the hypothalamus, which integrates peripheral metabolic cues and triggers adaptive responses to whole-body signals [40]. One mechanism by which the hypothalamus regulates energy homeostasis is by controlling food intake [41]. This brain structure is organized by several interconnected nuclei. The arcuate nucleus (ARC) is close to the median eminence (ME), a region characterized by an extensive vasculature and weakened blood-brain-barrier (BBB) (Figure 1). Thus, ARC is capable to primarily sense nutritional and hormonal signals derived from the periphery [42,43]. The regulation of FI by the ARC is related to the activity of two distinct neuronal populations: Orexigenic neurons co-express neuropeptide Y (NPY) and agouti-related protein (AgRP) [44], and anorexigenic neurons co-produce pro-opiomelanocortin (POMC) and cocaine- and amphetamine-regulated transcript (CART). These neurons have been shown to regulate feeding behavior and energy homeostasis [45,46], and are key targets of peripheral hormones, such as insulin, ghrelin and leptin [40,44,47]. POMC neurons are known to project to paraventricular nucleus (PVH), lateral hypothalamic area (LHA), ventromedial nucleus (VMH), and to other brain regions, such as brainstem and spinal cord [48].

PVH nuclei contains neurons that are involved in the regulation of peripheral metabolism through mediated production of neuropeptides and sympathetic innervation. Dorsomedial hypothalamic nuclei (DMH) contains leptin receptors and ARC-NPY/AgRP neurons projections. LHA, defined as the feeding center, has a large and diffuse population of neurons that express melanin concentrating hormone (MCH) and orexins. When stimulated, this hypothalamic structure increases FI, and when lesioned attenuates feeding and causes weight loss [49]. VMH is considered to be the primary satiety center in the hypothalamus due to its role in the regulation of energy homeostasis by controlling FI [50]. Stimulation of this nuclei suppresses feeding, while a lesion in this structure causes hyperphagia and weight gain [51,52] (Figure 1). Brain stem acts as a connector of peripheral metabolism and hypothalamic regulation of food intake. Nucleus tractus solitarius (NTS) receives signals from the gastro-intestinal tract (GIT) through the vagus nerve, which activation mediates peripheral effects on the brain and behavior, establishing the gut-brain axis [53,54].

Energy expenditure

Besides regulating FI, hypothalamus is responsible for the control of neuroendocrine responses [55], temperature [56], circadian rhythm [57], and energy expenditure (EE) in response to nutritional and hormonal signals [58]. EE encompasses basal metabolic rate (BMR), the level of physical activity and the presence of an adaptive thermogenesis for each individual [59,60]. Thus, the dietary content is able to induce thermogenesis. Diets with a great composition of protein and alcohol induce higher values of EE, whereas diets with a great amount of fat promote lower EE levels [61,62].

Thermogenesis occurs mainly in brown adipose tissue (BAT) upon exposure to cold, and also HFD feeding, which causes dissipation of energy as heat to regulate body weight [63,64] (Figure 1). WAT cells can be converted into BAT cells, under cold exposure or physical exercise circumstances, through a process called WAT browning, which increases EE. In WAT, there are also the so-called beige cells that can burn fat and dissipate energy as heat. However, the number of these cells is decreased in obesity [65]. Insulin and leptin signaling input in POMC neurons also mediate WAT browning and beige adipocytes development. Thermogenesis activates POMC neurons and promotes body weight loss, being essential as a defence against hypothermia and obesity development [65].

Besides being composed by lipid storage cells rich in mitochondria, BAT is innervated by the sympathetic nervous system (SNS). Upon a SNS-derived noradrenaline (NA) stimulation, β-adrenergic receptors (β-AR) are activated, leading to the activity of uncoupling protein 1 (UCP1) through lipolysis [64,66]. UCP1 can be found in the inner mitochondrial membrane and causes the uncoupling of mitochondrial respiratory chain, promoting the release of energy, commonly used to produce ATP, in the form of heat [38,67]. Hypothalamic nuclei, such as preoptic area (POA), VMH, DMH and ARC, can regulate thermogenesis through SNS actions [64,68].

Taken together, hypothalamic sensing and integration of peripheral metabolic signals, and subsequent triggering of responses, are crucial for FI and EE regulation. This, therefore, leads to a balanced energy homeostasis and healthy body weight.

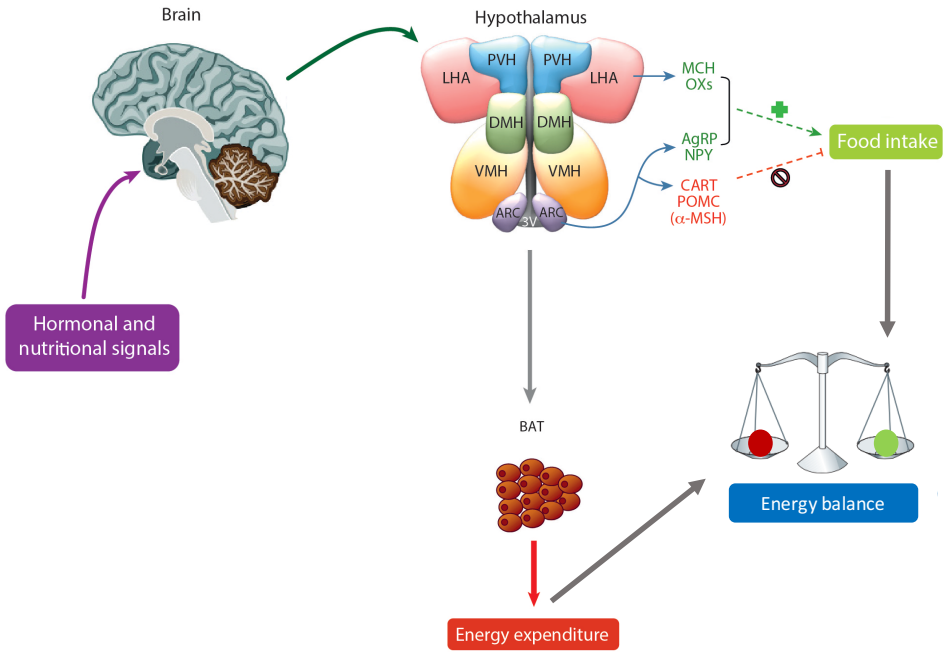

Figure 1. Hypothalamic regulation of energy homeostasis. Differences in energy availability, energy stores, and nutritional demands cause hypothalamic regulation of FI and trigger of functional changes in several tissues, such as BAT, controlling EE. This promotes a balanced energy system and body weight gain. Adapted from López et al (2013) and Seely et al (2013).

1.2.2. Glucose metabolism

Under fed or fasting conditions, blood glucose levels in healthy individuals remain within a narrow interval of concentrations, which characterizes a balanced glucose metabolism. This balance results from the interplay between several metabolic mechanisms, such as intestinal glucose uptake, hepatic glucose production (HGP), and also the uptake and metabolism of blood glucose by various peripheral tissues (Figure 2). These metabolic processes are controlled by hormones, particularly insulin and glucagon [69]. Some of insulin actions encompass the promotion of glucose uptake in insulin-sensitive tissues, glycolysis, storage of glucose as glycogen, and also suppression of HGP in the fed state [70]. Contrarily, glucagon counteracts the effects of insulin and promotes glycogenolysis and gluconeogenesis in a hypoglycemic state [71]. Energy production and substrate storage are the main results of glucose metabolism.

Glucose uptake

Glucose metabolism starts by intestinal absorption to bloodstream of glucose derived from diet or from endogenous production (e.g liver and kidney). Glucose transporters (GLUT) are subsequently crucial to facilitate the entry of glucose into cells. Several GLUT family members were identified, with GLUT4 involved in insulin-dependent glucose uptake by peripheral tissues, such as skeletal muscle and adipose tissue. In contrast, GLUT1, 2 and 3 act as insulin-independent glucose transporters, and are present in several tissues, such as the liver and brain [72]. Intracellular glucose can be stored in the form of glycogen, oxidized into pyruvate or converted into relevant metabolites, such as acetyl-CoA for FA production [73].

Glycogen synthesis and glycogenolysis

In fed state, glucose undergoes phosphorylation by glucokinase (GCK), which is activated in the presence of elevated blood glucose levels. This promotes glycogen synthase (GS) expression and glycogen synthesis. During fasting, the opposite mechanism occurs, with glycogen converted into glucose – glycogenolysis - under mediation of glycogen phosphorylase (GP) (Figure 2). GCK activity also increases glucose-6-phosphate (G6P) production. G6P stimulates glycogen synthesis by inhibition of GP and activation of GS [74]. Insulin production in fed state promotes glycogen synthesis by decreasing blood glucose levels through inhibitory post-translational modifications (PTMs) of GP and suppression of glycogenolysis [75]. This hormone also stimulates the expression of GCK and production of G6P by activation of its signaling pathway intermediates, such as Akt/Protein kinase B (PKB) and glycogen synthase kinase 3 beta (GSK3 β) [74]. Under fasting, insulin is counteracted by glucagon, which causes GS inhibition and GP activation [75].

Glycogen synthesis and glycogenolysis are crucial processes in liver and skeletal muscle for energy release and energy storage, respectively. Liver exports glucose obtained from stored glycogen to maintain blood glucose levels, and skeletal muscle uses glycogen to produce energy for contraction [73].

Glycolysis

Glucose is one of the main energy fuels of cells in fed state and is converted into pyruvate through mediation of several enzymes. Glycolytic flux is controlled by GCK [74], and

also by other enzymes, such as phosphofructokinase (PFK) isoenzymes that give rise to fructose-1,6-bisphosphate (FBP) [76,77] (Figure 2). The activity of these enzymes increases in the postprandial period [78].

Glucose also activates the transcription factor carbohydrate-responsive element-binding protein (ChREBP), which promotes glycolysis by binding and activating glycolytic enzymes [79]. Insulin stimulates glycolytic enzymes and increases glycolysis rate and pyruvate consumption [80]. Thus, pyruvate can be further oxidized in the citric acid cycle (TCA) under aerobic conditions and promote adenosine triphosphate (ATP) production in mitochondrial respiratory chain. Pyruvate can also be used to synthesize lipids and amino acids or for glucose production [81].

Gluconeogenesis

Gluconeogenesis is a metabolic pathway that leads to glucose production from nonsugar precursors, such as lactate and pyruvate. This process occurs mainly in the liver, which is tightly regulated by insulin and other relevant metabolic hormones. Under conditions of caloric restriction (CR) and fasting, the liver provides tissues with glucose to maintain blood glucose levels within normal values. In an early phase of fasting, liver mobilizes glucose trough glycogenolysis, and at a late phase of fasting, switches to gluconeogenesis [82]. Gluconeogenic substrates are either formed in the liver or obtained through circulation from other tissues. Lactate is transformed into pyruvate, which enters mitochondria and is metabolized to form oxaloacetate that is converted into phosphoenolpyruvate in the cytoplasm by a gluconeogenic key regulatory enzyme, phosphoenolpyruvate carboxykinase (PEPCK1) [76] (Figure 2). Hepatic transcription factors, such as forkhead box protein O1 (FOXO1) and peroxisome proliferator-activated receptor (PPAR)-γ coactivator (PGC)-1α, can also enhance the transcription of gluconeogenic enzymes genes, such as G6P, FBP and PEPCK1 [82].

A continuous supply of glucose is essential for a balanced metabolic homeostasis, particularly for CNS, which is unable to store glucose, or use other molecules as an energy source [83]. The hypothalamus contains glucose-sensing neurons that are activated upon changes in extracellular glucose concentrations [84,85]. These neurons are stimulated by increased levels of blood glucose [86] and inhibited by a hypoglycemic state [87].

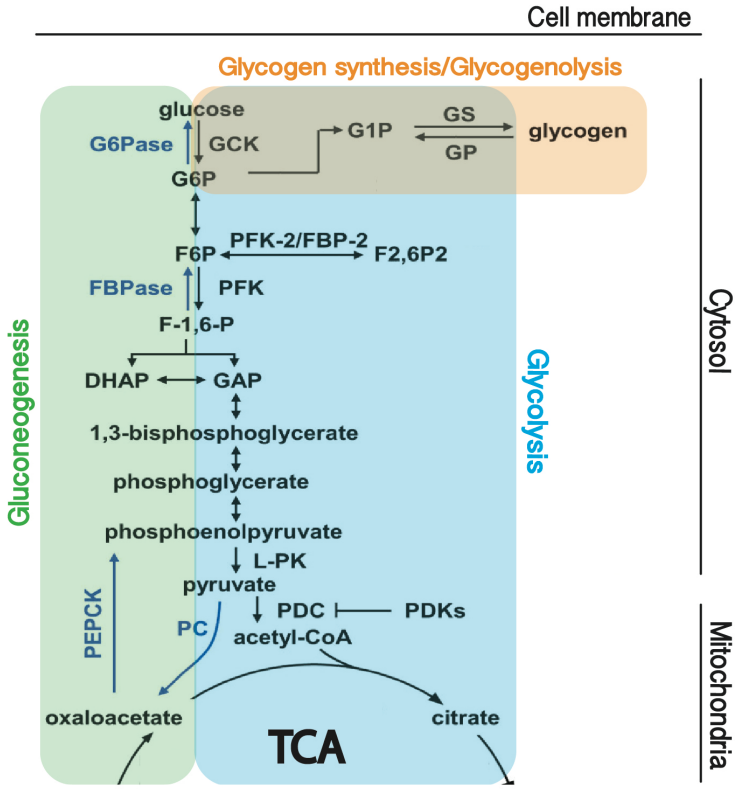

Figure 2. Glucose metabolism. In fed state, glucose enters into cells, and is transformed by several enzymes for energy production and glycogen storage. Under fasting conditions, glycogen is converted into glucose for energy usage, and glucose is also produced. All these metabolic pathways promote the maintenance of blood glucose levels within normal values in different nutritional status. Gluconeogenesis is defined in green; glycolysis/glycogenolysis in orange; and glycolysis in blue. Adapted from Rui (2014).

1.2.1. Lipid metabolism

Lipid metabolism integrates various cellular processes related to the uptake, oxidation, synthesis, and storage of lipids (Figure 3). These mechanisms demand metabolic balance, particularly under prolonged fasting or physical exercise. Several hormones underlie the regulation of lipid metabolic processes [88]. Insulin, besides participating in glucose metabolism, promotes triglycerides (TG) synthesis in the liver and its storage in WAT under nutritional abundance [89]. Contrarily, glucagon enhances lipolysis in WAT and fatty acid oxidation (FAO) in liver and other tissues under fasting conditions [90].

The liver is a key regulatory organ in lipid metabolism. This organ is able to use glucose and/or FA as metabolic fuels. Under a fed state, glucose is abundant and

glycolysis is the main source of energy, with glycolytic intermediates used to synthesize lipids, amino acids, and other substrates. However, in a fasted state, with lower glucose levels, the liver turns to FAO, and FA become other main fuel of energy production [76].

Adipogenesis

Another crucial organ in lipid metabolism is the adipose tissue [9,91]. Similar to the liver, adipose tissue adjusts its activities in accordance with energy availability. This tissue modulates adipocyte differentiation in order to store excess energy in the form of TG. Mature adipocytes differentiate from undifferentiated preadipocytes. Adipose tissue enlargement can occur by two mechanisms: through an increase in adipocyte size – hypertrophy – and/or an increase in number – hyperplasia. Hyperplastic growth happens in early stages of adipose tissue development, whereas hypertrophy develops after hyperplasia to support excess fat storage. Fat mass increase may lead to the development of obesity-associated metabolic disorders [92,93].

Adipogenesis is regulated by several transcription factors, such as PPARγ [94] and FOXO1. FOXO1 acts in the early phase of adipogenesis by suppressing the differentiation of preadipocytes. This protein binds PPARγ promoter gene, and inhibits its transcription and promotion of adipocyte differentiation [95]. Several proteins regulate FOXO1 activity, such as insulin, which promotes its phosphorylation and activity inhibition by nuclear exclusion [96].

Lipogenesis

Lipogenesis, which is characterized by *de novo* FA synthesis, occurs when carbohydrates levels are high or when insulin levels are increased. Thus, this process is enhanced when there is an excess of energy intake, which overcomes EE values. Carbohydrates transformation into FA and storage as TG requires a set of organized enzymatic reactions [76]. Glucose conversion into pyruvate provides a metabolic source for lipogenesis, which connects glycolysis to lipogenesis. Pyruvate is imported in mitochondria and transformed into acetyl-CoA, which is converted into citrate by citrate synthase [97]. Citrate is translocated to the cytosol and brokedown into acetyl-CoA and oxaloacetate by ATP-citrate lyase (ACLY). Acetyl-CoA performs as a building block for *de novo* lipogenesis, and once in the cytosol, is carboxylated by acetyl-CoA carboxylase (ACC) to form malonyl-

CoA that is used by fatty acid synthase (FasN) to synthesize palmitic acid, a common saturated fatty acid (SFA) (Figure 3). Palmitic acid can suffer elongation to give rise to long chain fatty acids (LCFAs), which are desaturated by stearoyl-CoA desaturase (SCDs), to form mono and poly-unsaturated LCFAs. SCD1 is responsible for synthesis of monounsaturated LCFAs and has been reported to be intrinsically associated to the development of obesity and related complications. SCD1 ablation was previously shown to protect against high carbohydrate diet-induced obesity and hepatic steatosis [98].

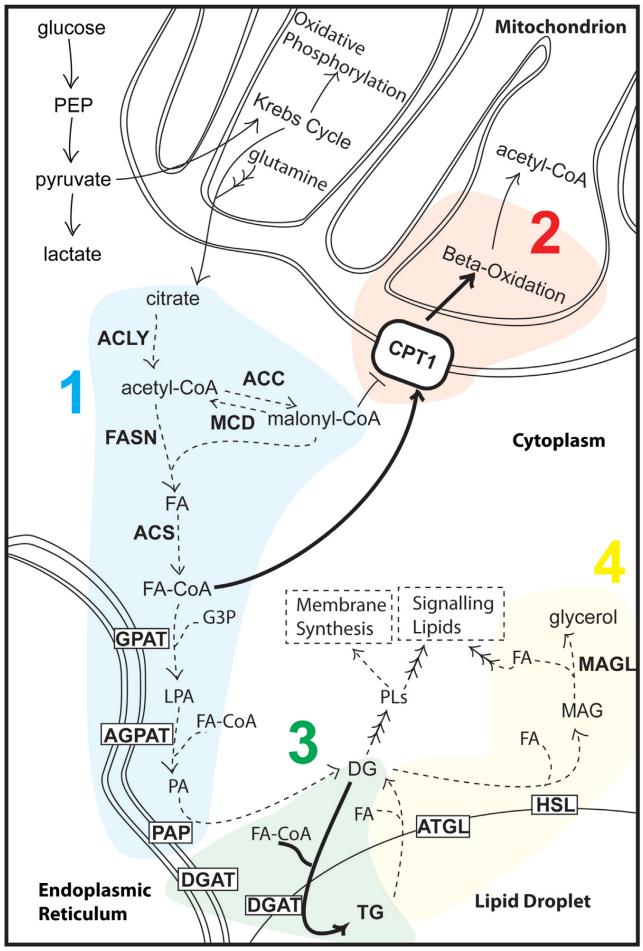

Figure 3. Lipid metabolism. In fed state, lipids are formed through lipogenesis, and are stored in lipid droplets. Under fasting conditions, lipids suffer lipolysis and FAO to be used as an energy source. 1 – *De novo* lipogenesis in blue; 2 – FAO in red; 3 – Lipid storage in green; 4 – Lipolysis in yellow. Adapted from Currie et al (2013).

Lipogenesis is also driven by several transcription factors and cofactors, such as ChREBP, PPAR proteins and sterol regulatory element-binding protein (SREBP), which

regulate the expression of lipogenic genes. SREBP-1c is a strong regulator of lipogenesis in the liver. This protein is involved in TG synthesis by promoting the expression of ACC, FasN and SCD1 [99]. Insulin enhances hepatic lipogenesis in conditions of nutritional abundance through its signaling intermediates, such as Akt/PKB [100]. Thus, activation of insulin signaling was shown to control SREBP-1c expression and consequently lipogenic proteins expression [89].

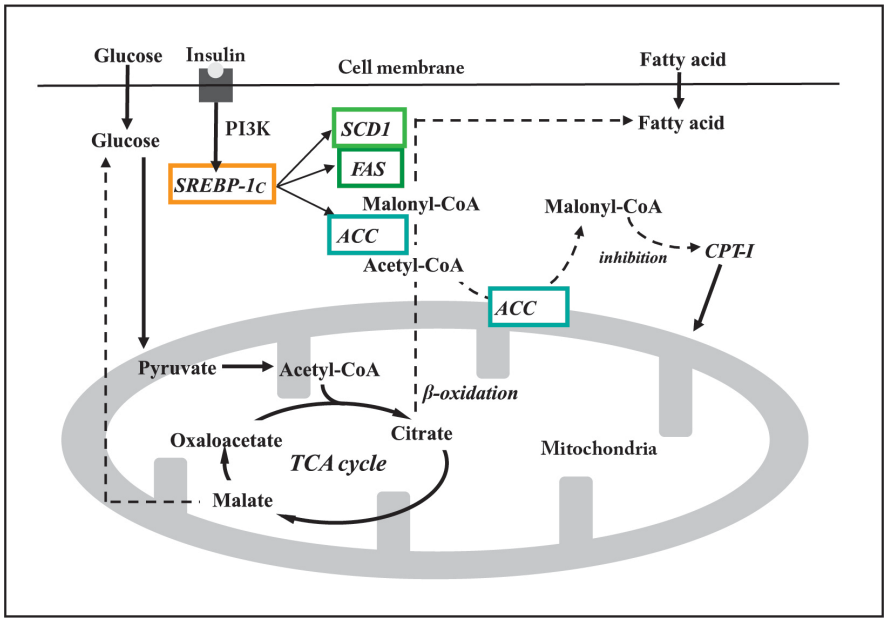

Figure 4. SREBP-1c target genes and the regulation of lipid homeostasis. SREBP-1c promotes the expression of lipogenic proteins, such as ACC, FasN (FAS) and SCD1. This protein action is controlled by insulin signaling, deeply involved in lipogenesis regulation. Adapted from Murase et al (2010).

Lipid storage and Lipolysis

SFAs are poorly used as energy fuel, and can be processed into TG and other lipid metabolites, such as diacylglycerol (DAG) and ceramides, and stored within cells [101,102] (Figure 3). TG can be stored in the so-called lipid droplets (LDs), and under starvation or exercise, can suffer lipolysis. Lipolysis consists in TG breakdown into glycerol and FA, which are consequently mobilized to other organs for use as energy substrates [103]. Impairment of lipolysis results in excess storage of TG, adipocyte hypertrophy and obesity [104].

In adipose tissue, lipolysis is strictly regulated by two crucial enzymes, adipose

triglyceride lipase (ATGL) and hormone-sensitive lipase (HSL) [105]. ATGL is considered the rate-limiting lipolytic enzyme, and catalyzes the initial step of lipolytic pathway, by converting TG into DAG. ATGL expression has been reported to be controlled by FOXO1 and PPARγ transcription factors. Insulin inhibits lipolysis by suppressing FOXO1 activity, which consequently reduces ATGL expression. Loss of ATGL has been reported to reduce lipolysis and promote increased adipose tissue weight gain [106]. HSL is phosphorylated by cAMP dependent protein kinase (PKA) that promotes its activation and translocation from cytosol to LDs. HSL converts DAG into monoacylglycerol (MAG) and glycerol, which are consequently transported to bloodstream and uptake by other organs [105]. Insulin anti-lipolytic action encompasses inhibition of HSL phosphorylation via lowered cAMP levels. Impairment in insulin action consequently increases HSL phosphorylation levels and lipolytic rate [107].

Fatty acid oxidation

FAO implicates several catabolic steps and occurs mainly in the mitochondrial matrix. This process consumes significant amounts of oxygen, affecting EE levels. In late stages of fasting, the increase in FA mobilization and FAO is critical to supply cells with energy. Contrarily, in fed state this process occurs at lower levels [76].

LCFAs enter the cell through specific transporters, and can be shuttled into mitochondrial matrix by the carnitine palmitoyltranferase system. Carnitine palmitoyltranferase 1 (CPT-1) enzyme is located at the outer membrane of mitochondria and is responsible for the transport of LCFAs from cytosol to mitochondrial matrix to be oxidized (Figure 3). CPT-1 is a rate-limiting step in FAO, and its activity is inhibited by malonyl-CoA [108]. The acyl-CoA dehydrogenases (ACAD), in particular the medium chain acyl-CoA dehydrogenase (MCAD) and the long chain acyl-CoA dehydrogenase (LCAD), are key players in FAO. These enzymes are regulated trough PTMs and their loss causes hepatic steatosis and insulin resistance [109]. An incomplete FAO can lead to the formation and increase of cellular FA metabolites (eg. ceramides and DAG) [110].

PPARα is a key regulator and promoter of FA β-oxidation, and is activated by LCFAs. This protein is highly expressed in the liver, and PPARα deletion was shown to decrease FAO in fasted state and potentiate fasting-induced hepatic steatosis [111,112]. Several PPARα coactivators have been discovered and studied in the liver, particularly

PGC-1α [113,114], which is phosphorylated by Akt/PKB and inhibited to promote FAO [115].

1.3. Metabolic dysregulation

1.3.1. Insulin resistance

Insulin resistance is a hallmark of metabolic disorders, such as obesity and type 2 diabetes, and has been shown to occur in various tissues, such as the pancreas, liver, adipose tissue, skeletal muscle, and also the brain [23,24,26]. In humans, insulin resistance is a complex polygenic and heterogeneous disease, both defined by a state of reduced insulin secretion by the pancreatic β-cells and a state of impaired insulin signaling in target tissues [116,117].

Insulin signaling starts by the binding of insulin to its receptor (IR), which causes the activation of the tyrosine kinase domain of the IR, and consequently the phosphorylation of insulin receptor substrate proteins (IRS). IRS proteins are the first critical node of insulin signaling network, and are essential for the maintenance of Akt/PKB pathway activity through phosphatidylinositol-4,5-bisphosphate 3-kinase (PI3K) kinase activation. IRS proteins are also responsible for the activation of the other insulin signaling branch, the Ras-mitogen-activated protein kinase (MAPK) pathway, responsible for cell growth and differentiation [118]. PI3K and Akt/PKB are also essential protein nodes in the insulin signaling cascade, with Akt activation promoting the stimulation of downstream proteins that are responsible for several cellular mechanisms, such as the promotion of glycogen synthesis (GSK3β), suppression of gluconeogenesis (FOXO1) and glucose uptake (GLUT4) [27,119,120]. Diets containing high-density foods have long been related to insulin resistance onset. HFD feeding was proved to have a critical role in promoting this disorder [121,122]. In previous studies, SFAs and trans-fatty acids were shown to block the PI3K-Akt/PKB pathway, and to disrupt the responses to insulin action [123]. FAs metabolites, particularly palmitate and stearate products, were also reported to promote the inhibition of IRS and PI3K-Akt/PKB activation, compromising insulin signaling [123–126]. Consequently, glucose and insulin levels increase, glycogen synthesis decrease, HGP decrease, and lipogenesis is suppressed [126–128].

In a prediabetic state, pancreatic β-cells secrete increased amounts of insulin to maintain normal glucose levels in insulin-resistant tissues (Figure 5). This process is

defined as compensatory hyperinsulinemia, and is present in obese and type 2 diabetic patients. In long-term, compensatory hyperinsulinemia leads to the exhaustion of pancreatic β-cells and impairment of glucose metabolism, promoting the development and progression of type 2 diabetes [129].

There is currently some controversy regarding the starting point of insulin resistance. Some studies indicate that central insulin resistance, particularly in hypothalamus, may be the primary defect for the development of obesity and type 2 diabetes [130,131]. Others, report the skeletal muscle as the initiating point for insulin resistance [132]. Liver [133] and adipose tissue [134] were also studied as metabolic organs predominantly affected by insulin resistance. Furthermore, a previous study showed that insulin resistance occurs in adipose tissue and liver before skeletal muscle [135].

Overall, insulin resistance is a widespread disorder caused by various insults, including dyslipidemia and inflammation.

1.3.2. Lipotoxicity

Chronic overnutrition leads to a positive energy balance, promoting hyperglycemia and hyperinsulinemia, but also the saturation of adipose tissue fat storage capacity. Under these conditions, adipocytes suffer hypertrophy and/or hyperplasia [136], and in long-term, fat storage limit is reached in adipose tissue. The excess of fat is consequently released into the bloodstream – dyslipidemia - and taken up by peripheral tissues, such as the liver and skeletal muscle. These tissues are not able to safely store an excess of lipids. This ectopic lipid accumulation – lipotoxicity - promotes metabolic dysfunction of tissues, which leads to development of insulin resistance and associated chronic diseases [137] (Figure 5).

Lipotoxicity in the pancreas may cause a decrease in pancreatic cell mass, leading to impaired insulin secretion and the development of diabetes [138]. Skeletal muscle becomes resistant to insulin-stimulated glucose uptake [139]. In the liver, lipotoxicity leads to hepatic steatosis (NAFLD) [140] and steatohepatitis (NASH) [141], causing hepatic dysregulation. Ectopic lipid accumulation is also known to promote inflammation and ultimately cell apoptosis [110].

Levels of dietary fat and FA composition have a crucial role in the modulation of lipidemia and also insulin resistance development in several tissues. In previous studies, it was shown that 6 weeks of fat-rich or cholesterol-rich diets can cause hyperlipidemia [142],

and also reported that HFD feeding decreases very low-density lipoproteins (VLDL) secretion in the liver, which inhibits TG transport out of the cells and promotes hepatic steatosis and insulin resistance development [143]. There is a negative correlation between lipid content and insulin action, and is yet to be fully understood if lipid metabolism dysregulation is a cause or result of insulin resistance development.

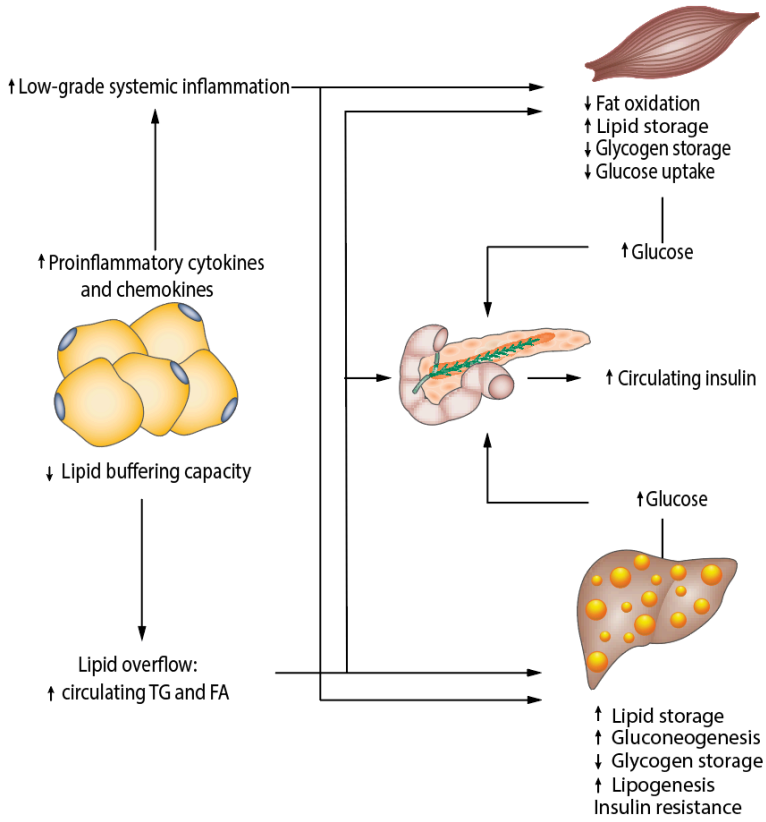

Figure 5. Metabolic dysfunction induced by interorgan crosstalk. Under a positive energy balance, adipose tissue can reach the limit to store fat, which results in increased release of lipids into blood flow. Lipids are mobilized to peripheral tissues, such as the pancreas, liver and skeletal muscle, causing ectopic lipid accumulation. Adipose tissue also increases the secretion and release of proinflammatory cytokines and chemokines, which contribute to peripheral tissues inflammation. All of these processes promote metabolic dysregulation and development of insulin resistance. Adapted from Canfora et al (2015).

1.3.3. Inflammation

Inflammation is a complex biological response that can be triggered by different insults, such as HFD feeding. This dietary pattern has been reported to induce inflammation in the liver, adipose tissue, skeletal muscle, and also the brain [144]. Inflammation and metabolic regulation are mechanisms functionally dependent on each other. When

dysregulated, inflammation can promote the development of metabolic disorders, such as obesity and type 2 diabetes, which have been defined as states of chronic low grade inflammation [145,146].

SFAs are tightly associated to the inflammatory mechanism. FA-increased intake in HFD feeding induces the activation of toll-like receptor 4 (TLR4) [147,148]. Consequently, TLR4 mediates nuclear factor kappa B (NF-κB) activation [149]. In the liver, NF-κB-activated pathway was reported to crosstalk and inhibit several steps in insulin signaling pathway, promoting hepatic insulin resistance [150]. Intracellular accumulation of palmitate and activation of protein kinase C (PKC) were also shown to activate NF-κB pathway and impair insulin sensitivity [133].

Under overnutrition, the adipose tissue releases chemokines and cytokines to report the feeding status to other organs [151]. Adipocytes from obese subjects express increased levels of pro-inflammatory cytokines, such as interleukin-6 (IL-6) and tumor necrosis factor alpha (TNF-α) [152] (Figure 5). TNF-α is highly expressed in WAT and related to proliferation and differentiation of cells [110]. This cytokine has been shown to impair IR activation by supressing its tyrosine kinase activity. Subsequently, tyrosine phosphorylation of IRS-1 is impaired, which compromises insulin action [153,154]. IL-6 is produced by T cells and macrophages, and its levels have also been positively correlated with both obesity and insulin resistance [155]. Both TNF-α and IL-6 lead to the activation of c-Jun amino-terminal kinase (JNK) and the IκB kinase-β (IKK-β) by classical receptor-mediated processes. These kinases induce the expression of inflammatory genes and NF-κB activity, which can promote insulin resistance onset [12,156].

1.4. Sirtuin family

1.4.1. Yeast Sir2

Silent information regulator 2 (Sir2) is the founding member of the sirtuin family, and was discovered in yeast *Saccharomyces cerevisiae* [157]. This protein was first defined as a genetic silencing factor [158,159], and later proved to extend lifespan in yeast by reducing the number of extrachromosomal ribosomal deoxyribonucleic acid (rDNA) [160]. Sir2 is a nicotinamide adenine dinucleotide $(NAD)^+$-dependent histone deacetylase, and targets

histones and non-histone proteins [161]. This protein was also shown to increase longevity in nematode *Caenorhabditis elegans* [162,163], fruit fly *Drosophila melanogaster* [164], and to be conserved in mammals [165].

1.4.2. Mammalian sirtuins

Sir2 homologs were subsequently identified in mammals and termed sirtuins. These evolutionary conserved proteins have also been studied in lifespan extension [194]. Although recent studies have questioned the role of mammalian sirtuins in lifespan extension [168], the current knowledge is that sirtuins may play an important role in health maintenance and stress responses, instead of acting as longevity determinants [169]. Thus, this family of proteins has been studied as metabolic [170] and stress [171] sensors, and have also been involved in several age-related diseases, such as type 2 diabetes [172], cancer [173], cardiovascular [174], inflammatory [175] and neurodegenerative diseases [176].

1.4.2.1. Isoforms

Mammalian sirtuins are composed by seven isoforms (SIRT1-7), of which SIRT1 is the closest homolog to Sir2. Sirtuins are the class III histone deacetylase family, and are characterized by a conserved NAD^+-binding site and catalytic core domain [167,177]. These enzymes deacetylase activity requires NAD^+ as a cofactor, with consequent formation of nicotinamide (NAM) (Figure 6). Sirtuins were reported to be inhibited by NAM in a non-competitive manner with NAD^+. NAM binds closely to NAD^+-binding site, and is essential to NAD^+ regeneration [178].

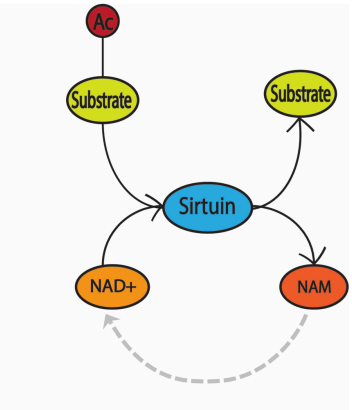

Figure 6. NAD^+-dependent deacetylase activity of sirtuins. These enzymes remove the acyl groups (Ac) from proteins substrates and cleave the cofactor NAD^+ to NAM.

Sirtuin isoforms display ubiquitous expression. These proteins are expressed in several peripheral tissues, such as the liver, kidney, adipose tissue and skeletal muscle, and also in several brain structures. Sirtuins expression levels and activity are strictly dependent on NAD^+ levels. The cofactor levels change due to physiological fluctuations of the cellular energetic and redox state. High energy demands, such as CR, fasting and physical activity, increase NAD^+ levels, which enhances sirtuins activation. Low energy demands, such as obesity, HFD feeding and stress, reduce NAD^+ levels, which decreases sirtuins activity [179,180].

Sirtuins have different subcellular localization, enzymatic activity, and targets (Table 1).These proteins can be divided in four different classes, with SIRT1–3 belonging to class I, SIRT4 to class II, SIRT5 to class III, and SIRT6 and SIRT7 to class IV [167]. SIRT1 is the most studied of all mammalian sirtuins, being mainly located in the nucleus, but can also be found in the cytosol [181]. SIRT3, 4 and 5 are mitochondrial sirtuins [182], and SIRT6 and 7 can be found in the nucleus and nucleolus, respectively [183]. SIRT2 is the only cytosolic sirtuin, but can also been found in other cellular organelles [184,185]. Only class I sirtuins appear to exhibit strong deacetylase activity in the presence of NAD^+, with SIRT4 and SIRT6 described to function as ADP-ribosyltransferases. SIRT5 was shown to primarily perform NAD^+-dependent dema-lonylase and desuccinylase reactions [167].

Mammalian sirtuins target proteins involved in cell cycle, mitochondrial function, transcription, metabolic and energy homeostasis, proving to be deeply involved in aging-related diseases and metabolic disorders [169].

1.4.2.2. General functions

Nuclear sirtuins (SIRT1, 6, and 7) have a well-documented role in transcriptional regulation, through targeting of transcription factors, cofactors or histones. SIRT1 has been reported as a deacetylase of several transcription factors, such as the tumor suppressor p53 [186,187]. SIRT1 inhibits p53 and promotes tumorigenesis. SIRT1 has also been related to lipid and glucose homeostasis in response to changes in nutrient availability. This sirtuin regulates positively PPARα and promotes the expression of genes that are critical for FAO in the liver [188]. SIRT6 is involved in DNA repair. This protein transfers adenosine diphosphase (ADP)-ribose moieties and deacetylases histones, such as histone (H) 3 lysine 9 and H3 lysine 56 [189]. SIRT6 deficiency was shown to lead to

genomic instability and a progeroid phenotype [190], and also to development of hepatic steatosis [78]. SIRT7 activates ribose ribonucleic acid (RNA) polymerase I transcription (Pol I), which is crucial for cell viability maintenance [191].

Mitochondrial SIRT3, 4 and 5 regulate the activity of enzymes and oxidative stress pathways. SIRT3 has been shown to deacetylate glutamate dehydrogenase (GDH) [192], complex I [193] and acetyl-CoA-synthetase 2 (AceCS2) [194]. This sirtuin is also involved in the regulation of mitochondrial FAO by deacetylating LCAD enzyme [195]. SIRT4 has a ADP-ribosylation activity and inhibits GDH, decreasing amino acid-dependent insulin secretion [196]. SIRT5 has the ability to remove malonyl and succinyl groups from carbamoyl phosphate synthetase 1 (CSP1) [197], and interact with other cellular metabolic protein, such as cytochrome c [192].

Cytosolic SIRT2 has been associated to adipose tissue development and function [177,198]. This protein was initially found to be a tubulin deacetylase [199], and later proved to act on multiple histone and non-histone proteins. SIRT2 has been reported to have a role in the stabilization of the transformed state of cancer cells [200,201] and also in metabolic regulation [202].

Table 1. Sirtuins subcellular localization, activities and targets

Sirtuin	Class	Subcellular localization	Activity	Key Targets
SIRT1	I	Nucleus, cytosol	Deacetylation	>PPAR α, PGC-1α, p53, FOXO, NF- κB, H3K9
SIRT2	I	Cytosol, nucleus	Deacetylation, demyristoylation	α-Tubulin, PGC-1α , PEPCK, FOXO, NF-κB, H4K16, ACLY, Akt e G6P
SIRT3	I	Mitochondria	Deacetylation	AceCS2, SOD2, LCAD, IDH2, FOXO, GDH, complex I
SIRT4	II	Mitochondria	ADP-ribosylation	GDH, MCD, ANT
SIRT5	III	Mitochondria	Deacetylation, demalonylation, desuccinylation,	CPS1, SOD1
SIRT6	IV	Nucleus	Deacetylation, ADP-ribosylation	H3K9, H3K56, HIF1α, PARP1, NF-κB
SIRT7	IV	Nucleolus	Deacetylation	H3K18, Pol I

1.4.2.1. Activity modulation

In recent years, modulation of sirtuins functions has been studied to better understand their roles and possible value as targets for the treatment of various diseases.

Animal genetic manipulation has been one of several approaches for sirtuins modulation. Mice overexpressing sirtuins or sirtuin-deficient mice have been developed and used to clarify the onset and progression of pathological symptoms, and explore potential therapeutic approaches [78,172,203]. Chemical modulation has also been studied, with several natural and synthetic compounds already used for sirtuins activity inhibition [204], such as synthetic AGK2 [205] and AK7 [206], potent and selective inhibitors for SIRT2. There are also robust activators, particularly described for SIRT1, such as the natural molecule found in red wine, resveratrol [207]. Dietary patterns, such as CR has been shown to prevent age- associated diseases, such as diabetes, cardiovascular diseases, and cancer, through sirtuins increased activity [192].

1.5. SIRT2

SIRT2 is one of the least understood of all mammalian sirtuins. Besides cytosolic, this protein can translocate to the nucleus during cell cycle [208]. More recently, SIRT2 was reported in the inner membrane of mitochondria, which loss caused a dysfunction in mitochondrial metabolism [185]. SIRT2 was shown to remove myristoyl groups [209]. This enzyme has been studied as deacetylase of several molecules that are key elements of different cellular mechanisms [210].

1.5.1. Distribution, expression modulation and activity regulation

SIRT2 exhibits a ubiquitous distribution, being expressed in several tissues, such as the brain, skeletal muscle, liver, kidney, and adipose tissue [211,212]. This protein is the most abundant sirtuin in both adipose tissue *in vivo* and adipocytes in culture [213]. SIRT2 is more abundantly expressed in the CNS, particularly in the cortex, striatum, hippocampus, and spinal cord, than in all other tissues [212]. Moreover, is expressed in different CNS cellular types, such as oligodendrocytes, microglia and neurons [212,214].

As all mammalian sirtuins, SIRT2 expression has been reported to be modulated by energy availability. This sirtuin is highly expressed during low-energy status, such as

fasting, or CR, and inhibited during high-energy states, such as HFD feeding or obesity. In previous studies, it was shown that mice subjected to a long-term CR had increased SIRT2 levels in WAT and kidney [211]. A short-term food deprivation was also proved to promote an increase in SIRT2 messenger RNA (mRNA) and protein expression in WAT [216]. In peripheral blood mononuclear cells (PBMC) samples of obese subjects, SIRT2 gene expression levels were proved to be increased after an 8-week hypocaloric diet [217]. Moreover, this protein expression in visceral WAT from obese subjects and HFD-fed mice was shown to be downregulated [7]. There are several transcript variants that result from an alternative splicing of SIRT2 gene, but only two were confirmed to have physiologically relevant protein products, the long variant 1 that encodes a 389-amino acid protein and has a predicted molecular weight of 43 kDa, and short variant 2 that encodes 352-amino acid protein and has a predicted molecular weight of 39 kDa [215].

SIRT2 activity has been proved to be regulated by PTMs. This protein enzymatic activity was reported to be reduced by the phosphorylation of residue serine (Ser) 331 by cyclin proteins, which consequently caused impaired deacetylation of core histones and α-tubulin [218]. SIRT2 was also shown to be acetylated by the lysine acetyltransferase p300 [219]. Pharmacological modulation of SIRT2 activity has also been studied, with sirtuin rearranging ligands (SirReals) molecules shown to be highly selective for human SIRT2, and proved by structure-activity relationships (SAR) analyses to be strongly efficient in modulating SIRT2 activity [220]. SirReal2, the most potent, was reported to promote tubulin hyperacetylation in HeLa cells and dysregulate other proteins when inhibiting SIRT2 [221]. A thiomyristol lysine compound, TM, was recently developed, and showed to be specific to SIRT2. This compound was also proved to have a tumor suppressor effect [222]. Currently, there are no pharmacological SIRT2 activators available. However, treatment with NAD^+ precursors has been reported as a booster of sirtuins activity and potential therapeutic strategy for several diseases [223,224].

1.5.2. General biological actions

Cell cycle and tumorigenesis

SIRT2 was proved to transiently shuttle to the nucleus during the G2/M transition phase of the cell cycle, where associates with chromatin and regulates chromosomal condensation by deacetylation of H4 lysine 16 [184,208] . SIRT2 was also shown to prevent

chromosomal instability by deacetylation of coactivators of anaphase promoting complex (APC/C) [225] and to deacetylate the lysine-668 of mitotic checkpoint BubR1, a protein associated with aging regulation and lifespan extension [226,227].

Regarding tumorigenesis regulation, SIRT2 activity is controversial [228]. SIRT2 was reported to act as a tumor suppressor by deacetylation and activation of p53 [229], and more recently, was shown to cause cancer cells metabolic reprograming towards carcinogenesis suppression [230]. Contrary to these results, in cervical cancer cell lines, SIRT2 levels were shown to continuously increase with cancer progression. This sirtuin was also reported to be increased in neuroblastoma and pancreatic cancer cells, promoting Myc proteins stability and cancer progression [231]. Overexpression of SIRT2 was also associated to enhanced cell mobility and invasiveness of hepatocellular carcinoma cells [232]. Taken together, further studies are required to clarify this contradiction of SIRT2 action and therapeutic potential in cancer.

Neurodegeneration

Several studies in cellular and animal models of neurodegenerative diseases, such as Parkinson's disease (PD) and Huntington's disease (HD), have brought a different perspective of SIRT2 activity [233]. Pharmacological and genetic inhibition of SIRT2 activity was reported to reduce sterol levels through alteration of SREBP-2 activity, which prevented mutant huntingtin (HTT) to increase sterols to toxic levels in CNS cells [234]. Moreover, it was reported in HD mouse models that SIRT2 inhibition by the small molecule AK7 reduced neuronal mutated HTT accumulation, improving symptomatic features of HD [235]. A similar study of SIRT2 inhibition, showed that depression of SIRT2 activity reduces mutated α-synuclein levels and protects dopaminergic neurons from toxicity both in *in vitro* and in *in vivo* PD models [205]. Contrary to these results, other study reported that genetic SIRT2 inhibition has no beneficial effects in neurodegenerative diseases, as HD [236]. Thus, more studies are required to fully understand whether SIRT2 inhibition promotes neuronal protection or if it is only under some conditions.

Inflammation

Several transcriptional factors, such as NF-κB and MAPKs, are able to regulate the expression of genes involved in the inflammatory response mechanism [237]. SIRT2 has

been reported to directly bind and deacetylate NF-κB p65 subunit at lysine 310. Consequently, NF-κB becomes unable to regulate the expression of inflammatory genes [238]. The loss of SIRT2 in microglial cells was shown to cause an increase in microglial activation and a proinflammatory phenotype [214]. Other study reported that SIRT2 deficiency in mice leads to severe colitis by NF-κB hyperacetylation and IκB activation [239]. These results support a protective role of SIRT2 against inflammatory processes that characterize several metabolic disorders.

1.5.3. Metabolic functions

1.5.3.1. Glucose metabolism

Glycolysis and gluconeogenesis

SIRT2 was shown to deacetylate glucokinase regulatory protein (GKRP) and regulate GCK-GKRP pathway. GCK binds GKRP in the nucleus and is inhibited to shuttle to cytoplasm to participate in glycolysis. Consequently, SIRT2 deacetylates GKRP and increases GCK nuclear export and glycolytic activity [240]. SIRT2 was also reported to deacetylate PEPCK1. Acetylation of human PEPCK1 was shown to be increased in response to hyperglycemia, which decreases PEPCK1 stability [241]. In contrast, SIRT2 has been reported to deacetylate and increase PEPCK1 stability under conditions of glucose deprivation [242]. Hepatic gluconeogenesis regulators, such as FOXO1 and PGC1α, have also been proved to be deacetylated by SIRT2 (Figure 7).

Insulin sensitivity

SIRT2 has been shown to interact with and regulate Akt activation in insulin-responsive cells under a normal diet [201,232] (Figure 7). This sirtuin overexpression was reported to increase insulin-induced Akt activation and downstream substrates phosphorylation (eg. GSK3β and p70S6 kinase) in 3T3-L1 preadipocytes and HeLa cells [201]. More recently, SIRT2 overexpression was reported to improve insulin sensitivity in insulin-resistant hepatocytes [243]. Contrarily to these studies, SIRT2 expression was shown to be increased in insulin-resistant C2C12 skeletal muscle cells, and when inhibited pharmacologically or genetically, insulin-induced phosphorylation of Akt and GSK3β was increased [244]. SIRT2 has also been proved to deacetylate TUG protein, which is implicated in GLUT4 cellular trafficking to plasma membrane by trapping GLUT4 storage vesicles in

insulin-unstimulated cells [245]. SIRT2-KO mice presented an increase in TUG acetylation state, which resulted in the accumulation of GLUT4 storage vesicles in unstimulated cells, and increased glucose uptake under insulin stimulation [246].

1.5.3.2. Lipid metabolism

Adipogenesis

Overexpression of SIRT2 inhibits adipocyte differentiation, whereas reducing SIRT2 expression promotes adipogenesis [216]. In 3T3-L1 preadipocytes, SIRT2 was shown to reduce acetylated and phosphorylated levels of FOXO1, which consequently leads to trapping of FOXO1 in the nucleus. FOXO1 represses the transcription of PPARγ gene by binding to gene promoter sites, and inhibits adipocyte differentiation [213]. SIRT2 was also reported to regulate adipogenesis through both modulation of PPARγ activity and enhancement of lipolysis when overexpressed in cultured adipocytes, in the presence or absence of insulin stimulation [200].

Lipogenesis

ACLY has been shown to be deacetylated by SIRT2. In *in vitro* and *in vivo* models under high-glucose conditions, ACLY is acetylated, which promotes protein stability and lipid synthesis [247]. SIRT2-mediated deacetylation of ACLY causes ubiquitination and degradation of this enzyme, and represses lipogenesis. [248] (Figure 7). By contrast, the study of SIRT2 action in cholesterol biosynthesis has brought conflicting results. SIRT2 inhibition has been shown to decrease cholesterol synthesis through SREBP-2 activity regulation, and subsequent gene transcription repression of crucial enzymes in the cholesterol synthesis pathway [234]. However, in SIRT2-KO mice the expression of these enzymes was shown to be unaltered. Neither the loss or pharmacological inhibition of SIRT2 caused an alteration in the expression of cholesterol biosynthesis enzymes [236]. Overall, the role of SIRT2 in lipogenesis requires to be further explored.

Fatty acid oxidation

The role of SIRT2 in FAO remains poorly understood. It has been reported that hypoxia inducible factor-1 alpha (HIF-1α) inhibits FAO, in an SIRT2-dependent manner. HIF-1α inactivation in WAT causes a nuclear accumulation of SIRT2 and subsequent increase

in PGC-1α deacetylation state and FAO (Figure 7). In a state of relative hypoxia induced by obesity, SIRT2 deacetylase activity is repressed, HIF-1α activation promoted, PGC-1α acetylated state increased, and FAO decreased [7].

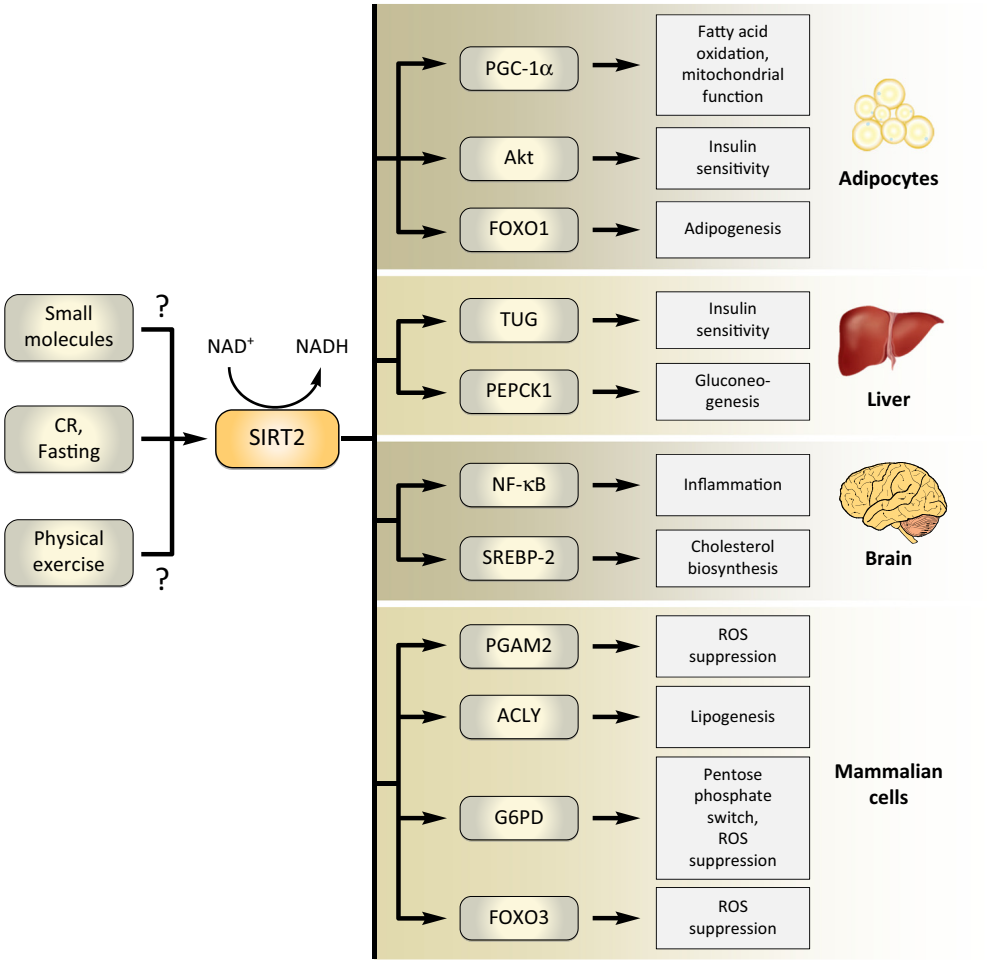

Figure 7. Metabolic actions and targets of SIRT2. Adapted from Gomes et al (2015).

1.5.3.1. Metabolic phenotype of SIRT2-KO mice

SIRT2 metabolic actions have been studied primarily in *in vitro* models [216,244], and few studies have shown relevant insights of SIRT2 role in *in vivo* metabolic homeostasis. Thus, was previously performed a thorough characterization of SIRT2-KO mice metabolic phenotype under regular CD feeding or HFD feeding for 4 weeks (Quatorze, 2016; unpublished data). Several metabolic parameters were measured both in WT control and SIRT2-KO mice.

SIRT2 ablation did not reveal an apparent impact in metabolic regulation of mice

fed a CD, whereas SIRT2 deficiency caused the development of exacerbated metabolic dysfunction in HFD-fed mice (Table 2).

Taken together, the results of this study suggest that SIRT2 may play key metabolic actions under stress inducer HFD conditions.

Table 2. Metabolic phenotype of SIRT2-KO mice compared to WT mice fed either a normal CD or a HFD

Parameters	Metabolic changes in SIRT2 KO mice compared to WT mice	
	CD	HFD
Body weight gain	=	+
Epididymal WAT weight gain	=	+
Food/energy intake	=	+
Blood glucose	=	+
Glucose tolerance	=	=
Insulin resistance	+	++

= - unaltered; + - mild; ++ - exacerbated

1.6. Aim and work plan

SIRT2 has emerged in recent years as a crucial regulator of mammalian metabolism, by targeting several proteins involved in crucial metabolic processes, such as adipogenesis, lipogenesis, gluconeogenesis and insulin sensitivity [210]. As the only cytosolic mammalian sirtuin, and ubiquitously distributed, particularly in metabolic relevant tissues (e.g adipose tissue, liver and skeletal muscle), the modulation of SIRT2 expression and activity may provide important insights into SIRT2 actions in metabolic homeostasis.

Our group previously performed a detailed metabolic characterization of SIRT2-KO mouse, and prompted several questions related to the role of SIRT2 in metabolic regulation. Under HFD feeding, SIRT2-KO mice developed exacerbated metabolic dysfunction, with increased body and adipose tissue weight gain, increased energy intake and serum TG levels and insulin resistance (Quatorze, 2016; unpublished data). Therefore, the overall aim of the present work was to expand the previous research (reviewed above

in the last topic of Chapter I) by studying, at histological and molecular level, the underlying mechanisms that could explain the metabolic phenotype of SIRT2-KO mice fed a HFD. We focused on the role of SIRT2 in the early onset of metabolic disorders (eg. obesity and type 2 diabetes) to identify potential targets to therapeutically counteract the progression of these diseases.

For this purpose, the work plan was divided into several experiments:

- To assess the effect of HFD on SIRT2 expression levels;
- To evaluate insulin signaling activation, particularly the phosphorylation levels of Akt protein, in WT and SIRT2-KO mice;
- To explore morphological alterations in the adipose tissue of WT and SIRT2-KO mice fed a HFD;
- To evaluate lipid accumulation in the liver of WT and SIRT2-KO fed a HFD;
- To assess mRNA levels of genes involved in crucial metabolic pathways under CD and HFD feeding.

Chapter II. Materials and Methods

2.1. Experimental animals and diets

Seven week-old wild-type (WT) C57BL/6 male mice were purchased from Charles River Laboratories. B6.129-Sirt2$^{tm1.1Fwa}$ (SIRT2-KO) male mice were purchased from The Jackson Laboratory (Ref. 012772). SIRT2-KO mice were generated in B6.129 genetic background and backcrossed to C57BL/6 for at least 8 generations to produce homozygous SIRT2$^{-/-}$ mice. A colony of these SIRT2-KO mice was established at the Centre for Neuroscience and Cell Biology (CNC) of the University of Coimbra. WT and SIRT2-KO mice were age- and sex-matched and maintained in a temperature-controlled room with 12h light/12h dark cycles. Animals were housed in groups of 2-5 animals and had free access to food and water. The experiments were carried out in accordance with the European Community Directive (2010/63/EU) and the Portuguese Decree-law 113/2013 for the care and use of laboratory animals, and guided by researchers who received adequate training (FELASA certified course) and certification from Portuguese national authority for animal health (DGAV). SIRT2-KO mice were subjected to a standard CD (4RF21, Mucedola, Italy) until the beginning of the dietary protocol. WT mice were fed the same CD for a 10-day acclimation period. Mice began the 31-day dietary protocol with, on average, 8 weeks of age. During this dietary protocol, mice were fed either a CD or HFD (Table 3). This particular HFD (D12492, Research Diets, US) is the most widely used to induce obesity and metabolic dysfunction and is composed of 60% Kcal from fat and lard- enriched.

Table 3. Standard CD and HFD nutritional composition.

Content			CD	HFD
Proteins			18.5%	20%
Carbohydrates			54%	20%
Fats	Soybean oil		3%	5%
	Lard		-	55%
	of which	Saturated FA	21%	32%
		Unsaturated FA	79%	68%
Energy			2.67	5.24

2.2. Metabolic phenotyping

2.2.1. Body weight and food intake assessment

Food intake and body weight were assessed twice a week during the 31 days of the study (Figure 8). Food was weighed and refilled whenever a minimum weight value was achieved. Mice were weighed and transferred to clean cages with free access to fresh water in each time. Food intake per mouse was calculated dividing food intake by the number of mice in the cage.

2.2.2. Intraperitoneal glucose tolerance test (ipGTT)

ipGTT was performed on day 24 of the dietary protocol (Figure 8). Mice were fasted overnight for 15-16 hours (6 p.m to 9/10 a.m) after being transferred to clean cages without food or faeces. Before starting the experiment, mice were housed individually. Basal blood glucose levels were measured before ip glucose injection (1.5 g D-glucose/Kg of body weight) after tail cut (~1 mm) and vein blood collection. Blood glucose levels were subsequently measured at minutes 15, 30, 60, 90 and 120 following glucose injection. Glucose concentration was determined with a glucose meter (Free Style Precision Neo glucometer, Abbott). Area under the curve (AUC) of the ipGTT was calculated using the trapezoidal rule.

2.2.3. Intraperitoneal insulin tolerance test (ipITT)

ipITT was performed on day 28 of the dietary protocol (Figure 8). Mice were fasted for 5-6 hours (9 a.m to 2/3 p.m) and housed individually for the experiment. Blood glucose levels were measured before insulin injection (0.75 U/Kg of body weight, Humalog, Lilly) after tail cut and vein blood collection. Blood glucose levels were measured at minutes 15, 30, 60, 90 and 120 after injection, using a glucose meter (Free Style Precision Neo glucometer, Abbott). AUC was calculated by using the trapezoidal rule.

2.2.4. Insulin stimulation and tissue collection

Mice were fasted overnight after being transferred to clean cages without food or faeces. Animals were injected ip with insulin (2U/Kg of body weight, Humalog, Lilly) or saline solution. After 30 minutes of insulin stimulation, mice were anesthetized with isoflurane

and sacrificed by cervical dislocation. Tissues were rapidly dissected, weighed and divided in 3 pieces. 2 pieces were immediately frozen in liquid nitrogen and stored at -80°C for later analysis. A third piece was fixed at room temperature in a solution of 10% neutral buffered formalin (Prolabo®, formaldehyde 4% aqueous solution, buffered, VWR chemicals) for a maximum of 60 days, for posterior histological analysis (Figure 8).

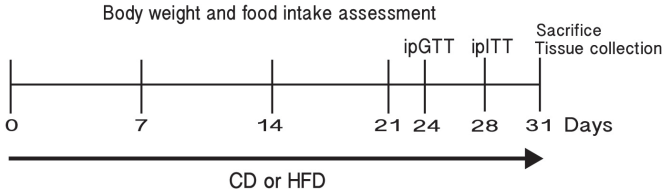

Figure 8. Experimental design of metabolic phenotyping under a CD or HFD.

2.3. Insulin signaling

2.3.1. Protein extraction and quantification

Tissues were lysed with radioimmunoprecipitation assay (RIPA) buffer (50 mM Tris-base; 150 mM NaCl; 5 mM egtazic acid (EGTA); 1% (v/v) Triton X-100; 0.5 % (w/v) deoxycholate (DOC); 0.1 % (w/v) sodium dodecyl sulphate (SDS)); complete mini protease inhibitor cocktail tablet (Roche Diagnostics, GmbH); 1 mM sodium orthovanadate ($NaVO_4$); 1 mM dithiothreitol (DTT); 10 mM sodium fluoride (NaF); 200 μM phenylmethylsulfonylfluoride (PMSF). Tissue lysates were prepared using manual homogenizers and followed by sonication (3/4 pulses, amplitude 60, 3/4 seconds each). Lysates were centrifuged at 13.000 rpm during 20 minutes at 4°C. Protein concentration was determined by the bicinchoninic acid (BCA) method. The samples were denatured with 6x concentrated sample buffer (0.5 M Tris-HCl, pH 6.8; 30% (v/v) glycerol; 10% (w/v) SDS; 0.6 M DTT; 0.01% (w/v) bromophenol blue), and heated at 95ºC for 5 min and stored at -80ºC until use.

2.3.2. SDS-PAGE and Western blotting

Proteins were resolved by sodium dodecyl sulphate-polyacrylamide gel electrophoresis (SDS–PAGE) using 8% and 10% polyacrylamide gels. Electrophoresis was run on a Tris-Bicine buffer (125 mM Tris-base; 125 mM Bicine; 0.5% (w/v) SDS; pH 8.3) at 70 V in the first 10 minutes and at 100 V until an appropriate separation of the molecular weight standards. Proteins were electrotransferred to polyvinylidene difluoride (PVDF) membrane in CAPS transfer buffer (10 mM CAPS, pH 11.0; 10% (v/v) metanol) upon a constant current of 750 mA, during 2 hours. Membranes were blocked for ~1 hour at room temperature with blocking buffer (5% non-fat dry milk or 5% bovine serum albumin (BSA) in Tris buffered saline (200 mM Tris-base; 137 mM NaCl; pH7.6 with 0.1% Tween-20). Membranes were incubated overnight at 4ºC with the following primary antibodies: rabbit polyclonal anti-P-Akt Ser473 (1:1000; Cell Signaling 9271S); rabbit polyclonal anti-Akt (1:1000; Cell Signaling 9272S); rabbit anti- SIRT2 (1:1000; Sigma S8447); rabbit polyclonal anti-P-HSL Ser660 (1:1000; Cell Signaling 4126S), mouse monoclonal anti-ATGL (1:1000; Santa Cruz Biotechnology F-7); mouse monoclonal anti-α tubulin (1:10000; Sigma T6074); mouse monoclonal anti-β tubulin (1:10000; Sigma T7816), followed by 1 hour incubation with the corresponding alkaline phosphatase-linked secondary goat anti-mouse or anti-rabbit antibody (1:10000; Thermo Scientific). Proteins were visualized with enhanced chemifluorescence substrate (ECF) (GE Healthcare) and scanned by VersaDoc Imaging System Model 3000 (Bio-Rad). Densitometry analysis of the blots was performed using Quantity One Version 4.6.9 (Bio-Rad).

2.4. Histological analysis

Tissues previously stored and conserved in a 10% neutral buffered formalin solution (Prolabo®, formaldehyde 4% aqueous solution, buffered, VWR chemicals) were passed through several steps for paraffin (Histosec® pastilles, Merck KGaA, EMO Millipore Corporation) blocks inclusion: 1 hour at ethanol 70%; two series of ethanol 95%, 45 minutes each; two series of ethanol 100%, 1 hour each; two series of xylene, 1 hour each and two series of paraffin, 1 hour each. In the end, tissues were included in paraffin blocks.

2.4.1. Hematoxylin & Eosin (H&E) staining

Paraffin blocks were sectioned at 4 μm thickness with microtome (Thermo Scientific HM325). Tissue sections were collected to microscope slides (SuperFrost™, Thermo Scientific). H&E staining was performed according to the manufacturer guidelines. Liver and epididymal white adipose tissue (eWAT) paraffin sections were deparaffinized in xylene and rehydrated in 100% ethanol and then in 95% ethanol. Slides were incubated with Hematoxylin Solution modified acc. to Gill III (Merck KGaA, EMO Millipore Corporation), and then washed in distilled water (dH_2O). After, sections were counterstained with Eosin Y-solution 0.5% aqueous (Merck KGaA, EMO Millipore Corporation), washed with distilled water and finally dehydrated in 95% ethanol, 100% ethanol and xylene. Mowiol mounting medium (Thermo Scientific) and a coverslip (Thermo Scientific) were added to prepare tissue sections for microscopy. Preparations were left to dry overnight. Microscope images were obtained using Axio Imager Z2 (Transmission Light, Objective plan-Apochromat 20x/0.8 M27, 0,512 μm/pixel) for qualitative and quantitative analysis. Adipocyte size and diameter were determined in a blind manner. A minimum of 200 adipocytes for each animal was quantified using ImageJ software (National Health Institute, Bethesda, MD, USA, Java 1.6.0_24).

2.4.2. Oil Red O (ORO) staining

Hepatic lipid content was determined by using ORO staining on frozen livers. Tissues were embedded in OCT Tissue-tek optimum cutting temperature (Sakura Finetek) and cut at a cryostat-microtome (Leica CM3050S, Leica Microsystems Nussloch GmbH, Nußloch, Germany) in 8-10 μm sections, and collected to microscope slides (SuperFrost™, Thermo Scientific) After 10 min at room temperature, slices were added ~1 mL ORO working solution (1.5 parts ORO stock solution (1.25 g ORO (Sigma-Aldrich) + 200 mL Isopropyl 99% solution) to 1 part of dH_2O) for 10 minutes, and then rinse with dH_2O to remove the solution. Tissue sections were left to dry and then prepared with Mowiol (Thermo Scientific) and a coverslip (Thermo Scientific) for microscopy. Microscope images were obtained using Axio Imager Z2 (Transmission Light, Objective plan-Apochromat 20x/0.8 M27, 0,512 μm/pixel). ORO percent stained area was determined in a blind manner. 10 images for each animal were quantified using ImageJ software (National Health Institute, Bethesda, MD, USA, Java 1.6.0_24).

2.5. mRNA quantification

2.5.1. Total RNA extraction

Total RNA was extracted from the liver using the NucleoSpin® RNA Isolation kit for tissue and according to the manufacturer's manual (Macherey-Nagel). DNase digestion was performed during the process to exclude any contamination with genomic DNA. Total RNA was quantified by optical density (OD) measurements using a ND-1000 Nanodrop Spectrophotometer (Thermo Scientific) and the purity was assessed with the ratio of OD at 260 and 280 nm. Total RNA samples were kept at -80ºC.

2.5.2. Real-time quantitative PCR analysis (RT-qPCR)

The mRNA levels of genes involved in selected metabolic pathways were assessed by RT-qPCR. cDNA was obtained from the conversion of 1000 ng of liver total RNA using the iScript™cDNA Synthesis Kit (Bio-Rad) according to the manufacturer's protocol. Prior to cDNA preparation, RNA samples of liver were diluted in RNase-free water (2 dilutions, 40 µL each) and stored at -20ºC. For mRNA quantification, the SsoAdvanced SYBR Green Supermix (Bio-Rad) was used in combination with pre-designed PCR primer sets (Alfagene) (Table 4). These primer sets were optimized to our liver samples, together with a reference gene. The reference gene was previously validated in our laboratory by GeNorm and NormFinder softwares. PCR primer sets were also validated by PrimerBlast (PubMED) and Oligocalc softwares before use.

2.6. Statistical analysis

Results are expressed as mean ± standard error of the mean (SEM). Statistical analysis was performed with parametric Student's t-test or ordinary One-way ANOVA, and effectuated using GraphPad Prism Software (v.7). Statistical significance is displayed as ns = non-significant, *p<0.05, **p<0.01, ***p<0.001, ****p<0.0001.

Table 4. Metabolic genes quantified by RT-qPCR. Identification of accession number, primer sequence and annealing temperature for the genes analyzed in the mouse liver.

Gene	Accession number	Primer Sequence (5'-3')	Annealing TºC
G6P	NM_0080614	F: CTGTGAGACCGGACCAGGA R: GACCATAACATAGTATACACCTGCTGC	60ºC
PEPCK	NM_011044.2	F: CCAACGTGGCCGAGACTAGCG R: GGCACATGGTTCCGCGTCCT	65ºC
SREBP-1c	NM_001313979.1 NM_011480.4	F: GATCAAAGAGGAGCCAGTGC R: TAGATGGTGGCTGCTGAGTG	60ºC
ACC	NM_133360.2	F: GGAGATGTACGCTGACCGAGAA R: ACCCGACGCATGGTTTTCA	60ºC
FasN	NM_007988.3	F: AGCTTCGGCTGCTGTTGGAAGT R: TCGGATGCCTCTGAACCACTCACA	65ºC
SCD1	NM_009127.4	F: CCGGAGACCCCTTAGATCGA R: TAGCCTGTAAAAGATTTCTGCAAACC	60ºC
CPT1	XM_006531658.3 XM_006531655.2 XM_006531654.2 XM_011248602.2	F: GGTTGCTGATGACGGCTATGGTGT R: GCGGTGAGGCCAAACAAGGTGATA	65ºC
ACLY	NM_001199296.1 NM_134037.3	F: GCCAGCGGGAGCACATC R: CTTTGCAGGTGCCACTTCATC	60ºC
MCAD	NM_007382.5	F: AACACTTACTATGCCTCGATTGCA R: CCATAGCCTCCGAAAATCTGAA	60ºC
HPRT	NM_0135562	F: GCTYACCTCACTGCTTTCCG R: CATCATCGCTAATCACGACGC	60ºC

Chapter III. Results

3.1. SIRT2 expression pattern in WT mice

3.1.1. SIRT2 expression in metabolically relevant tissues

SIRT2 has a ubiquitous distribution, being abundantly expressed in the CNS, but also in peripheral tissues [212,213]. In order to evaluate SIRT2 relative expression in several metabolically relevant tissues, and also to confirm the ablation of SIRT2 in our animal model, we first explored SIRT2 expression levels in the liver, adipose tissue, skeletal muscle and hypothalamus of WT and SIRT2-KO (KO) mice fed a regular CD. We observed that SIRT2 is expressed in all tissues examined from WT (Figure 9). We also found higher SIRT2 expression levels in hypothalamus in comparison with the other tissues. As expected, the absence of SIRT2 protein expression in KO mice was confirmed in all tissues tested.

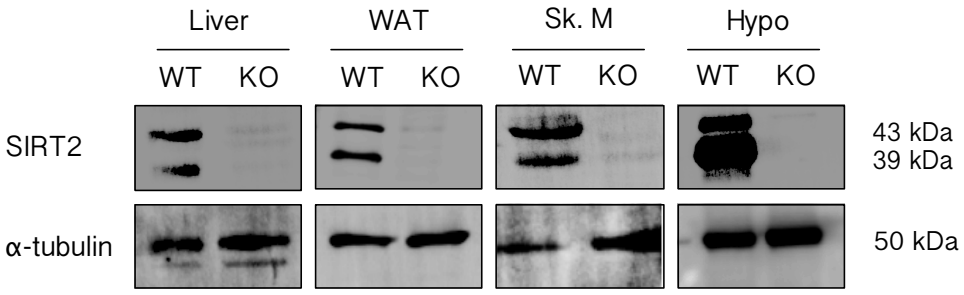

Figure 9. SIRT2 expression in metabolically relevant tissues. Representative immunoblots of tissue lysates (50 μg) from WT and SIRT2-KO mice fed a CD. Samples were analyzed by SDS-PAGE and Western blotting using antibodies against SIRT2 and α-tubulin (loading control). WAT – white adipose tissue; Sk. M – skeletal muscle; Hypo – hypothalamus.

3.1.1. Effect of HFD feeding on SIRT2 expression levels

The expression levels and deacetylase activity of sirtuins may change according to nutritional availability [180]. Thus, we investigated the impact of HFD feeding in SIRT2 expression levels in the tissues examined in Figure 1.

We observed that SIRT2 expression levels were not significantly altered after HFD when compared to CD, except in the adipose tissue of WT mice (Figure 10). We analyzed the expression levels of two reported SIRT2 isoforms, the long isoform with a molecular weight of 43 kDa (43) and the short isoform with a molecular weight of 39 kDa (39), and

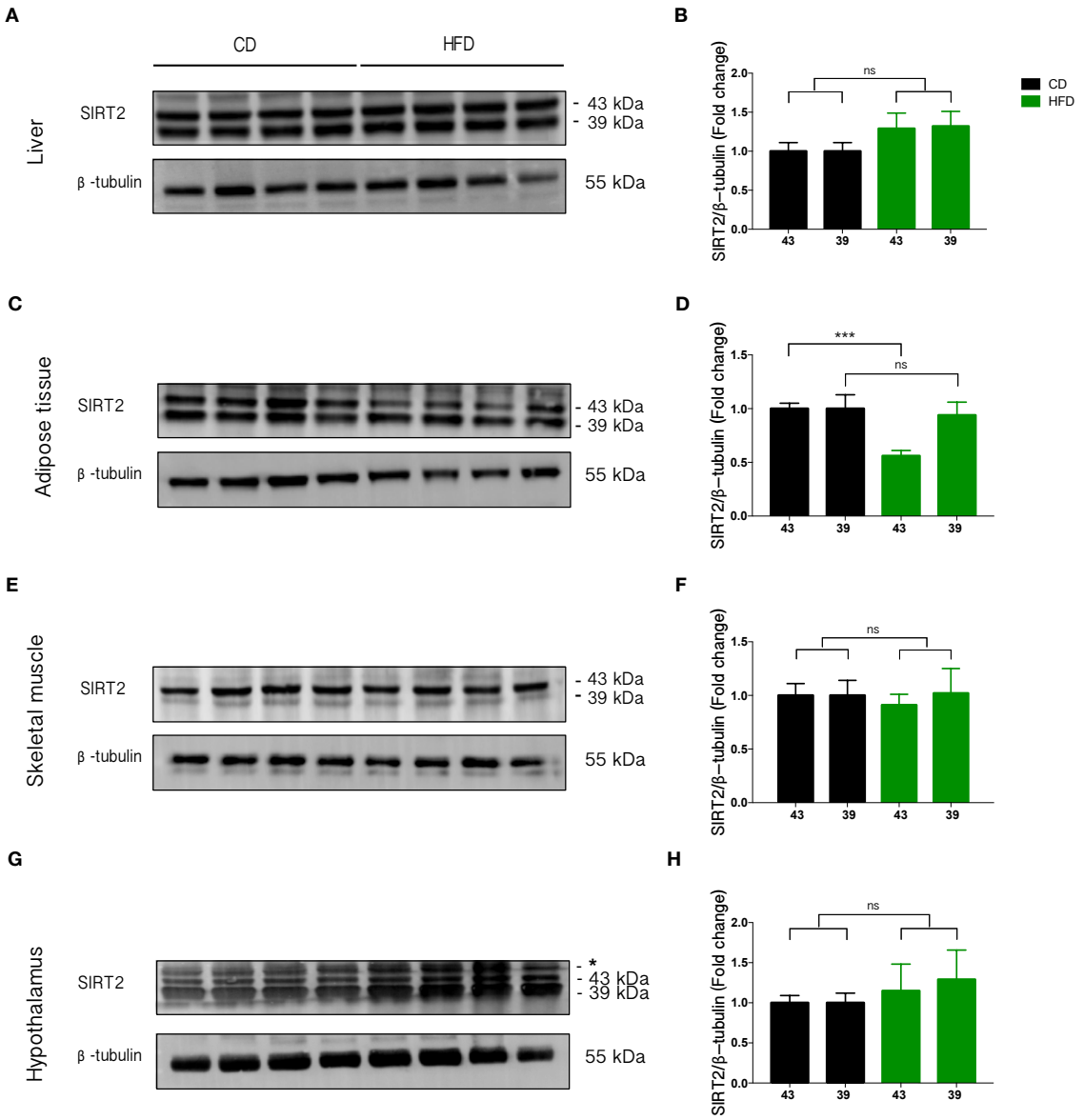

Figure 10. SIRT2 expression in metabolic tissues of WT mice fed a HFD for 4 weeks (A, C, E, G) Representative immunoblots of tissue lysates (50-80 μg) from WT mice fed either a CD or a HFD. Samples were analyzed by SDS-PAGE and Western blotting using antibodies against SIRT2 and β−tubulin (loading control) **(B, D, F, H)** Quantification of SIRT2/β−tubulin ratios. Levels of SIRT2 isoforms were normalized to β−tubulin in the same lane. All SIRT2/β−tubulin ratios were normalized to the value from WT mice fed a CD. Each lane corresponds to a distinct animal. Results are represented as mean ± SEM; n= 4/group. Statistical significance was determined by ordinary One-way ANOVA; ns=non-significant, ***p<0.001 compared to WT mice fed a CD. * represents a previously reported 51-kDa SIRT2 CNS isoform [249].

found similar expression levels in the liver, skeletal muscle and hypothalamus of WT mice fed a HFD in comparison with WT mice fed a CD (Figure 10A-B and E-H). Despite unaltered expression levels of isoform 39, we found a significant decrease in the expression levels of isoform 43 in the adipose tissue of WT mice fed a HFD, in comparison to WT mice fed

a CD (Figure 10C and D).

Taken together, these results suggest that 4 weeks of HFD feeding were not sufficient to induce significant alterations in SIRT2 expression levels in the liver, skeletal muscle, and hypothalamus, but reduced SIRT2 expression levels in the adipose tissue of WT mice.

3.2. Effect of HFD on insulin signaling activation in WT and SIRT2-KO mice

3.2.1. Insulin signaling in WT and SIRT2-KO mice under regular CD

SIRT2-KO (KO) mice fed a CD previously showed a mild insulin resistance (Quatorze, 2016; unpublished data). Thus, to investigate the impact of SIRT2 deficiency on insulin sensitivity, we assessed insulin signaling activation in KO mice fed a CD, in comparison to WT mice fed the same diet (Figure 11). We examined insulin signaling in several tissues collected from fasted mice ip injected with 0.9% saline or human insulin (2U/kg of body weight) for 30 minutes before sacrifice, and used Akt phosphorylation at Ser 473 (P-Akt^{473}) as a readout of insulin signaling activation.

We found a similar increase (~15-fold) in P-Akt in the livers from both WT and KO mice stimulated with insulin, in comparison with the livers from saline-administered animals (Figure 11A and B). In the adipose tissue and skeletal muscle, we observed an approximately 8-fold increase in P-Akt in WT and KO mice stimulated with insulin, when comparing to the animals administered with the saline solution (Figure 11C-F).

In the hypothalamus, we found that Akt is phosphorylated under saline conditions, and that insulin stimulation failed to further induce Akt phosphorylation (Figure 11G and H).

Taken together, insulin-induced Akt phosphorylation in the liver, adipose tissue and skeletal muscle of KO mice was indistinguishable from the levels in the tissues of WT mice. These results suggest that the absence of SIRT2 may not have impact on the molecular response to insulin under CD conditions.

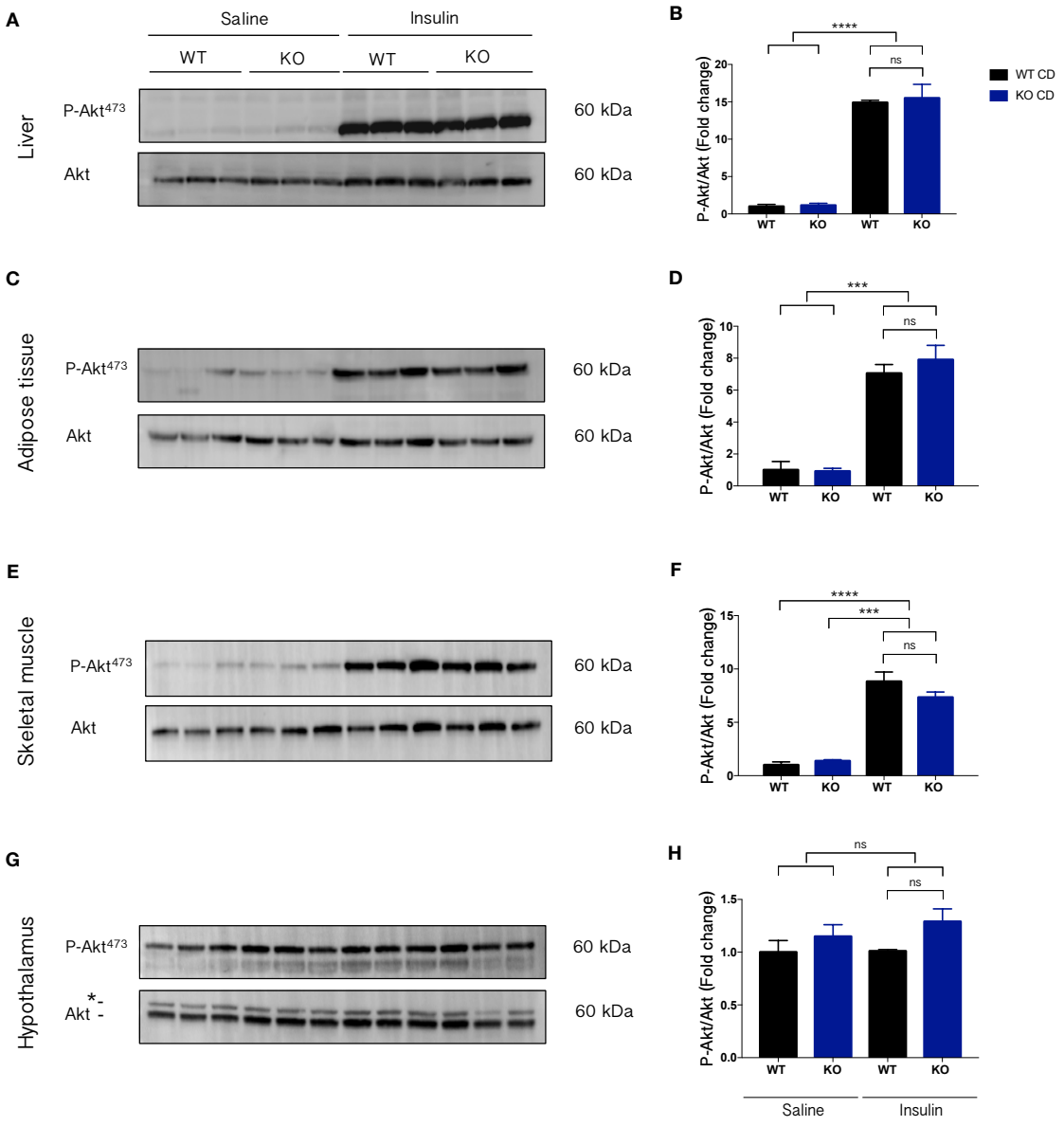

Figure 11. Insulin signaling in WT and SIRT2-KO (KO) mice fed a CD (A, C, E, G) Representative immunoblots of tissue lysates (50-80 μg) from WT and KO mice fed a CD and ip injected with 0.9% saline or human insulin (2U/kg body weight) for 30 minutes before sacrifice. Samples were analyzed by SDS-PAGE and Western blotting using antibodies against P-Akt and Akt **(B, D, F, H)** Quantification of P-Akt/Akt ratios. Levels of P-Akt were normalized to total Akt protein in the same lane. All P-Akt/Akt ratios were normalized to the value from WT mice injected with saline. Each lane corresponds to a distinct animal. Results are represented as mean ± SEM; n= 3/group. Statistical significance was determined by ordinary One-way ANOVA; ns= non-significant compared to WT insulin and saline; ***p<0.001, ****p<0.0001 compared to saline. * represents a lane of unspecific binding.

3.2.1. WT and SIRT2-KO mice insulin signaling under HFD

SIRT2-KO (KO) mice previously showed exacerbated insulin resistance when fed a HFD (Quatorze, 2016; unpublished data). Thus, we explored the impact of SIRT2 deficiency

on insulin signaling activation in KO mice fed a HFD, in comparison to WT fed the same diet (Figure 12).

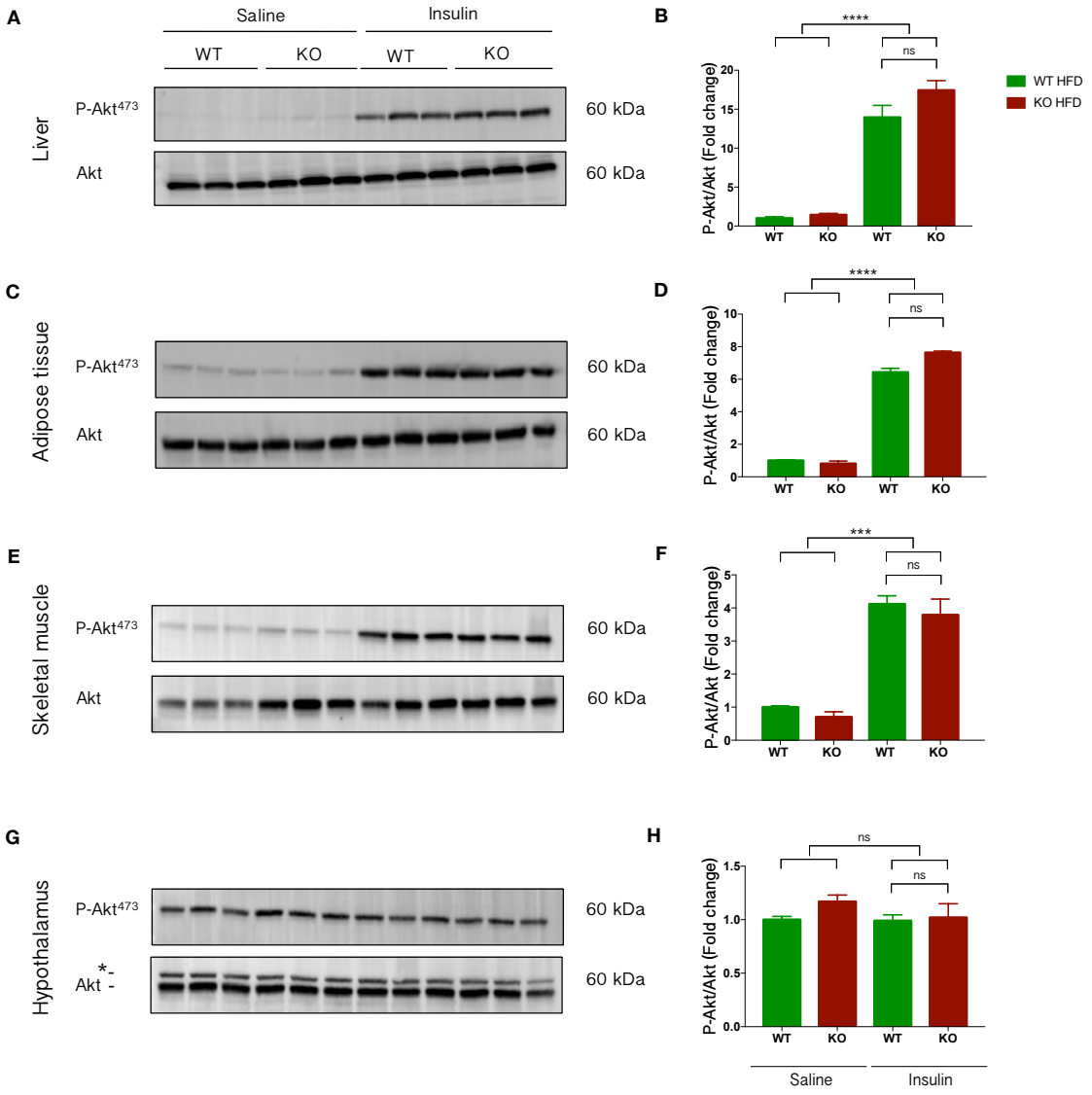

Figure 12. Insulin signaling in WT and SIRT2-KO (KO) mice fed a HFD (A, C, E, G) Representative immunoblots of tissue lysates (50-80 μg) from WT and KO mice fed a HFD and ip injected with 0.9% saline or human insulin (2U/kg body weight) for 30 minutes before sacrifice. Samples were analyzed by SDS-PAGE and Western blotting using antibodies against P-Akt and Akt **(B, D, F, H)** Quantification of P-Akt/Akt ratios. Levels of P-Akt were normalized to total Akt protein in the same lane. All P-Akt/Akt ratios were normalized to the value from WT mice injected with saline. Each lane corresponds to a distinct animal. Results are represented as mean ± SEM; n= 3/group. Statistical significance was determined by ordinary One-way ANOVA; ns= non-significant compared to WT insulin and saline, ***p<0.001, ****p<0.0001 compared to saline. * represents a lane of unspecific binding.

We assessed Akt phosphorylation at Ser 473 (P-Akt^{473}) in several tissues collected from fasted mice ip injected with 0.9% saline or human insulin (2U/kg of body

weight) for 30 minutes before sacrifice.

We found a similar increase in P-Akt in the livers (~15-fold) (Figure 12A and B), adipose tissue (~7-fold) (Figure 12C and D) and skeletal muscle (~4-fold) (Figure 12E and F) from WT and KO mice stimulated with insulin, when comparing to saline-administered animals.

In the hypothalamus, as observed in CD mice, we found that Akt is phosphorylated under saline conditions, however insulin stimulation did not result in further Akt phosphorylation (Figure 12G and H).

Overall, insulin-induced Akt phosphorylation levels in the liver, adipose tissue, and skeletal muscle of KO mice were indistinguishable from the levels in the tissues of WT mice. These results suggest that SIRT2 deficiency may also not have impact on the molecular response to insulin in mice fed a HFD for 4 weeks.

3.3. Adipose tissue morphology in WT and SIRT2-KO mice after HFD feeding

SIRT2-KO mice fed a HFD had increased body weight gain and also a higher eWAT mass when compared to WT mice fed a HFD (Quatorze 2016, unpublished data). Thus, to explore underlying mechanisms of exacerbated metabolic dysfunction in SIRT2-KO (KO) mice fed a HFD, we investigated possible morphological alterations in eWAT using hematoxylin and eosin (H&E) staining (Figure 13). Enlargement of adipose tissue mass can result from increased adipocyte size (hypertrophy) and/or adipocyte number (hyperplasia). Therefore, we used eWAT H&E staining to further assess changes in the adipocyte size and diameter (Figure 14) of WT and KO mice fed a CD or HFD, and also to study the adipocyte number in these animal groups (Figure 15).

As observed in the representative images of H&E-stained eWAT sections (Figure 13), we found larger adipocytes in both WT and KO mice fed a HFD, in comparison with mice fed a CD. This data suggests that HFD feeding for 4 weeks is sufficient to induce morphological changes in the adipocytes of animals fed a HFD.

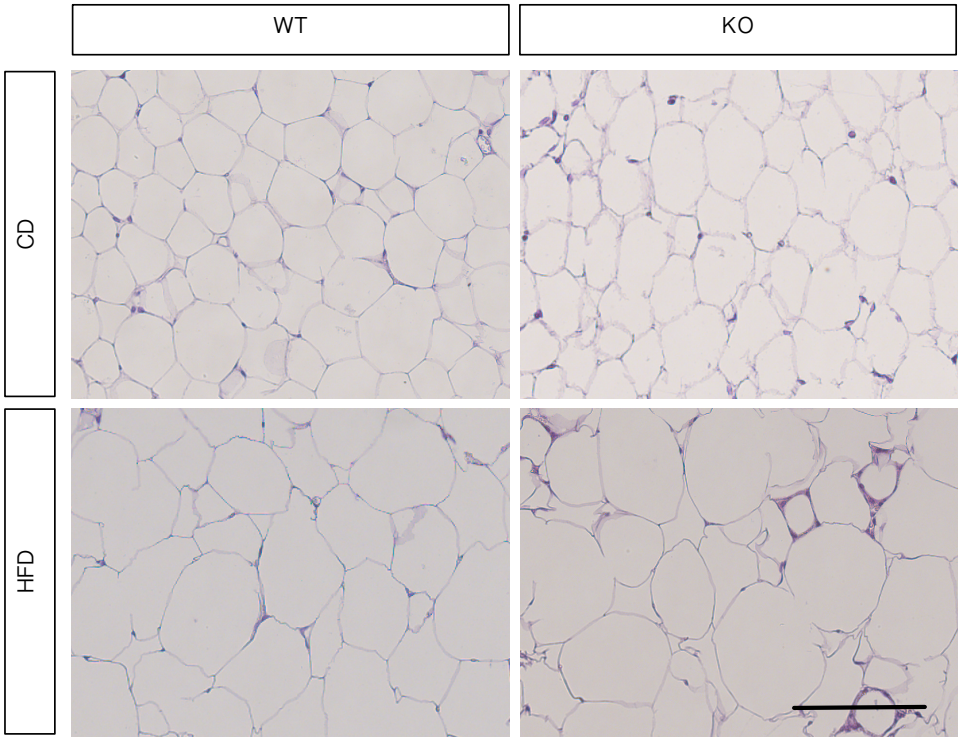

Figure 13. Morphology of eWAT from WT and SIRT2-KO (KO) mice fed a CD or HFD. Representative images of H&E-stained eWAT sections from WT and KO mice fed a CD or HFD. Scale bar, 100 μm.

3.3.1. Adipocyte size in WT and SIRT2-KO mice after HFD feeding

In order to explore if enlarged eWAT mass resulted from adipocyte hypertrophy, the previous qualitative results (Figure 13) were supported by cell size and diameter quantification. Adipocyte size was significantly increased in the WT mice fed a HFD (WT HFD) when compared to WT mice fed a CD (WT CD) (Figure 14A). SIRT2-KO (KO) animals fed a HFD (KO HFD) had also a significant increase in adipocyte size when compared to KO animals fed a CD (KO CD). We also observed larger adipocytes in KO HFD, when compared to WT HFD. The quantification of adipocyte diameter showed a significant increase in WT HFD, in comparison with WT CD (Figure 14C). KO HFD also had increased adipocyte diameter when compared to KO CD. However, adipocyte diameter was not significantly increased in KO HFD in comparison with WT HFD.

Frequency distribution of adipocyte size and diameter was different between WT and KO HFD mice (Figure 14B and D).

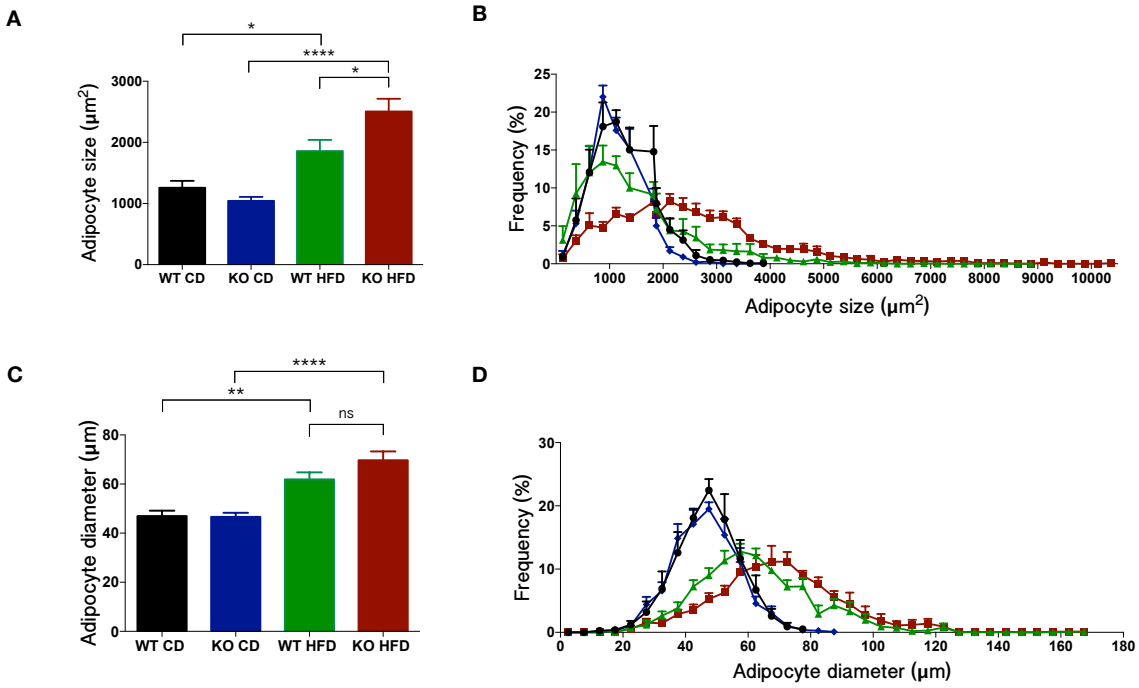

Figure 14. Adipocyte size and diameter of eWAT from WT and SIRT2-KO (KO) mice fed a CD or HFD (A, C) Adipocyte size and diameter was measured using ImageJ software. Results are represented as mean ± SEM; n=5/group. Statistical significance was determined by ordinary One-way ANOVA; *p<0.05, **p<0.01, ****p<0.0001 compared to CD mice **(B, D)** Adipocyte distribution and frequency with respect to the mean size and diameter measured using ImageJ software.

For both adipocyte size and diameter, KO HFD presented fewer small adipocytes, and an increase in the number of large adipocytes. Contrarily, WT HFD presented an increase in the number of small adipocytes, and fewer large adipocytes.

Taken together, this data suggests that SIRT2 deficiency promotes exacerbated adipocyte hypertrophy in eWAT of mice after 4 weeks of HFD feeding.

3.3.1. WT and SIRT2-KO mice adipocyte number after HFD feeding

We performed adipocyte number quantification in order to further study the enlargement of eWAT in SIRT2-KO (KO) mice under HFD feeding. We found that the number of adipocytes was decreased in the WT and KO HFD when compared to the WT and KO CD mice (Figure 15A). We further evaluate morphological changes of eWAT adipocytes by correlating adipocyte size with adipocyte number of all animal groups. A negative correlation between these two variables was found (Figure 15B). Adipocyte hypertrophy was correlated to a decrease in adipocyte number.

Overall, our results suggest that the enlargement of eWAT mass in SIRT2-KO mice

fed HFD eWAT was a result of significant increase in adipocyte size and reduction of total adipocyte number.

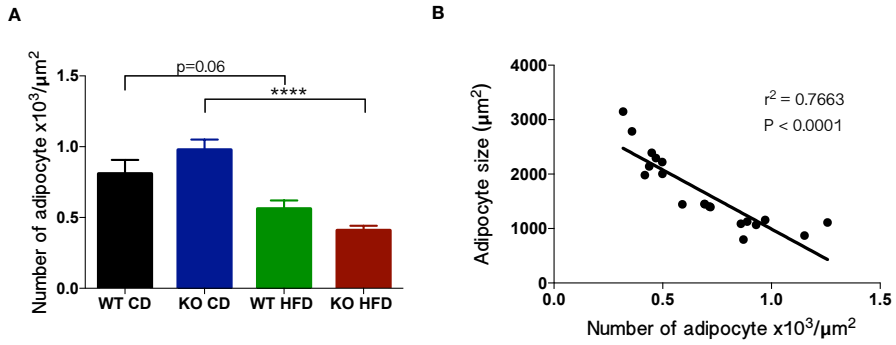

Figure 15. Adipocyte number of eWAT from WT and SIRT2-KO (KO) mice fed a CD or HFD (A) The number of adipocytes/µm^2 was measured using ImageJ software. Results are represented as mean ± SEM; n=5/group. Statistical significance was determined by parametric Student's t-test; p=0.06, ****p<0.0001 compared to CD mice **(B)** Adipocyte size plotted against adipocyte number. n=20; r and P value were determined by Pearson correlation test for normalized adipocyte size versus adipocyte number in eWAT of mice. Plotted line was determined by linear regression analysis.

3.4. Morphological alterations in the liver of WT and SIRT2-KO mice after HFD feeding

After the observation of adipocyte hypertrophy and decreased adipocyte number in SIRT2-KO mice under HFD feeding (Figure 13-15), we focused on another relevant metabolic organ, the liver, which was previously reported to accumulate lipids mobilized from an enlarged adipose tissue [250,251]. Thus, we investigated morphological alterations in the liver caused by increased lipid accumulation, which may possibly have been the underlying cause for insulin resistance development in KO mice fed a HFD (Figure 16 and 17).

3.4.1. Histopathological changes in WT and SIRT2-KO mice after HFD feeding

We performed H&E staining to assess histopathological changes in liver sections of WT and SIRT2-KO (KO) mice fed a CD or a HFD (Figure 16). H&E staining revealed normal morphologic features of hepatocytes of WT and KO mice fed a CD (Figure 16A-E and B-F). However, we observed lipid droplets (LDs) formation in the livers of WT and KO

mice fed a HFD (Figure 16C and D). KO mice under HFD showed formation of larger LDs when compared to WT mice fed a HFD (Figure 16G and H).

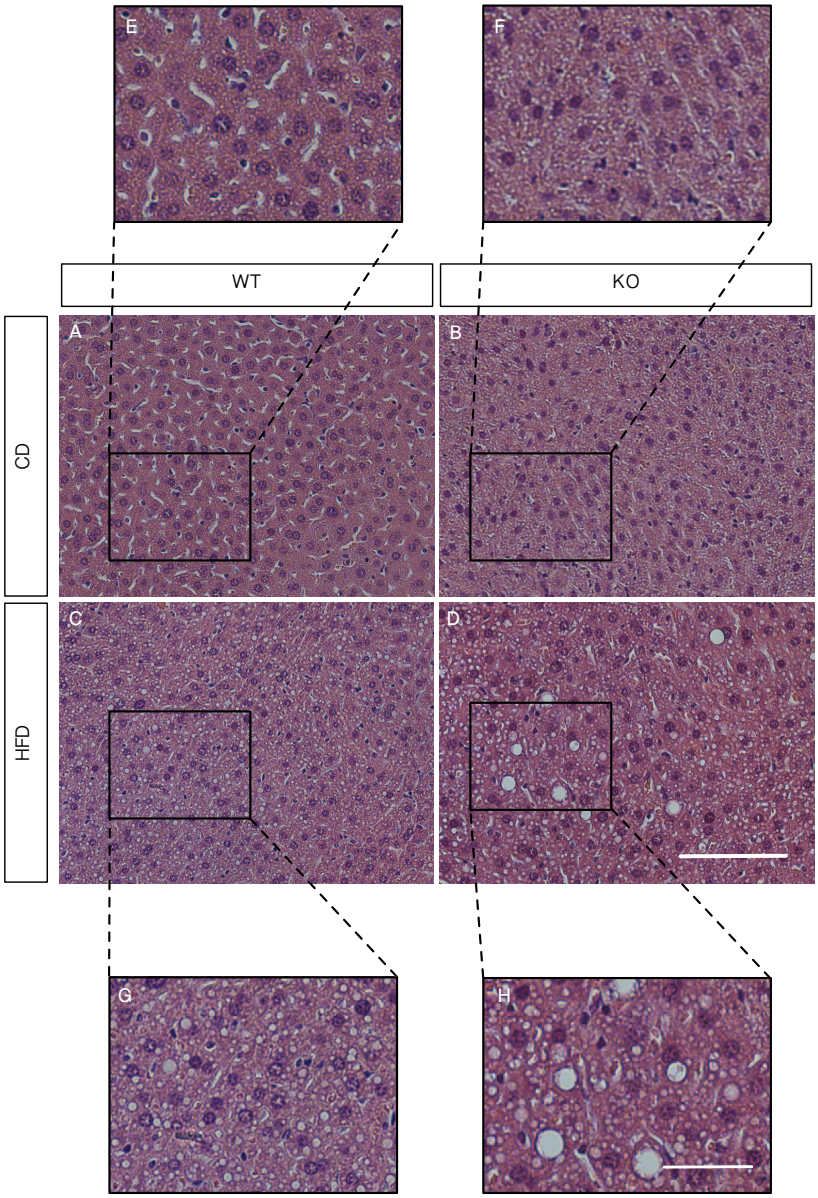

Figure 16. Morphology of liver from WT and SIRT2-KO (KO) mice fed a CD or HFD (A-D) Representative images of H&E-stained liver sections for WT and KO mice fed a CD or a HFD **(E-H)** Magnified regions of A-D images of liver H&E staining. Scale bar, 100 μm.

These results suggest that the absence of SIRT2 may cause increased accumulation and storage of lipids in the liver of mice under HFD feeding, promoting the development of hepatic steatosis.

3.4.2. Lipid accumulation in WT and SIRT2-KO mice after HFD feeding

To further evaluate lipid accumulation in the liver, we also performed Oil Red O (ORO) staining in liver sections of WT and SIRT2-KO (KO) mice (Figure 17) fed a CD (WT CD and KO CD) or a HFD (WT HFD and KO HFD) for 4 weeks. ORO staining was used to assess hepatic lipid content and stain neutral lipids, such as TG, which were previously observed

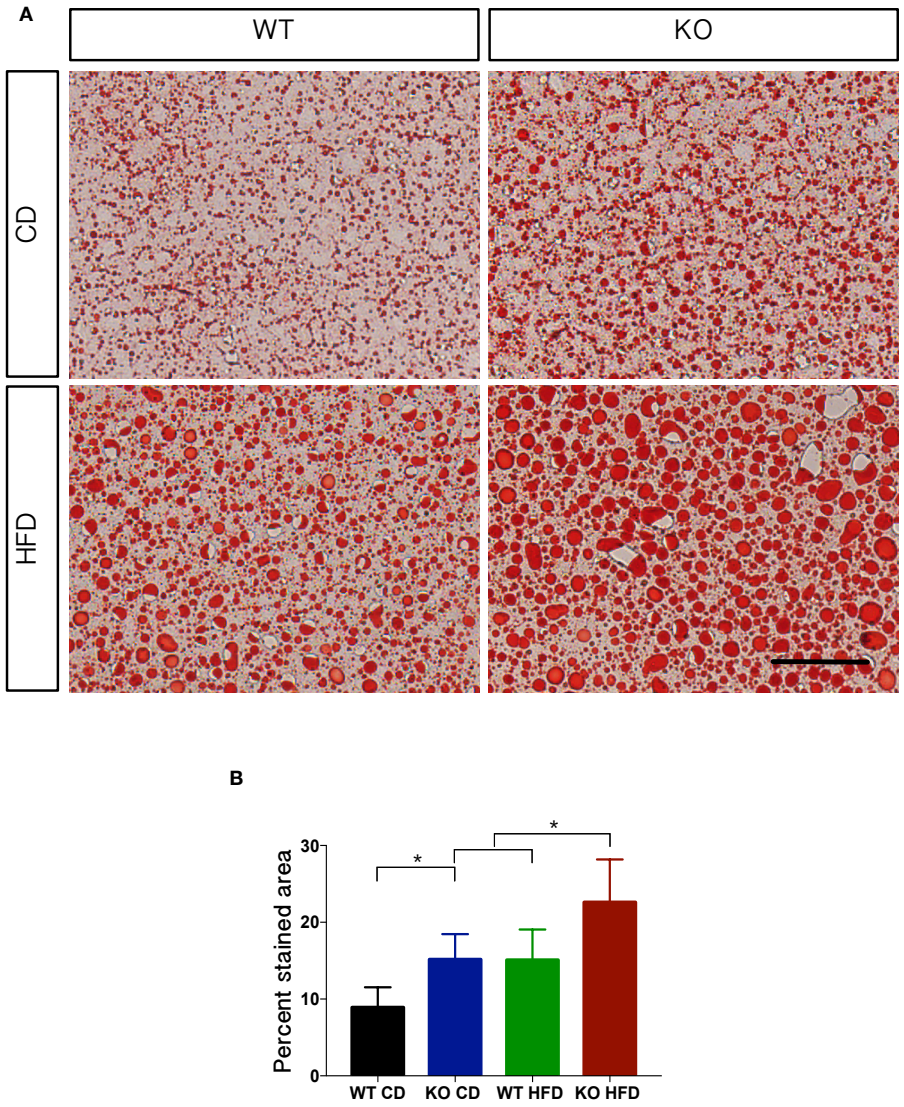

Figure 17. Hepatic lipid content in liver from WT and SIRT2-KO (KO) mice fed a CD or HFD **(A)** Representative images of ORO-stained liver sections for WT and KO mice fed a CD or a HFD. Scale bar, 100 µm **(B)** ORO-percent stained area was measured using Image J software. Results are represented as mean ± SEM; n=5/group. Statistical significance was determined by ordinary One-way ANOVA; *p<0.05 compared to CD and WT HFD mice.

to have increased serum concentrations in KO mice fed a HFD (Quatorze, 2016; unpublished data).

We observed a significant increase in the percentage of ORO staining in the livers of KO HFD, in comparison with WT HFD mice (Figure 17A and B). KO mice also showed increased staining percentage under CD feeding. These results further suggest that SIRT2 deficiency may promote increased lipid accumulation in the liver, which appears to occur in HFD feeding, but also under CD conditions.

3.5. Lipolysis in the adipose tissue of WT and SIRT2-KO mice fed a HFD

In order to determine whether the markedly adipocyte hypertrophy and lipid content accumulation in SIRT2-KO mice fed a HFD were result of altered lipolytic activity, we investigated by Western blotting the phosphorylation levels of HSL (P-HSL^{660}) and the expression levels of ATGL in eWAT of WT and KO mice fed a HFD (Figure 18).

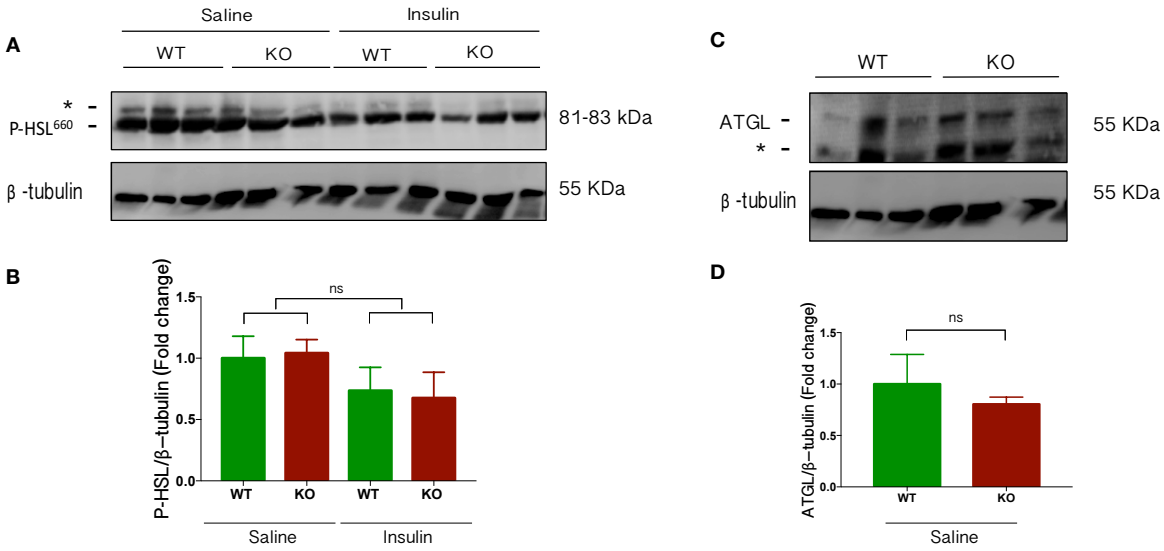

Figure 18. Lipolytic enzyme expression in WT and SIRT2-KO (KO) mice fed a HFD (A, C) Representative immunoblots of adipose tissue lysates (50 µg) from WT and KO mice fed a HFD. Samples were analyzed by SDS-PAGE and Western blotting using antibodies against P-HSL, ATGL and β–tubulin (loading control) **(B, D)** Quantification of P-HSL/β-tubulin and ATGL/β-tubulin ratios. Levels of P-HSL and ATGL were normalized to β–tubulin in the same lane. All P-HSL/β–tubulin and ATGL/β-tubulin ratios were normalized to the value from WT mice injected with saline. Each lane corresponds to a distinct animal. Results are represented as mean ± SEM; n= 3/group. Statistical significance was determined by ordinary One-way ANOVA and parametric Student's t-test; ns= non-significant compared to WT saline.

Our results showed trend towards decreased phosphorylation levels of HSL upon insulin stimulation of WT and KO mice fed a HFD, in comparison with saline-stimulated animal groups (Figure 18A and B). We also found similar ATGL expression levels in KO mice when compared to WT mice fed a HFD (Figure 18C and D).

Overall, this data suggests that SIRT2 deficiency may not have impact in lipolysis, and that 4 weeks of HFD feeding may also not have been sufficient to significantly alter lipolytic activity in eWAT adipocytes.

3.6. Gene expression of key metabolic regulators in WT and SIRT2-KO mice under HFD

To further investigate the underlying mechanisms responsible for increased lipid accumulation in the liver of SIRT2-KO mice fed a HFD, liver gene expression of key proteins in several metabolic mechanisms, such as gluconeogenesis, *de novo* lipogenesis, and fatty acid β-oxidation proteins, was evaluated by RT-qPCR technique (Figure 19).

We evaluated the mRNA levels of PEPCK and G6P and did not find significant alterations in these gluconeogenic proteins gene expression in KO mice fed a HFD (KO HFD) in comparison with WT mice fed the same diet (WT HFD) (Figure 19A and B). These results suggest that SIRT2 ablation may not have impact on the gluconeogenic pathway in HFD-fed mice.

We also analyzed mRNA levels of genes involved in *de novo* lipogenic pathway (Figure 19C-G). mRNAs encoding SREBP-1c, FasN and SCD1 showed alterations in KO mice fed a HFD. The results showed trend towards increased SREBP-1c mRNA levels in KO HFD when compared to WT HFD (Figure 19C). SREBP1-c gene expression in KO CD also tended to be upregulated, in comparison with WT CD. We also observed SCD1 and FasN mRNA levels tended increase in KO HFD when compared to WT HFD (Figure 19D and E). ACC and ACLY mRNA levels did not show significant changes in KO HFD, in comparison with WT HFD (Figure 19F and G). Overall, our results suggest that SIRT2 deficiency may have impact on lipogenic gene expression after 4 weeks of HFD feeding.

For the mRNA levels of genes encoding fatty acid β-oxidation proteins, we found increased levels of CPT-1 mRNA in KO HFD when compared to KO CD animals (Figure 19I). MCAD mRNA levels did not show significant alterations for all animal groups (Figure

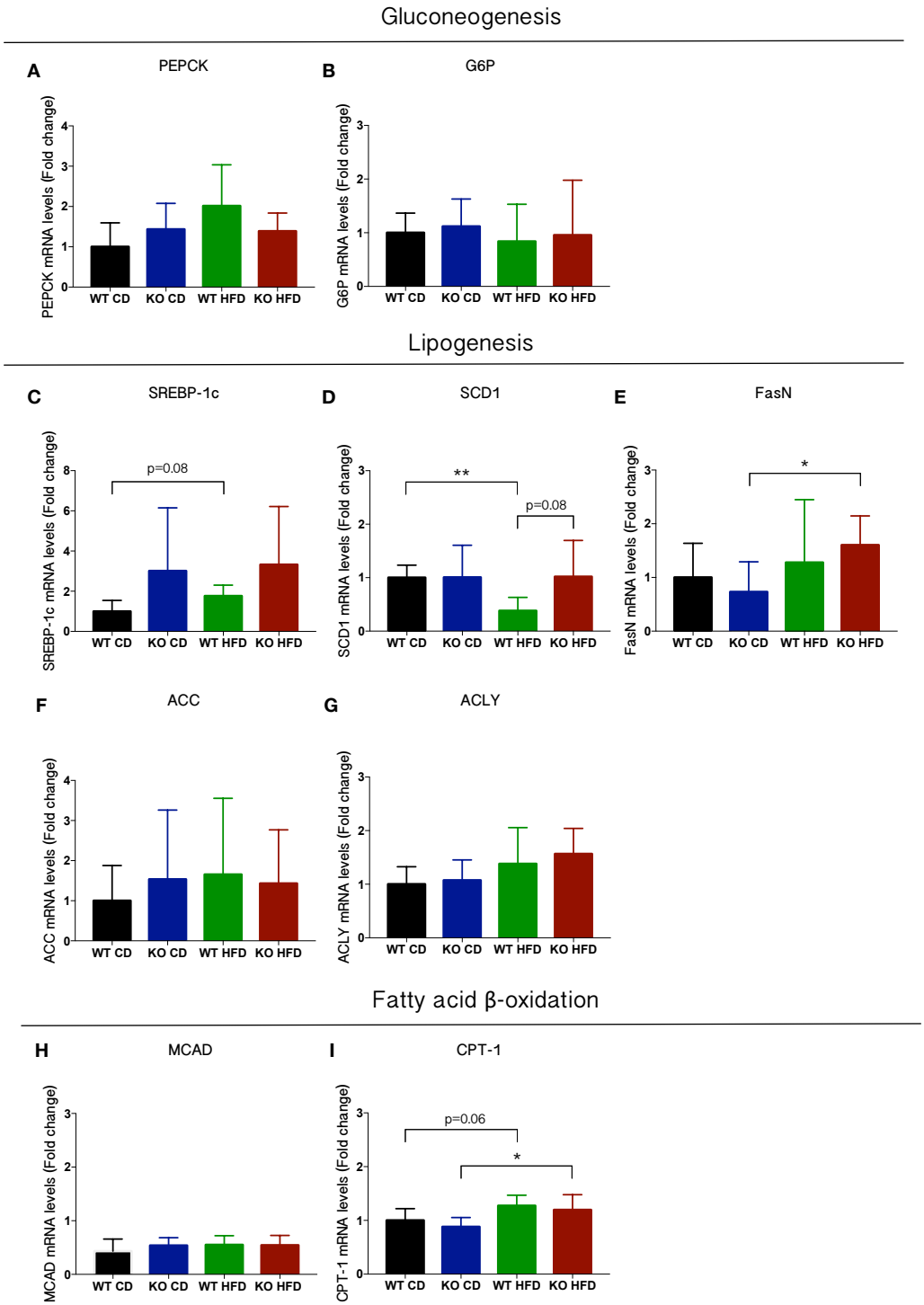

Figure 19. Hepatic mRNA levels of genes involved in key metabolic pathways of WT and SIRT2-KO (KO) mice fed a CD or HFD (A and B) RT-qPCR analysis of gluconeogenesis gene expression in livers of WT and KO mice fed a CD or HFD. Results represented as mean ± SEM; n=5-6/group **(C - G)** RT-qPCR analysis of lipogenesis gene expression in livers of WT and KO mice fed a CD or HFD. Results represented as mean ± SEM; n=5-6/group. Statistical significance was determined by parametric Student's t-test; p=0.08, * p<0.05, ** p<0.01 compared to WT CD and HFD mice **(H and I)** RT-qPCR analysis of fatty acid β-oxidation expression in livers of WT and KO mice fed a CD or HFD. Results represented as mean ± SEM; n=5-6/group. Statistical significance was determined by parametric Student's t-test; p=0.06, *p<0.05 compared to CD mice.

19H). These results suggest that the absence of SIRT2 may affect fatty acid β-oxidation gene expression, such as CPT-1, under HFD feeding.

Taken together, RT-qPCR results show a dysregulation of some key metabolic proteins gene expression in SIRT2-KO mice after 4 weeks of HFD feeding, which may possibly explain the morphological changes previously assessed in the liver of KO HFD-fed mice (Figure 16 and 17).

Chapter IV. Discussion

Obesity and type 2 diabetes are becoming highly prevalent worldwide. Current health treatments for these diseases have either severe effects or low effectiveness, which magnifies the urgency to develop novel therapeutic approaches. In recent years, mammalian sirtuins have been studied as potential targets to prevent or ameliorate metabolic disorders [252]. SIRT2 has been emerging as a crucial metabolic regulator [200,201,210], although its role in the development of obesity and associated complications has not been clarified in an *in vivo* mouse model. Our work, therefore, aims to provide critical insights into the role of SIRT2 in the pathogenesis of metabolic disorders using a SIRT2-KO mouse model. This work is focused on early onset of these diseases and aims to identify potential targets to therapeutically prevent or counteract their development.

In the present study, we aimed to expand and understand previous research showing a markedly metabolic dysregulation in SIRT2-KO mice under HFD feeding (Quatorze 2016; unpublished data). Obesity is defined by an enlargement in adipose tissue, which has been reported to be caused by adipocyte hypertrophy and/or hyperplasia during obesity progression [93,136]. This study revealed increased adipocyte size and decreased adipocyte number in SIRT2-KO mice fed a HFD for 4 weeks, which consisted with previous results of increased body and eWAT weight gain in SIRT2-KO mice fed a HFD (Quatorze 2016; unpublished data). A previous study of fat-specific SIRT6 ablation also showed markedly adipocyte hypertrophy and adiposity in mice fed a HFD for 8-12 weeks [253]. Enlargement of adipose tissue is also associated with mobilization of lipids from this tissue to other peripheral tissues [137]. We observed exacerbated lipid accumulation and histopathological changes in the liver of SIRT2-KO mice fed a HFD. These results are consistent with previous studies of other SIRT-KO mouse models. Liver-specific deletion of SIRT6 was shown to promote increased LDs formation, which ultimately lead to hepatic steatosis onset [78]. Under HFD feeding, liver-specific ablation of SIRT1 also altered hepatic lipid content and contributed to fatty liver development [188].

Hepatic lipid overload in SIRT2-KO mice fed a HFD might have been the result of increased lipogenesis. SREBP-1c is known to be the master regulator of lipid metabolism [254]. In our study, there was a trend towards increased SREBP-1c mRNA levels in the livers of HFD-fed mice for 4 weeks. Interestingly, in SIRT2-KO mice fed a CD, SREBP-1c gene expression also tended to be upregulated, which appears to consist with the ORO staining results. SREBP-1c has several target genes, such as FasN, and SCD1 [255]. As expected,

SCD1 and FasN mRNA levels also tended to be increased in SIRT2-KO mice fed a HFD. This data consists with previous studies where FasN and SREBP-1c mRNA levels were shown to be increased in mice after 10 weeks of HFD feeding [256]. In another *in vivo* study, after 6 weeks of HFD, both SCD1 and FasN expression levels were also reported to be increased, together with SREBP-1c mRNA levels [257]. Unexpectedly, as another SREBP-1c gene target, ACC did not show significant alterations in mRNA levels, which contradicts previous studies of ACC upregulated gene expression in mice fed a HFD [258]. These previous studies were performed under a long-term HFD feeding and in different animal models, which might explain the absent alteration of ACC mRNA levels in our short-term HFD feeding study. ACLY has been reported to be deacetylated by SIRT2, which consequently causes ACLY degradation and lipogenesis repression [248]. Taking this into account, ACLY could possibly be altered in SIRT2-KO mice. However, our study did not show significant changes in ACLY mRNA levels. The SIRT2 deacetylation activity towards ACLY was previous studied under high-glucose conditions, in contrast to our HFD conditions.

Gluconeogenesis is an anabolic process that generates glucose from several precursors (pyruvate, glycerol, amino acids). This mechanism is regulated by two key proteins, PEPCK and G6P [255]. Our results revealed unaltered PEPCK and G6P mRNA levels in the livers of HFD-fed SIRT2-KO mice, in apparent contrast to previous data. In an 8 week-HFD feeding protocol, the expression of gluconeogenic proteins was reported to be significantly upregulated in mice [259]. Moreover, other previous study with only 4 days of HFD feeding also showed increased mRNA expression levels of PEPCK and G6P in mice [260]. These previous studies used different experimental mouse models and periods of HFD feeding, in comparison to our 4 weeks of HFD feeding of SIRT2-KO mice. SIRT2 was shown to deacetylate and increase PEPCK stability, preventing its degradation and decreased levels under fasting and glucose deprivation conditions [261]. Our results might show that there might not be an effect of SIRT2 under nutritional abundance conditions, which might explain SIRT2 absent impact in gluconeogenic proteins gene expression, such as PEPCK, after HFD feeding.

FAO encompasses a translocation of FA from cytosol to mitochondria, through CPT-1 transport, to be oxidized into acetyl-CoA [255]. Dehydrogenases, such as MCAD, are also key players in this metabolic process [109]. In our study, no significant changes were

observed in MCAD mRNA levels among all animal groups. Despite this data, CPT-1 revealed increased expression levels in the livers of SIRT2-KO HFD-fed mice. These results are consistent with a previous study showing that after 18 weeks of HFD, CPT1 mRNA levels were increased in mice [262]. Interestingly, MCAD expression levels were also reported to be increased in mice after 5 weeks of HFD feeding [263]. In contradiction, other study reported that both CPT-1 and MCAD expression were decreased in mice after 16 weeks of HFD [264]. These studies were developed using different animal models and periods of HFD, and performed in other peripheral tissues, particularly the adipose tissue [262], skeletal muscle [263], and kidney [264], which raises the possibility that HFD feeding might have tissue-specific effects in FAO proteins expression levels.

Adipose tissue lipolysis is a process of TG breakdown into FA and glycerol to be used by other tissues as an energy source. This metabolic process is regulated by two crucial lipases, ATGL and HSL, and when impaired results in excess storage of TG that causes adipocyte hypertrophy and obesity. In this study, no significant results were observed towards HSL phosphorylation levels and ATGL expression levels in adipose tissue of WT and KO mice fed a HFD. Unfortunately, this data does not give enough insights into the impact of SIRT2 ablation in lipolysis under HFD conditions.

In our study, we also observed a decrease in SIRT2 expression levels in the adipose tissue, but no significant changes were observed in the liver, skeletal muscle and hypothalamus of HFD-fed mice. Our results may suggest that under a 4 week-period of HFD feeding, the adipose tissue may be the primarily affected tissue, with consequent alterations in SIRT2 expression levels in response to the metabolic stress condition. Despite previous studies of SIRT2 expression downregulated in HFD feeding [265], our dietary protocol may not have been sufficient to cause changes in SIRT2 expression levels in other metabolic relevant tissues besides adipose tissue.

Other interesting result was the observation of an apparently normal insulin signaling activation in insulin-resistant SIRT2-KO mice fed a HFD (Quatorze, 2016; unpublished data). Previous studies have associated insulin resistance to defects in the insulin signaling cascade, particularly in upstream proteins, such as IR and IRS [27,266], which compromise the activation of downstream molecules, such as Akt. The phosphorylation levels of this protein have been reported to be decreased under HFD feeding of *in vivo* models [124,267]. As expected, no differences were found in Akt phosphorylation levels

between insulin-stimulated SIRT2-KO mice and control mice fed a CD. Surprisingly, similar results were observed in the SIRT2-KO mice fed a HFD. Our data suggests that exacerbated insulin resistance development in SIRT2-KO mice might not have been caused by dysregulated insulin signaling activation. In fact, insulin resistance has been suggested to occur independently of insulin signaling proteins. In a previous study, insulin signaling pathway was compared to another pathway that recapitulates several aspects of insulin action, but in an IRS-independent manner [268]. After analyzing six models of insulin resistance, including chronic low-dose inflammation and hyperinsulinemia, both pathways were shown to be defective, despite the insulin-specific insults within IRS-Akt node. In this previous study, insulin resistance was pointed to occur independently to IRS1 protein, and disruption in insulin activity was suggested to be a consequence, and not a cause, of insulin resistance development after HFD feeding [268].

One potential explanation for the lack of differences in insulin signaling might be related to the insulin stimulation period selected in our work (30 minutes). This period is suggested to be extensive to evaluate Akt phosphorylation levels [120], and might have caused a saturation of the phosphorylation levels of the insulin signaling proteins, compromising the assessment of a possible impairment in insulin signaling activation in HFD-fed SIRT2-KO mice. In fact, it was previously shown that depending on the tissue examined, insulin signaling proteins have a different time course of phosphorylation [269]. A 10-minute ip injection of insulin was suggested to be an appropriate time to assess phosphorylation levels in peripheral tissues, particularly in the liver and in the skeletal muscle. Thus, in future studies we should stimulate SIRT2-KO mice with insulin for a 10 to 15-minute period, to adequately study the phosphorylation events in peripheral tissues. Despite this short period of insulin stimulation required to activate insulin signaling in these tissues, hypothalamic insulin signaling activation might need a longer time of insulin stimulation, in consistence with previous mice studies [270]. Another limitation of our study might be the smaller number of animals used in RT-qPCR analysis. We should use a larger number of animals per group to obtain more robust data and further assess if our results with trend towards increased mRNA levels are in fact significant alterations in lipogenic gene expression. Furthermore, our study has other limitations regarding the assessment of alterations in the lipolytic activity. We only assessed HSL phosphorylation levels upon insulin stimulation in HFD-fed mice, being also crucial to evaluate insulin action in CD

conditions. If found a significant decrease in HSL phosphorylation levels in CD mice in comparison to HFD mice, insulin activity might be impaired after HFD feeding. However, this speculation might have another limitation. To properly assess insulin inhibitory effects in lipolysis, mice should be injected with isoproterenol (ISO) before sacrifice [253]. We also only studied ATGL expression levels, and we should evaluate its phosphorylation levels using an antibody against P-ATGL [253].

To fully understand SIRT2 metabolic actions in both adipose tissue and liver, several follow-up experiments should be performed. In the adipose tissue, increased adiposity and insulin resistance development have been associated to inflammation and infiltration of macrophages [136]. These conditions have been reported in other SIRT-KO mice under HFD feeding [253]. Thus, we should analyze macrophage markers, such as CD11c and F4/80, by immunochemistry, and also perform RT-qPCR, to further assess the mRNA levels of these markers in adipose tissue of SIRT2-KO mice fed a HFD. Gene expression levels of several pro-inflammatory cytokines, such as IL-6 and TNF-α, should also be assessed. Moreover, it is also crucial to study mRNA expression levels of the gluconeogenic, lipogenic and FAO proteins in the adipose tissue of SIRT2-KO and control mice under CD and HFD feeding. In the liver, hepatic steatosis has been associated to the development of inflammation and fibrosis [271]. Therefore, gene expression of pro-inflammatory markers should be evaluated, and liver sections should be stained with fibrosis markers (eg. collagen staining with Sirius red). FA uptake transporters, such as CD36, gene expression analysis should also be performed to further understand increased hepatic lipid accumulation [253]. In regard to the study of impaired lipolysis in SIRT2-KO mice fed a HFD, we should inject our mice with ISO, in order to evaluate glycerol release and measure lipolytic rate in WAT explants [253].

Other experiments should also be performed to further understand previous results of enhanced energy intake and increased body weight in SIRT2-KO mice fed a HFD (Quatorze, 2016; unpublished data). Gene expression of thermogenesis proteins, such as PGC-1α, and UCP1, sould be analyzed in BAT. Moreover, hypothalamic gene expression of anorexigenic, such as POMC, and orexigenic neuropeptides, such as NPY and AgRP, should be performed to assess FI dysregulation in SIRT2-KO mice under HFD feeding.

In conclusion, the present study suggests that exacerbated metabolic dysfunction in SIRT2-KO mice fed a HFD might have been caused by an increase in lipogenesis, which

led to marked lipid accumulation in the liver, possibly promoting the development of insulin resistance after 4 weeks. Our study provides critical insights into the role of SIRT2 in HFD-induced metabolic stress conditions. The modulation of SIRT2 might constitute a novel therapeutic strategy against the development of metabolic disorders, such as obesity and type 2 diabetes. Therefore, the present study suggests that tissue- and cell type-specific SIRT2 stimulation might counteract the development of metabolic dysfunction induced by HFD feeding.

Chapter V. Concluding remarks

The present study was developed in order to gain mechanistic insight, at the molecular level, into the role of SIRT2 in metabolic homeostasis. In this study, SIRT2 deficiency was associated with adipocyte hypertrophy and exacerbated lipid accumulation in the liver of HFD-fed mice. Unexpectedly, SIRT2-KO mice exhibited normal activation of the insulin signaling pathway under both diets. Despite this fact, SIRT2 ablation led to lipid overload in peripheral tissues, with consistent alterations in metabolic mechanisms, such as lipogenesis in the liver. Early-onset insulin resistance in SIRT2-KO mice may be the result of lipid metabolic dysregulation. Further studies should be performed to fully understand the liver-specific metabolic role of SIRT2, and also SIRT2 actions in other metabolically relevant tissues, such as the adipose tissue and skeletal muscle.

This study provides critical insights into SIRT2 connection to the development of metabolic disorders, such as obesity and type 2 diabetes, and identifies potential tissues and cellular mechanisms to target and therapeutically counteract the progression of these disorders. Our data suggests that SIRT2 stimulation under HFD feeding may ameliorate the metabolic dysregulation associated to the early onset of metabolic disorders.

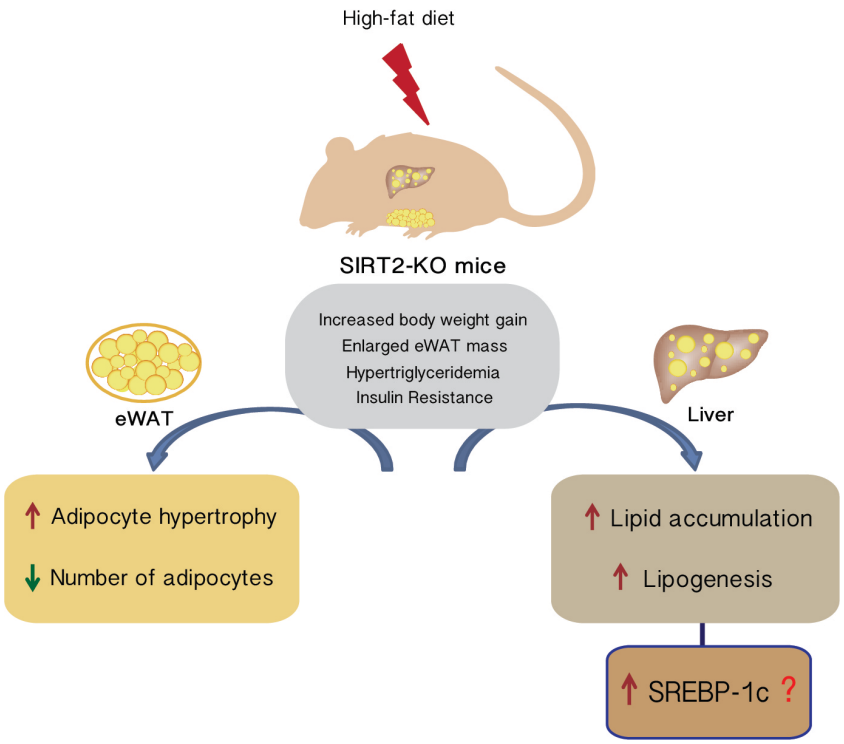

Figure 20. Exacerbated metabolic dysfunction of SIRT2-KO mice under HFD feeding. SIRT2-KO mice showed a markedly metabolic dysregulation after 4 weeks of high-fat diet (HFD) that may have been a result of altered metabolic mechanisms, such as lipogenesis, and increased lipid overload in peripheral tissues, possibly promoting the development of insulin resistance.

References

1. Ahima, R. S. Digger deeper into obesity. *J. Clin. Invest.* **121,** 3–6 (2011).
2. Scheen, A. J. & Van Gaal, L. F. Combating the dual burden: Therapeutic targeting of common pathways in obesity and type 2 diabetes. *Lancet Diabetes Endocrinol.* **2,** 911–922 (2014).
3. Kelly, T., Yang, W., Chen, C.-S., Reynolds, K. & He, J. Global burden of obesity in 2005 and projections to 2030. *Int. J. Obes. (Lond).* **32,** 1431–7 (2008).
4. Shaw, J. E. *et al.* Global estimates of the prevalence of diabetes for 2010 and 2030. *Diabetes Res. Clin. Pract.* **87,** 4–14 (2010).
5. Kushner, R. F. Weight loss strategies for treatment of obesity. *Prog. Cardiovasc. Dis.* **56,** 465–472 (2014).
6. Caballero, B. The Global Epidemic of Obesity: An Overview. *Epidemiol. Rev.* **29,** 1–5 (2007).
7. Krishnan, J. *et al.* Dietary obesity-associated hif1α activation in adipocytes restricts fatty acid oxidation and energy expenditure via suppression of the Sirt2-NAD+ system. *Genes Dev.* **26,** 259–270 (2012).
8. Boden, G. Obesity, insulin resistance and free fatty acids. *Curr Opin Endocrinol Diabetes Obes.* **18,** 139–143 (2003).
9. Scherer, P. E. Adipose tissue: from lipid storage compartment to endocrine organ. *Diabetes* **55,** 1537–45 (2006).
10. Mohamed-Ali, V. *et al.* Subcutaneous Adipose Tissue Releases Interleukin-6, But Not Tumor Necrosis Factor-α, *in Vivo* [1]. *J. Clin. Endocrinol. Metab.* **82,** 4196–4200 (1997).
11. Fain, J. N., Madan, A. K., Hiler, M. L., Cheema, P. & Bahouth, S. W. Comparison of the Release of Adipokines by Adipose Tissue, Adipose Tissue Matrix, and Adipocytes from Visceral and Subcutaneous Abdominal Adipose Tissues of Obese Humans. *Endocrinology* **145,** 2273–2282 (2004).
12. Kahn, S. E., Hull, R. L. & Utzschneider, K. M. Mechanisms linking obesity to insulin resistance and type 2 diabetes. *Nature* **444,** 840–846 (2006).
13. Pascot, A. *et al.* Reduced HDL particle size as an additional feature of the atherogenic dyslipidemia of abdominal obesity. *J. Lipid Res.* **42,** 2007–14 (2001).
14. Poirier, P. & Eckel, R. H. Obesity and cardiovascular disease. *Curr. Atheroscler. Rep.* **4,** 448–53 (2002).
15. Gholam, P. M., Flancbaum, L., Machan, J. T., Charney, D. A. & Kotler, D. P. Nonalcoholic Fatty Liver Disease in Severely Obese Subjects. *Am. J. Gastroenterol.* **102,** 399–408 (2007).
16. Van Gaal, L. F., Mertens, I. L. & De Block, C. E. Mechanisms linking obesity with cardiovascular disease. *Nature* **444,** 875–80 (2006).
17. Calle, E. E. & Kaaks, R. Overweight, obesity and cancer: epidemiological evidence and proposed mechanisms. *Nat. Rev. Cancer* **4,** 579–591 (2004).
18. Fader, A. N., Arriba, L. N., Frasure, H. E. & von Gruenigen, V. E. Endometrial cancer and obesity: Epidemiology, biomarkers, prevention and survivorship. *Gynecol. Oncol.* **114,** 121–127 (2009).
19. James, P. T., Rigby, N., Leach, R. & International Obesity Task, F. The obesity epidemic, metabolic syndrome and future prevention strategies. *Eur. J. Cardiovasc. Prev. Rehabil.* **11,** 3–8 (2004).
20. Wang, Y. C. *et al.* Health and economic burden of the projected obesity trends in the USA and the UK. *Lancet (London, England)* **378,** 815–25 (2011).
21. Jaacks, L. M., Siegel, K. R., Gujral, U. P. & Narayan, K. M. V. Type 2 diabetes: A 21st century epidemic. *Best Pract. Res. Clin. Endocrinol. Metab.* **30,** 331–343 (2016).
22. Donath, M. Y. & Halban, P. A. Decreased beta-cell mass in diabetes: significance, mechanisms and therapeutic implications. *Diabetologia* **47,** 581–589 (2004).
23. Reaven, G. Role of insulin resistance in human disease. *Diabetes* **37,** 1596–1607 (1988).
24. Martin, B. C. *et al.* Role of glucose and insulin resistance in development of type 2 diabetes mellitus: results of a 25-year follow-up study. *Lancet* **340,** 925–929 (1992).
25. Shirakawa, J., De Jesus, D. F. & Kulkarni, R. N. Exploring inter-organ crosstalk to uncover mechanisms that regulate β-cell function and mass. *Eur. J. Clin. Nutr.* **71,** 896–913 (2017).
26. Cefalu, W. T. Insulin Resistance : Cellular and Clinical Concepts. **226,** 13–26 (2008).
27. Könner, A. C. & Brüning, J. C. Selective Insulin and Leptin Resistance in Metabolic Disorders.

Cell Metab. **16,** 144–152 (2012).
28. Wild, S., Roglic, G., Green, A., Sicree, R. & King, H. Global prevalence of diabetes: estimates for the year 2000 and projections for 2030. *Diabetes Care* **27,** 1047–53 (2004).
29. Chen, L., Magliano, D. J. & Zimmet, P. Z. The worldwide epidemiology of type 2 diabetes mellitus--present and future perspectives. *Nat. Rev. Endocrinol.* **8,** 228–36 (2012).
30. A.J., K. & M.B., P. New drugs for type 2 diabetes mellitus: What is their place in therapy? *Drugs* **68,** 2131–2162 (2008).
31. Lovshin, J. A., Kramer, C. K., Zinman, B. & Retnakaran, R. Glucagon-like Peptide-1 Receptor Agonists: A Class Update for Treating Type 2 Diabetes. *Can. J. Diabetes* **384,** 2228–2234 (2017).
32. Prevention, D. & Diabetes Prevention Program Research Group. Reduction in the incidence of type 2 diabetes with lifestyle intervention or metformin. *N. Engl. J. Med.* **346,** 393–403 (2002).
33. Bogacka, I., Xie, H., Bray, G. A. & Smith, S. R. The Effect of Pioglitazone on Peroxisome Proliferator-Activated Receptor-γ Target Genes Related to Lipid Storage In Vivo. *Diabetes Care* **27,** 1660–1667 (2004).
34. Marín-Peñalver, J. J., Martín-Timón, I., Sevillano-Collantes, C. & Del Cañizo-Gómez, F. J. Update on the treatment of type 2 diabetes mellitus. *World J. Diabetes* **7,** 354–95 (2016).
35. Howells, L., McKay, A. J., Hussain, S. & Majeed, A. Management of a patient at high risk of type 2 diabetes. *London J. Prim. Care (Abingdon).* **8,** 76–79 (2016).
36. Reusch, J. E. B., Manson, J. E., C, W. & JM, L. Management of Type 2 Diabetes in 2017. *JAMA* **317,** 1015 (2017).
37. Meng, J. *et al.* Effect of Diabetes Treatment-Related Attributes on Costs to Type 2 Diabetes Patients in a Real-World Population. *J. Manag. Care Spec. Pharm.* **23,** 446–452 (2017).
38. Spiegelman, B. M. & Flier, J. S. Obesity and the regulation of energy balance. *Cell* **104,** 531–543 (2001).
39. Woods, S. C., Seeley, R. J., Jr., D. P. & Schwartz, M. W. Signals That Regulate Food Intake and Energy Homeostasis. *Science (80-.).* **280,** 1378–1383 (1998).
40. Yu, J. H., and Kim, M. S. Molecular mechanisms of appetite regulation. *Diabetes Metab. J.* **36,** 391–398 (2012).
41. Coll, A. P. & Yeo, G. S. H. The hypothalamus and metabolism: Integrating signals to control energy and glucose homeostasis. *Curr. Opin. Pharmacol.* **13,** 970–976 (2013).
42. Broadwell, R. D. & Brightman, M. W. Entry of peroxidase into neurons of the central and peripheral nervous systems from extracerebral and cerebral blood. *J. Comp. Neurol.* **166,** 257–283 (1976).
43. Coppari, R. *et al.* The hypothalamic arcuate nucleus: A key site for mediating leptin's effects on glucose homeostasis and locomotor activity. *Cell Metab.* **1,** 63–72 (2005).
44. Williams, G. *et al.* The hypothalamus and the control of energy homeostasis. *Physiol. Behav.* **74,** 683–701 (2001).
45. Kalra, S. P. P. *et al.* NPY and cohorts in regulating appetite, obesity and metabolic syndrome: Beneficial effects of gene therapy. *Neuropeptides* **38,** 201–211 (2004).
46. Henry, M., Ghibaudi, L., Gao, J. & Hwa, J. J. Energy metabolic profile of mice after chronic activation of central NPY Y1, Y2, or Y5 receptors. *Obes. Res.* **13,** 36–47 (2005).
47. Schwartz, M. W., Woods, S. C., Porte, D., Seeley, R. J. & Baskin, D. G. Central nervous system control of food intake. *Nature* **404,** 661–671 (2000).
48. Bouret, S. G., Draper, S. J. & Simerly, R. B. Formation of Projection Pathways from the Arcuate Nucleus of the Hypothalamus to Hypothalamic Regions Implicated in the Neural Control of Feeding Behavior in Mice. *J. Neurosci.* **24,** 2797–2805 (2004).
49. Elias, C. F. *et al.* Chemically defined projections linking the mediobasal hypothalamus and the lateral hypothalamic area. *J. Comp. Neurol.* **402,** 442–459 (1998).
50. Choi, Y.-H., Fujikawa, T., Lee, J., Reuter, A. & Kim, K. W. Revisiting the Ventral Medial Nucleus of the Hypothalamus: The Roles of SF-1 Neurons in Energy Homeostasis. *Front. Neurosci.* **7,** 71 (2013).

51. Klöckener, T. *et al.* High-fat feeding promotes obesity via insulin receptor/PI3K-dependent inhibition of SF-1 VMH neurons. *Nat. Neurosci.* **14,** 911–918 (2011).
52. King, B. M. The rise, fall, and resurrection of the ventromedial hypothalamus in the regulation of feeding behavior and body weight. *Physiol. Behav.* **87,** 221–244 (2006).
53. Geerling, J. C., Shin, J.-W., Chimenti, P. C. & Loewy, A. D. Paraventricular hypothalamic nucleus: Axonal projections to the brainstem. *J. Comp. Neurol.* **518,** 1460–1499 (2010).
54. Forsythe, P., Bienenstock, J. & Kunze, W. A. in *Microbial Endocrinology: The Microbiota-Gut-Brain Axis in Health and Disease* 115–133 (Springer New York, 2014).
55. Mittag, J. *et al.* Thyroid hormone is required for hypothalamic neurons regulating cardiovascular functions. *J. Clin. Invest.* **123,** 509–516 (2013).
56. Dimitrov, E. L., Kim, Y. Y. & Usdin, T. B. Regulation of Hypothalamic Signaling by Tuberoinfundibular Peptide of 39 Residues Is Critical for the Response to Cold: A Novel Peptidergic Mechanism of Thermoregulation. *J. Neurosci.* **31,** 18166–18179 (2011).
57. Moore, R. Y. Suprachiasmatic nucleus in sleep-wake regulation. *Sleep Med* **8,** 27–33 (2007).
58. Coll, A. P. *et al.* The hypothalamus and the control of energy homeostasis. *Physiol. Behav.* **13,** 683–701 (2013).
59. Weststrate, J. A. Resting metabolic rate and diet-induced thermogenesis: a methodological reappraisal. *Am. J. Clin. Nutr.* **58,** 592–601 (1993).
60. Westerterp, K. R. Diet induced thermogenesis. *Nutr. Metab. (Lond).* **1,** 5 (2004).
61. Weststrate, J. A., Wunnink, I., Deurenberg, P. & Hautvast, J. G. A. J. Alcohol and its acute effects on resting metabolic rate and diet-induced thermogenesis. *Br. J. Nutr.* **64,** 413 (1990).
62. Raben, A., Agerholm-Larsen, L., Flint, A., Holst, J. J. & Astrup, A. Meals with similar energy densities but rich in protein, fat, carbohydrate, or alcohol have different effects on energy expenditure and substrate metabolism but not on appetite and energy intake. *Am. J. Clin. Nutr.* **77,** 91–100 (2003).
63. Bachman, S. E. *et al.* βAR Signaling Required for Diet-Induced Thermogenesis and Obesity Resistance. *Science (80-.).* **297,** 843–845 (2002).
64. Cannon, B. & Nedergaard, J. Brown adipose tissue: function and physiological significance. *Physiol. Rev.* **84,** 277–359 (2004).
65. Dodd, G. T. *et al.* Leptin and insulin act on POMC neurons to promote the browning of white fat. *Cell* **160,** 88–104 (2015).
66. Sell, H., Deshaies, Y. & Richard, D. The brown adipocyte: update on its metabolic role. *Int. J. Biochem. Cell Biol.* **36,** 2098–2104 (2004).
67. Nedergaard, J. *et al.* UCP1: The only protein able to mediate adaptive non-shivering thermogenesis and metabolic inefficiency. *Biochim. Biophys. Acta - Bioenerg.* **1504,** 82–106 (2001).
68. Morrison, S. F., Madden, C. J. & Tupone, D. Central neural regulation of brown adipose tissue thermogenesis and energy expenditure. *Cell Metab.* **19,** 741–756 (2014).
69. Triplitt, C. L. Examining the mechanisms of glucose regulation. *Am. J. Manag. Care* **18,** S4-10 (2012).
70. Wilcox, G. Insulin and insulin resistance. *Clin. Biochem. Rev.* **26,** 19–39 (2005).
71. Aljabri, K. S., Bokhari, S. A. & Khan, M. J. Serum Glucagon Counterregulatory Hormonal Response to Hypoglycemia Is Blunted in Congenital Hyperinsulinism. *Ann. Saudi Med.* **30,** 10–12 (2010).
72. Barrett, M. P., Walmsley, A. R. & Gould, G. W. Structure and function of facilitative sugar transporters. *Curr. Opin. Cell Biol.* **11,** 496–502 (1999).
73. Bouché, C., Serdy, S., Kahn, C. R. & Goldfine, A. B. The cellular fate of glucose and its relevance in type 2 diabetes. *Endocr. Rev.* **25,** 807–830 (2004).
74. Agius, L. Glucokinase and molecular aspects of liver glycogen metabolism. *Biochem. J.* **414,** 1–18 (2008).
75. Zhang, T. *et al.* Acetylation negatively regulates glycogen phosphorylase by recruiting protein phosphatase 1. *Cell Metab.* **15,** 75–87 (2012).
76. Rui, L. Energy Metabolism in the Liver. *Compr Physiol* **4,** 177–197 (2014).

77. Rider, M. H. *et al.* 6-Phosphofructo-2-kinase/fructose-2,6-bisphosphatase: head-to-head with a bifunctional enzyme that controls glycolysis. *Biochem. J* **381,** 561–579 (2004).
78. Kim, H. S. *et al.* Hepatic-specific disruption of SIRT6 in mice results in fatty liver formation due to enhanced glycolysis and triglyceride synthesis. *Cell Metab.* **12,** 224–236 (2010).
79. Uyeda, K. *et al.* Carbohydrate response element binding protein, ChREBP, a transcription factor coupling hepatic glucose utilization and lipid synthesis. *Cell Metab.* **4,** 107–10 (2006).
80. Jeoung, N. H. & Harris, R. A. Role of pyruvate dehydrogenase kinase 4 in regulation of blood glucose levels. *Korean Diabetes J.* **34,** 274–83 (2010).
81. Lin, H. V. & Accili, D. Hormonal regulation of hepatic glucose production in health and disease. *Cell Metab.* **14,** 9–19 (2011).
82. Puigserver, P. *et al.* Insulin-regulated hepatic gluconeogenesis through FOXO1–PGC-1α interaction. *Nature* **423,** 550–555 (2003).
83. Mergenthaler, P., Lindauer, U., Dienel, G. A. & Meisel, A. Sugar for the brain: The role of glucose in physiological and pathological brain function. *Trends Neurosci.* **36,** 587–597 (2013).
84. Anand, B. K., Chhina, G. S., Sharma, K. N., Dua, S. & Singh, B. Activity of single neurons in the hypothalamic feeding centers: effect of glucose. *Am. J. Physiol. -- Leg. Content* **207,** 1146–1154 (1964).
85. Oomura, Y., Ono, T., Ooyama, H. & Wayner, M. J. Glucose and Osmosensitive Neurones of the Rat Hypothalamus. *Nature* **222,** 282–284 (1969).
86. Dunn-Meynell, A. A., Rawson, N. E. & Levin, B. E. Distribution and phenotype of neurons containing the ATP-sensitive K+ channel in rat brain. *Brain Res.* **814,** 41–54 (1998).
87. Routh, V. H. Glucose-sensing neurons: Are they physiologically relevant? *Physiol. Behav.* **76,** 403–413 (2002).
88. Wang, Y., Viscarra, J., Kim, S.-J. & Sul, H. S. Transcriptional regulation of hepatic lipogenesis. *Nat. Rev. Mol. Cell Biol.* **16,** 678–89 (2015).
89. Yecies, J. L. *et al.* Akt stimulates hepatic SREBP1c and lipogenesis through parallel mTORC1-dependent and independent pathways. *Cell Metab.* **14,** 21–32 (2011).
90. Schade, D. S., Woodside, W., Eaton, R. P. & al., et. The role of glucagon in the regulation of plasma lipids. *Metabolism.* **28,** 874–86 (1979).
91. Kershaw, E. E. & Flier, J. S. Adipose Tissue as an Endocrine Organ. *J. Clin. Endocrinol. Metab.* **89,** 2548–2556 (2004).
92. Unger, R. H., Clark, G. O., Scherer, P. E. & Orci, L. Lipid homeostasis, lipotoxicity and the metabolic syndrome. *Biochim. Biophys. Acta - Mol. Cell Biol. Lipids* **1801,** 209–214 (2010).
93. Jo, J. *et al.* Hypertrophy and/or hyperplasia: Dynamics of adipose tissue growth. *PLoS Comput. Biol.* **5,** e1000324 (2009).
94. Tontonoz, P., Hu, E., Graves, R. A., Budavari, A. I. & Spiegelman, B. M. mPPAR gamma 2: Tissue-specific regulator of an adipocyte enhancer. *Genes Dev.* **8,** 1224–1234 (1994).
95. Armoni, M. *et al.* FOXO1 represses peroxisome proliferator-activated receptor-gamma1 and -gamma2 gene promoters in primary adipocytes. A novel paradigm to increase insulin sensitivity. *J. Biol. Chem.* **281,** 19881–91 (2006).
96. Nakae, J. *et al.* The forkhead transcription factor Foxo1 regulates adipocyte differentiation. *Dev. Cell* **4,** 119–29 (2003).
97. Srere, A. The Citrate Cleavage Enzyme. Distribution and purification. *J. Biol. Chem.* **234,** 2544–2547 (1959).
98. Binczek, E. *et al.* Obesity resistance of the stearoyl-CoA desaturase-deficient (scd1 -/-) mouse results from disruption of the epidermal lipid barrier and adaptive thermoregulation. *Biol. Chem.* **388,** 405–418 (2007).
99. Horton, J. D., Goldstein, J. L. & Brown, M. S. SREBPs: activators of the complete program of cholesterol and fatty acid synthesis in the liver. *J. Clin. Invest.* **109,** 1125–31 (2002).
100. Wan, M. *et al.* Postprandial hepatic lipid metabolism requires signaling through Akt2 independent of the transcription factors FoxA2, FoxO1, and SREBP1c. *Cell Metab.* **14,** 516–27 (2011).
101. DeLany, J. P., Windhauser, M. M., Champagne, C. M. & Bray, G. A. Differential oxidation of

individual dietary fatty acids in humans. *Am. J. Clin. Nutr.* **72,** 905–911 (2000).
102. Storlien, L. H. *et al.* Dietary fat subtypes and obesity. *World Rev. Nutr. Diet.* **88,** 148–54 (2001).
103. Greenberg, A. S. *et al.* The role of lipid droplets in metabolic disease in rodents and humans. *J. Clin. Invest.* **121,** 2102–10 (2011).
104. Langin, D. *et al.* Adipocyte Lipases and Defect of Lipolysis in Human Obesity. *Diabetes* **54,** 3190–3197 (2005).
105. Perry, R. J., Samuel, V. T., Petersen, K. F. & Shulman, G. I. The role of hepatic lipids in hepatic insulin resistance and type 2 diabetes. *Nature* **510,** 84 (2014).
106. Zhang, W. *et al.* Integrated Regulation of Hepatic Lipid and Glucose Metabolism by Adipose Triacylglycerol Lipase and FoxO Proteins. *Cell Rep.* **15,** 349–359 (2016).
107. Holm, C. Molecular mechanisms regulating hormone-sensitive lipase and lipolysis. *Biochem Soc Trans* **31,** 1120–1124 (2003).
108. Power, G. W., Yaqoob, P., Harvey, D. J., Newsholme, E. A. & Calder, P. C. The effect of dietary lipid manipulation on hepatic mitochondrial phospholipid fatty acid composition and carnitine palmitoyltransferase I activity. *Biochem. Mol. Biol. Int.* **34,** 671–84 (1994).
109. Gan, L. *et al.* α-MSH and Foxc2 promote fatty acid oxidation through C/EBPβ negative transcription in mice adipose tissue. *Sci. Rep.* **6,** 36661 (2016).
110. Paniagua, J. A. Nutrition, insulin resistance and dysfunctional adipose tissue determine the different components of metabolic syndrome. *World J. Diabetes* **7,** 483–514 (2016).
111. Kersten, S. *et al.* Peroxisome proliferator-activated receptor alpha mediates the adaptive response to fasting. *J. Clin. Invest.* **103,** 1489–98 (1999).
112. Leone, T. C., Weinheimer, C. J. & Kelly, D. P. A critical role for the peroxisome proliferator-activated receptor alpha (PPARalpha) in the cellular fasting response: the PPARalpha-null mouse as a model of fatty acid oxidation disorders. *Proc. Natl. Acad. Sci. U. S. A.* **96,** 7473–8 (1999).
113. Vega, R. B., Huss, J. M. & Kelly, D. P. The coactivator PGC-1 cooperates with peroxisome proliferator-activated receptor alpha in transcriptional control of nuclear genes encoding mitochondrial fatty acid oxidation enzymes. *Mol. Cell. Biol.* **20,** 1868–76 (2000).
114. Wu, Z. *et al.* Mechanisms controlling mitochondrial biogenesis and respiration through the thermogenic coactivator PGC-1. *Cell* **98,** 115–24 (1999).
115. Li, X., Monks, B., Ge, Q. & Birnbaum, M. J. Akt/PKB regulates hepatic metabolism by directly inhibiting PGC-1α transcription coactivator. *Nature* **447,** 1012–1016 (2007).
116. Almind, K., Doria, A. & Kahn, C. R. Putting the genes for type II diabetes on the map. *Nat. Med.* **7,** 277–279 (2001).
117. Biddinger, S. B. *et al.* Effects of Diet and Genetic Background on Sterol Regulatory Element-Binding Protein-1c, Stearoyl-CoA Desaturase 1, and the Development of the Metabolic Syndrome. *Diabetes* **54,** 1314–1323 (2005).
118. Taniguchi, C. M., Emanuelli, B. & Kahn, C. R. Critical nodes in signalling pathways: insights into insulin action. *Nat. Rev. Mol. Cell Biol.* **7,** 85–96 (2006).
119. White, M. F. Insulin Signaling in Health and Disease. *Science (80-.).* **302,** 1710–1711 (2003).
120. Kubota, H. *et al.* Temporal Coding of Insulin Action through Multiplexing of the AKT Pathway. *Mol. Cell* **46,** 820–832 (2012).
121. Turner, N. *et al.* Distinct patterns of tissue-specific lipid accumulation during the induction of insulin resistance in mice by high-fat feeding. *Diabetologia* **56,** 1638–1648 (2013).
122. Buettner, R. *et al.* Defining high-fat-diet rat models: metabolic and molecular effects of different fat types. *J. Mol. Endocrinol.* **36,** 485–501 (2006).
123. Lipina, C. & Hundal, H. S. Sphingolipids: Agents provocateurs in the pathogenesis of insulin resistance. *Diabetologia* **54,** 1596–1607 (2011).
124. Teruel, T., Hernandez, R. & Lorenzo, M. Ceramide Mediates Insulin Resistance by Tumor Necrosis Factor-alpha in Brown Adipocytes by Maintaining Akt in an Inactive Dephosphorylated State. *Diabetes* **50,** 2563–2571 (2001).
125. Emken, E. A., Adlof, R. O., Rohwedder, W. K. & Gulley, R. M. Influence of linoleic acid on desaturation and uptake of deuterium-labeled palmitic and stearic acids in humans. *Biochim.*

Biophys. Acta (BBA)/Lipids Lipid Metab. **1170,** 173–181 (1993).
126. Chavez, J. A. & Summers, S. A. Characterizing the effects of saturated fatty acids on insulin signaling and ceramide and diacylglycerol accumulation in 3T3-L1 adipocytes and C2C12 myotubes. *Arch. Biochem. Biophys.* **419,** 101–109 (2003).
127. Stratford, S., Hoehn, K. L., Liu, F. & Summers, S. A. Regulation of insulin action by ceramide: Dual mechanisms linking ceramide accumulation to the inhibition of Akt/protein kinase B. *J. Biol. Chem.* **279,** 36608–36615 (2004).
128. Magkos, F. *et al.* Intrahepatic diacylglycerol content is associated with hepatic insulin resistance in obese subjects. *Gastroenterology* **142,** 1444–1446 (2012).
129. Muoio, D. M. & Newgard, C. B. Mechanisms of disease: Molecular and metabolic mechanisms of insulin resistance and β-cell failure in type 2 diabetes. *Nat. Rev. Mol. Cell Biol.* **9,** 193–205 (2008).
130. Pagotto, U. Where does insulin resistance start? The brain. *Diabetes Care* **32 Suppl 2,** 0–3 (2009).
131. Wang, J. *et al.* Overfeeding Rapidly Induces Leptin and Insulin Resistance. *Diabetes* **50,** 2786–2791 (2001).
132. DeFronzo, R. A. & Tripathy, D. Skeletal muscle insulin resistance is the primary defect in type 2 diabetes. *Diabetes Care* **32 Suppl 2,** S157-63 (2009).
133. Van Beek, M. *et al.* Bcl10 Links Saturated Fat Overnutrition with Hepatocellular NF-kB Activation and Insulin Resistance. *Cell Rep.* **1,** 444–452 (2012).
134. Tan, S. X. *et al.* Selective insulin resistance in adipocytes. *J. Biol. Chem.* **290,** 11337–11348 (2015).
135. Kraegen, E. W. *et al.* Development of muscle insulin resistance after liver insulin resistance in high-fat-fed rats. *Diabetes* **40,** 1397–403 (1991).
136. Kraakman, M. J., Murphy, A. J., Jandeleit-dahm, K. & Kammoun, H. L. Macrophage polarization in obesity and type 2 diabetes : weighing down our understanding of macrophage function ? **5,** 1–7 (2014).
137. Shulman, G. I. Ectopic Fat in Insulin Resistance, Dyslipidemia, and Cardiometabolic Disease. *N. Engl. J. Med.* **371,** 1131–1141 (2014).
138. Lupi, R. *et al.* Prolonged Exposure to Free Fatty Acids Has Cytostatic and Pro-Apoptotic Effects on Human Pancreatic Islets. *Diabetes* **51,** 1437–1442 (2002).
139. Pimenta, A. S. *et al.* Prolonged exposure to palmitate impairs fatty acid oxidation despite activation of AMP-activated protein kinase in skeletal muscle cells. *J. Cell. Physiol.* **217,** 478–485 (2008).
140. Lavoie, J.-M. & Gauthier, M.-S. Regulation of fat metabolism in the liver: link to non-alcoholic hepatic steatosis and impact of physical exercise. *Cell. Mol. Life Sci.* **63,** 1393–1409 (2006).
141. Day, C. P., Matsumine, H., Kobayashi, T., Friedman, S. & Anania, F. Pathogenesis of steatohepatitis. *Best Pract. Res. Clin. Gastroenterol.* **16,** 663–678 (2002).
142. Annamária ónody, Csaba Csonka, Zoltán Giricz, P. F., ónody, A., Csonka, C., Giricz, Z. & Ferdinandy, P. Hyperlipidemia induced by a cholesterol-rich diet leads to enhanced peroxynitrite formation in rat hearts. *Cardiovasc. Res.* **58,** 663–670 (2003).
143. Oosterveer, M. H. *et al.* High fat feeding induces hepatic fatty acid elongation in mice. *PLoS One* **4,** e6066 (2009).
144. Glass, C. K. & Olefsky, J. M. Inflammation and lipid signaling in the etiology of insulin resistance. *Cell Metab.* **15,** 635–45 (2012).
145. Hotamisligil, G. S. Inflammation and metabolic disorders. *Nature* **444,** 860–867 (2006).
146. Wellen, K. E. & Hotamisligil, G. S. Inflammation , stress , and diabetes. *J. Clin. Invest.* **115,** 1111–1119 (2005).
147. Fessler, M., Rudel, L. & Brown, M. Toll-like receptor signaling links dietary fatty acids to the metabolic syndrome. *Natl. Inst. Heal.* **20,** 379–385 (2011).
148. Lee, J. J. *et al.* High-fat diet induces toll-like receptor 4-dependent macrophage/Microglial cell activation and retinal impairment. *Investig. Ophthalmol. Vis. Sci.* **56,** 3041–3050 (2015).
149. Lee, J. Y., Sohn, K. H., Rhee, S. H. & Hwang, D. Saturated Fatty Acids, but Not Unsaturated

Fatty Acids, Induce the Expression of Cyclooxygenase-2 Mediated through Toll-like Receptor 4. *J. Biol. Chem.* **276,** 16683–16689 (2001).
150. Baker, R. G., Hayden, M. S. & Ghosh, S. NF-kB, inflammation, and metabolic disease. *Cell Metab.* **13,** 11–22 (2011).
151. Wiedemann, M. S. F. *et al.* Adipose tissue inflammation contributes to short-term high-fat diet-induced hepatic insulin resistance. *Am. J. Physiol. Endocrinol. Metab.* **305,** E388-95 (2013).
152. Kern, P. a *et al.* Adipose tissue tumor necrosis factor and interleukin-6 expression in human obesity and insulin resistance. *Am J Physiol Endocr Metab* **280,** 745–751 (2013).
153. Hotamisligil, G. S. *et al.* IRS-1-Mediated Inhibition of Insulin Receptor Tyrosine Kinase Activity in TNF-α- and Obesity-Induced Insulin Resistance. *Science (80-.).* **271,** 665 (1996).
154. Peraldi, P., Hotamisligil, G. S., Buurman, W. A., White, M. F. & Spiegelman, B. M. Tumor necrosis factor (TNF)-alpha inhibits insulin signaling through stimulation of the p55 TNF receptor and activation of sphingomyelinase. *J. Biol. Chem.* **271,** 13018–22 (1996).
155. Fernández-Real, J. M. & Ricart, W. Insulin Resistance and Chronic Cardiovascular Inflammatory Syndrome. *Endocr. Rev.* **24,** 278–301 (2003).
156. Baud, V. & Karin, M. Signal transduction by tumor necrosis factor and its relatives. *Trends Cell Biol.* **11,** 372–7 (2001).
157. Ivy, J. M., Klar, A. J. & Hicks, J. B. Cloning and characterization of four SIR genes of Saccharomyces cerevisiae. *Mol. Cell. Biol.* **6,** 688–702 (1986).
158. Rine, J. & Herskowitz, I. Four genes responsible for a position effect on expression from HML and HMR in Saccharomyces cerevisiae. *Genetics* **116,** 9–22 (1987).
159. Bryk, M. *et al.* Transcriptional silencing of Tyl elements in the RDNI locus of yeast. *Genes Dev.* **11,** 255–269 (1997).
160. Kaeberlein, M., Mcvey, M. & Guarente, L. The SIR2/3/4 complex and SIR2 alone promote longevity in Saccharomyces cerevisiae by two different mechanisms. *Genes Dev.* **13,** 2570–2580 (1999).
161. Imai, S., Armstrong, C. M., Kaeberlein, M. & Guarente, L. Transcriptional silencing and longevity protein Sir2 is an NAD-dependent histone deacetylase. *Nature* **403,** 795–800 (2000).
162. Wang, Y. & Tissenbaum, H. A. Overlapping and distinct functions for a Caenorhabditis elegans SIR2 and DAF-16/FOXO. *Mech. Ageing Dev.* **127,** 48–56 (2006).
163. Tissenbaum, H. a & Guarente, L. Increased dosage of a sir-2 gene extends lifespan in Caenorhabditis elegans. *Nature* **410,** 227–230 (2001).
164. Rogina, B. & Helfand, S. L. Sir2 mediates longevity in the fly through a pathway related to calorie restriction. *Proc. Natl. Acad. Sci. U. S. A.* **101,** 15998–6003 (2004).
165. Mair, W. & Dillin, A. Aging and Survival: The Genetics of Life Span Extension by Dietary Restriction. *Annu. Rev. Biochem.* **77,** 727–754 (2008).
166. Rae, M. It's Never Too Late: Calorie Restriction is Effective in Older Mammals. *Rejuvenation Res.* **7,** 3–8 (2004).
167. Haigis, M. C. & Guarente, L. P. Mammalian sirtuins - Emerging roles in physiology, aging, and calorie restriction. *Genes Dev.* **20,** 2913–2921 (2006).
168. Burnett, C. *et al.* Absence of effects of Sir2 overexpression on lifespan in C. elegans and Drosophila. *Nature* **477,** 482–5 (2011).
169. Houtkooper, R. H., Pirinen, E. & Auwerx, J. Sirtuins as regulators of metabolism and healthspan. *Nat. Rev. Mol. Cell Biol.* **13,** 225–238 (2012).
170. Houtkooper, R. H., Williams, R. W. & Auwerx, J. Metabolic networks of longevity. *Cell* **142,** 9–14 (2010).
171. Verdin, E., Hirschey, M. D., Finley, L. W. S. & Haigis, M. C. Sirtuin regulation of mitochondria: energy production, apoptosis, and signaling. *Trends Biochem. Sci.* **35,** 669–675 (2010).
172. Banks, A. S. *et al.* SirT1 Gain of Function Increases Energy Efficiency and Prevents Diabetes in Mice. *Cell Metab.* **8,** 333–341 (2008).
173. Bradbury, C. A. *et al.* Histone deacetylases in acute myeloid leukaemia show a distinctive pattern of expression that changes selectively in response to deacetylase inhibitors. *Leukemia* **19,** 1751–1759 (2005).

174. Alcendor, R. R. *et al.* Sirt1 Regulates Aging and Resistance to Oxidative Stress in the Heart. *Circ. Res.* **100,** 1512–1521 (2007).
175. Kawahara, T. L. A. A. *et al.* SIRT6 Links Histone H3 Lysine 9 Deacetylation to NF-κB-Dependent Gene Expression and Organismal Life Span. *Cell* **136,** 62–74 (2009).
176. Jiang, M. *et al.* Neuroprotective role of Sirt1 in mammalian models of Huntington's disease through activation of multiple Sirt1 targets. *Nat. Med.* **18,** 153–8 (2011).
177. Hall, J. A., Dominy, J. E., Lee, Y. & Puigserver, P. The sirtuin family's role in aging and age-associated pathologies. *J. Clin. Invest.* **123,** 973–979 (2013).
178. Sauve, A. A., Schramm, V. L., and, A. A. S. & Schramm*, V. L. Sir2 regulation by nicotinamide results from switching between base exchange and deacetylation chemistry. *Biochemistry* **42,** 9249–9256 (2003).
179. Verdin, E. The Many Faces of Sirtuins: Coupling of NAD metabolism, sirtuins and lifespan. *Nat. Med.* **20,** 25–27 (2014).
180. Chalkiadaki, A. & Guarente, L. Sirtuins mediate mammalian metabolic responses to nutrient availability. *Nat Rev Endocrinol* **8,** 287–296 (2012).
181. Tanno, M., Sakamoto, J., Miura, T., Shimamoto, K. & Horio, Y. Nucleocytoplasmic shuttling of the NAD+-dependent histone deacetylase SIRT1. *J. Biol. Chem.* **282,** 6823–6832 (2007).
182. Huang, J. Y., Hirschey, M. D., Shimazu, T., Ho, L. & Verdin, E. Mitochondrial sirtuins. *Biochim. Biophys. Acta - Proteins Proteomics* **1804,** 1645–1651 (2010).
183. Michishita, E., Park, J. Y., Burneskis, J. M., Barrett, J. C. & Horikawa, I. Evolutionarily conserved and nonconserved cellular localizations and functions of human SIRT proteins. *Mol. Biol. Cell* **16,** 4623–35 (2005).
184. Vaquero, A. *et al.* SirT2 is a histone deacetylase with preference for histone H4 Lys 16 during mitosis. *Genes Dev.* **20,** 1256–1261 (2006).
185. Liu, G. *et al.* Loss of NAD-Dependent Protein Deacetylase Sirtuin-2 Alters Mitochondrial Protein Acetylation and Dysregulates Mitophagy. *Antioxid. Redox Signal.* **27,** 849–863 (2016).
186. Chen, W. Y. *et al.* Tumor suppressor HIC1 directly regulates SIRT1 to modulate p53-dependent DNA-damage responses. *Cell* **123,** 437–48 (2005).
187. Vaziri, H. *et al.* hSIR2(SIRT1) functions as an NAD-dependent p53 deacetylase. *Cell* **107,** 149–59 (2001).
188. Purushotham, A. *et al.* Hepatocyte-specific deletion of SIRT1 alters fatty acid metabolism and results in hepatic steatosis and inflammation. *Cell Metab.* **9,** 327–38 (2009).
189. Xu, Y. *et al.* Dual-mode of insulin action controls GLUT4 vesicle exocytosis. *J. Cell Biol.* (2011).
190. Ghosh, S., Liu, B., Wang, Y., Hao, Q. & Zhou, Z. Lamin A Is an Endogenous SIRT6 Activator and Promotes SIRT6-Mediated DNA Repair. *Cell Rep.* **13,** 1396–1406 (2015).
191. Ford, E. *et al.* Mammalian Sir2 homolog SIRT7 is an activator of RNA polymerase I transcription. *Genes Dev.* **20,** 1075–80 (2006).
192. Schlicker, C. *et al.* Substrates and Regulation Mechanisms for the Human Mitochondrial Sirtuins Sirt3 and Sirt5. *J. Mol. Biol.* **382,** 790–801 (2008).
193. Ahn, B.-H. H. *et al.* A role for the mitochondrial deacetylase Sirt3 in regulating energy homeostasis. *Proc Natl Acad Sci U S A* **105,** 14447–14452 (2008).
194. Hallows, W. C., Lee, S. & Denu, J. M. Sirtuins deacetylate and activate mammalian acetyl-CoA synthetases. *Proc. Natl. Acad. Sci. U. S. A.* **103,** 10230–5 (2006).
195. Hirschey, M. D. *et al.* SIRT3 regulates mitochondrial fatty-acid oxidation by reversible enzyme deacetylation. *Nature* **464,** 121–5 (2010).
196. Haigis, M. C. *et al.* SIRT4 Inhibits Glutamate Dehydrogenase and Opposes the Effects of Calorie Restriction in Pancreatic β Cells. *Cell* **126,** 941–954 (2006).
197. Nakagawa, T., Lomb, D. J., Haigis, M. C. & Guarente, L. SIRT5 Deacetylates carbamoyl phosphate synthetase 1 and regulates the urea cycle. *Cell* **137,** 560–70 (2009).
198. Mei, Z. *et al.* Sirtuins in metabolism, DNA repair and cancer. *J. Exp. Clin. Cancer Res.* **35,** 182 (2016).
199. North, B. J. *et al.* The Human Sir2 Ortholog, SIRT2, Is an NAD(+) -Dependent Tubulin Deacetylase Brian. *Mol. Cell* **11,** 437–444 (2003).

200. Wang, F. & Tong, Q. SIRT2 suppresses adipocyte differentiation by deacetylating FOXO1 and enhancing FOXO1's repressive interaction with PPARgamma. *Mol. Biol. Cell* **20,** 801–8 (2009).
201. Ramakrishnan, G. *et al.* Sirt2 deacetylase is a novel AKT Binding partner critical for AKT activation by insulin. *J. Biol. Chem.* **289,** 6054–6066 (2014).
202. Barber, M. F. *et al.* SIRT7 links H3K18 deacetylation to maintenance of oncogenic transformation. *Nature* **487,** 114–8 (2012).
203. Herranz, D. *et al.* Sirt1 improves healthy ageing and protects from metabolic syndrome-associated cancer. *Nat. Commun.* **1,** 3 (2010).
204. Villalba, J. M. & Alcaín, F. J. Sirtuin activators and inhibitors. *BioFactors* **38,** 349–359 (2012).
205. Outeiro, T. F. *et al.* Sirtuin 2 inhibitors rescue alpha-synuclein-mediated toxicity in models of Parkinson's disease. *Science* **317,** 516–519 (2007).
206. Chen, X. *et al.* The sirtuin-2 inhibitor AK7 is neuroprotective in models of parkinson's disease but not amyotrophic lateral sclerosis and cerebral ischemia. *PLoS One* **10,** 1–15 (2015).
207. Howitz, K. T. *et al.* Small molecule activators of sirtuins extend Saccharomyces cerevisiae lifespan. *Nature* **425,** 191–196 (2003).
208. North, B. J. & Verdin, E. Interphase nucleo-cytoplasmic shuttling and localization of SIRT2 during mitosis. *PLoS One* **2,** e784 (2007).
209. Teng, Y.-B. B. *et al.* Efficient demyristoylase activity of SIRT2 revealed by kinetic and structural studies. *Sci. Rep.* **5,** 8529 (2015).
210. Gomes, P., Fleming Outeiro, T. & Cavadas, C. Emerging Role of Sirtuin 2 in the Regulation of Mammalian Metabolism. *Trends Pharmacol. Sci.* **36,** 756–768 (2015).
211. Wang, F., Nguyen, M., Qin, F. X. F. & Tong, Q. SIRT2 deacetylates FOXO3a in response to oxidative stress and caloric restriction. *Aging Cell* **6,** 505–514 (2007).
212. Maxwell, M. M. *et al.* The Sirtuin 2 microtubule deacetylase is an abundant neuronal protein that accumulates in the aging CNS. *Hum. Mol. Genet.* **20,** 3986–3996 (2011).
213. Jing, E., Gesta, S. & Kahn, C. R. SIRT2 Regulates Adipocyte Differentiation through FoxO1 Acetylation/Deacetylation. *Cell Metab.* **6,** 105–114 (2007).
214. Jing, E. *et al.* The NAD-dependent deacetylase sirtuin 2 is a suppressor of microglial activation and brain inflammation. *Nature* **5,** 327–331 (2013).
215. Voelter-mahlknecht, S., Ho, A. D. & Mahlknecht, U. FISH-mapping and genomic organization of the NAD-dependent histone deacetylase gene , Sirtuin 2 (Sirt2). *Int. J. Oncol.* **2,** 1187–1196 (2005).
216. Enxuan Jing, Stephane Gesta, and C. R. K. Sirt2 Regulates Adipocyte Differentiation Involving FoxO1 Acetylation/Deacetylation. *Cell Metab.* **6,** 105–114 (2007).
217. Crujeiras, A. B., Parra, D., Goyenechea, E. & Martínez, J. A. Sirtuin gene expression in human mononuclear cells is modulated by caloric restriction. *Eur. J. Clin. Invest.* **38,** 672–678 (2008).
218. Pandithage, R. *et al.* The regulation of SIRT2 function by cyclin-dependent kinases affects cell motility. *J. Cell Biol.* **180,** 915–929 (2008).
219. Han, Y. *et al.* Acetylation of Sirt2 by p300 attenuates its deacetylase activity. *Biochem. Biophys. Res. Commun.* **375,** 576–580 (2008).
220. Schiedel, M. *et al.* Aminothiazoles as Potent and Selective Sirt2 Inhibitors: A Structure–Activity Relationship Study. *J. Med. Chem.* **59,** 1599–1612 (2016).
221. Rumpf, T. *et al.* Selective Sirt2 inhibition by ligand-induced rearrangement of the active site. *Nat. Commun.* **6,** 6263 (2015).
222. Jing, H. *et al.* A SIRT2-Selective Inhibitor Promotes c-Myc Oncoprotein Degradation and Exhibits Broad Anticancer Activity. *Cancer Cell* **29,** 297–310 (2016).
223. Yoshino, J., Mills, K. F., Yoon, M. J. & Imai, S. Nicotinamide mononucleotide, a key NAD(+) intermediate, treats the pathophysiology of diet- and age-induced diabetes in mice. *Cell Metab.* **14,** 528–36 (2011).
224. Cantó, C. *et al.* The NAD+ Precursor Nicotinamide Riboside Enhances Oxidative Metabolism and Protects against High-Fat Diet-Induced Obesity. *Cell Metab.* **15,** 838–847 (2012).
225. Kim, H. S. *et al.* SIRT2 Maintains Genome Integrity and Suppresses Tumorigenesis through Regulating APC/C Activity. *Cancer Cell* **20,** 487–499 (2011).

226. Baker, D. J. *et al.* Increased expression of BubR1 protects against aneuploidy and cancer and extends healthy lifespan. *Nat. Cell Biol.* **15,** 96–102 (2013).
227. North, B. J. *et al.* SIRT2 induces the checkpoint kinase BubR1 to increase lifespan. *EMBO J.* **33,** 1438–53 (2014).
228. McGlynn, L. M. *et al.* SIRT2: Tumour suppressor or tumour promoter in operable breast cancer? *Eur. J. Cancer* **50,** 290–301 (2014).
229. Sanderson, L. M. *et al.* Peroxisome proliferator-activated receptor beta/delta (PPARbeta/delta) but not PPARalpha serves as a plasma free fatty acid sensor in liver. *Mol. Cell. Biol.* **29,** 6257–67 (2009).
230. Park, S.-H. *et al.* SIRT2-mediated deacetylation and tetramerization of pyruvate kinase directs glycolysis and tumor growth. *Cancer Res.* **76,** 3802–3812 (2016).
231. Liu, P. Y. *et al.* The histone deacetylase SIRT2 stabilizes Myc oncoproteins. *Cell Death Differ.* **20,** 503–514 (2013).
232. Chen, J. *et al.* SIRT2 overexpression in hepatocellular carcinoma mediates epithelial to mesenchymal transition by protein kinase B/glycogen synthase kinase-3β/β-catenin signaling. *Hepatology* **57,** 2287–2298 (2013).
233. Donmez, G. & Outeiro, T. F. SIRT1 and SIRT2: Emerging targets in neurodegeneration. *EMBO Mol. Med.* **5,** 344–352 (2013).
234. Luthi-Carter, R. *et al.* SIRT2 inhibition achieves neuroprotection by decreasing sterol biosynthesis. *Proc. Natl. Acad. Sci. U. S. A.* **107,** 7927–32 (2010).
235. Chopra, V. *et al.* The Sirtuin 2 Inhibitor AK-7 Is Neuroprotective in Huntington's Disease Mouse Models. *Cell Rep.* **2,** 1492–1497 (2012).
236. Bobrowska, A., Donmez, G., Weiss, A., Guarente, L. & Bates, G. SIRT2 ablation has no effect on tubulin acetylation in brain, cholesterol biosynthesis or the progression of Huntington's disease phenotypes in vivo. *PLoS One* **7,** e34805 (2012).
237. Lumeng, C. N. & Saltiel, A. R. Inflammatory links between obesity and metabolic disease. *Life Sci.* **121,** 2111–2117 (2011).
238. Rothgiesser, K. M., Erener, S., Waibel, S., Lüscher, B. & Hottiger, M. O. SIRT2 regulates NF-κB dependent gene expression through deacetylation of p65 Lys310. *J. Cell Sci.* **123,** 4251–8 (2010).
239. Lo Sasso, G. *et al.* SIRT2 Deficiency Modulates Macrophage Polarization and Susceptibility to Experimental Colitis. *PLoS One* **9,** e103573 (2014).
240. Park, J.-M., Kim, T.-H., Jo, S.-H., Kim, M.-Y. & Ahn, Y.-H. Acetylation of glucokinase regulatory protein decreases glucose metabolism by suppressing glucokinase activity. *Sci. Rep.* **5,** 17395 (2015).
241. Zhao, S. *et al.* Regulation of cellular metabolism by protein lysine acetylation. *Science* **327,** 1000–4 (2010).
242. Jiang, W. *et al.* Acetylation regulates gluconeogenesis by promoting PEPCK1 degradation via recruiting the UBR5 ubiquitin ligase. *Mol. Cell* **43,** 33–44 (2011).
243. Magro, F., Cavadas, C., Rego, A. C. & Costa, V. The NAD+-dependent deacetylase SIRT2 attenuates oxidative stress and mitochondrial dysfunction and improves insulin sensitivity in hepatocytes. *Hum. Mol. Genet.* (2017).
244. Arora, A. & Dey, C. S. SIRT2 negatively regulates insulin resistance in C2C12 skeletal muscle cells. *Biochim. Biophys. Acta - Mol. Basis Dis.* **1842,** 1372–1378 (2014).
245. Bogan, J. S., Hendon, N., McKee, A. E., Tsao, T.-S. & Lodish, H. F. Functional cloning of TUG as a regulator of GLUT4 glucose transporter trafficking. *Nature* **425,** 727–733 (2003).
246. Belman, J. P. *et al.* Acetylation of TUG protein promotes the accumulation of GLUT4 glucose transporters in an insulin-responsive intracellular compartment. *J. Biol. Chem.* **290,** 4447–63 (2015).
247. Wang, Q. *et al.* Abrogation of hepatic ATP-citrate lyase protects against fatty liver and ameliorates hyperglycemia in leptin receptor-deficient mice. *Hepatology* **49,** 1166–1175 (2009).
248. Ruiting Lin et al. Acetylation Stabilizes ATP-Citrate Lyase to Promote Lipid Biosynthesis and

Tumor Growth Ruiting. *Mol. Cell* **51,** 506–518 (2013).
249. Dryden, S. C., Nahhas, F. A., Nowak, J. E., Goustin, A. & Tainsky, M. A. Role for Human SIRT2 NAD-Dependent Deacetylase Activity in Control of Mitotic Exit in the Cell Cycle. *Mol. Cell. Biol.* **23,** 3173–3185 (2003).
250. Konige, M., Wang, H. & Sztalryd, C. Role of adipose specific lipid droplet proteins in maintaining whole body energy homeostasis. *BBA - Mol. Basis Dis.* **1842,** 393–401 (2013).
251. Smith, B. W. & Adams, L. A. Nonalcoholic fatty liver disease and diabetes mellitus: pathogenesis and treatment. *Nat. Rev. Endocrinol.* **7,** 456–465 (2011).
252. Haigis, M. C. & Sinclair, D. A. Mammalian Sirtuins: Biological Insights and Disease Relevance. *Annu. Rev. Pathol. Mech. Dis.* **5,** 253–295 (2010).
253. Kuang, J. *et al.* Fat-specific Sirt6 ablation sensitizes mice to high-fat diet-induced obesity and insulin resistance by inhibiting lipolysis. *Diabetes* **50,** db161225 (2017).
254. Murase, T. *et al.* Coffee polyphenols suppress diet-induced body fat accumulation by downregulating SREBP-1c and related molecules in C57BL / 6J mice. *Am J Physiol Endocr Metab* **300,** E122–E133 (2011).
255. Dimitriadis, G., Mitrou, P., Lambadiari, V., Maratou, E. & Raptis, S. A. Insulin effects in muscle and adipose tissue. *Diabetes Res. Clin. Pract.* **93,** 52–59 (2011).
256. Xiangyu Meng et al. Liver microRNA-291b-3p promotes hepatic lipogenesis through negative regulation of Adenosine 5'-monophosphate (AMP)-activated protein kinase α1. *Am. Soc. Biochem. Mol. Biol.* **291,** 0625–10634 (2016).
257. Quan, H., Yuan, H., Jung, M. I. S. & Ko, S. K. Ginsenoside Re lowers blood glucose and lipid levels via activation of AMP-activated protein kinase in HepG2 cells and high-fat diet fed mice. *Int. J. Mol. Med.* **29,** 73–80 (2012).
258. Cansby, E. *et al.* Increased expression of STK25 leads to impaired glucose utilization and insulin sensitivity in mice challenged with a high-fat diet. *FASEB J.* **27,** 3660–3671 (2013).
259. Chu, Y. *et al.* Liver Med23 ablation improves glucose and lipid metabolism through modulating FOXO1 activity. *Cell Res.* **24,** 1250–1265 (2014).
260. Schneeberger, M., Altirriba, J., Zorzano, A., Gomis, R. & Claret, M. Reduced alpha-MSH Underlies Hypothalamic ER-Stress- Induced Hepatic Gluconeogenesis Report Reduced a -MSH Underlies Hypothalamic ER-Stress-Induced Hepatic Gluconeogenesis. *Cell Rep.* **12,** 361–370 (2015).
261. Badalà, F., Nouri-mahdavi, K. & Raoof, D. A. Acetylation regulates gluconeogenesis by promoting PEPCK1 degradation via recruiting the UBR5 ubiquitin ligase. *Mol. Cell* **144,** 724–732 (2008).
262. Joseph, J. W. *et al.* Uncoupling Protein 2 Knockout Mice Have Enhanced Insulin Secretory Capacity After a High-Fat Diet. *Diabetes* **51,** 3211–3219 (2002).
263. Willems, K., Dijk, V. & Jeneson, J. A. Fiber-type-specific sensitivities and phenotypic adaptations to dietary fat overload differentially impact fast- versus slow-twitch muscle contractile function in. *J. Nutr. Biochem.* **26,** 155–164 (2015).
264. Kume, S., Uzu, T., Araki, S., Sugimoto, T. & Isshiki, K. Role of Altered Renal Lipid Metabolism in the Development of Renal Injury Induced by a High-Fat Diet. *J Am Soc Nephrol* **18,** 2715–2723 (2007).
265. Krishnan, J. *et al.* Dietary obesity-associated Hif1 a activation in adipocytes restricts fatty acid oxidation and energy expenditure via suppression of the Sirt2-NAD + system. *Genes Dev.* **26,** 259–270 (2012).
266. Kubota, T., Kubota, N. & Kadowaki, T. Imbalanced Insulin Actions in Obesity and Type 2 Diabetes: Key Mouse Models of Insulin Signaling Pathway. *Cell Metab.* **25,** 797–810 (2017).
267. Powell, D. J., Turban, S., Gray, A., Hajduch, E. & Hundal, H. S. Intracellular ceramide synthesis and protein kinase Czeta activation play an essential role in palmitate-induced insulin resistance in rat L6 skeletal muscle cells. *Biochem. J.* **382,** 619–29 (2004).
268. Hoehn, K. L. *et al.* IRS1-Independent Defects Define Major Nodes of Insulin Resistance. *Cell Metab.* **7,** 421–433 (2010).
269. Agouni, A., Owen, C., Czopek, A., Mody, N. & Delibegovic, M. In vivo differential effects of

fasting , re-feeding , insulin and insulin stimulation time course on insulin signaling pathway components in peripheral tissues. *Biochem. Biophys. Res. Commun.* **401,** 104–111 (2010).

270. Scherer, T. *et al.* Insulin regulates hepatic triglyceride secretion and lipid content via signaling in the brain. *Diabetes* **65,** 1511–1520 (2016).
271. Tilg, H. & Moschen, A. R. Evolution of inflammation in nonalcoholic fatty liver disease: The multiple parallel hits hypothesis. *Hepatology* **52,** 1836–1846 (2010).